

9-30-2011

Functional Characterization of Putative Non-Specific Phospholipase C (NPC) in *Arabidopsis thaliana*

Carlotta Antonetta Peters

University of Missouri-St. Louis, capxd@umsl.edu

Follow this and additional works at: <https://irl.umsl.edu/dissertation>



Part of the [Biology Commons](#)

Recommended Citation

Peters, Carlotta Antonetta, "Functional Characterization of Putative Non-Specific Phospholipase C (NPC) in *Arabidopsis thaliana*" (2011). *Dissertations*. 411.

<https://irl.umsl.edu/dissertation/411>

This Dissertation is brought to you for free and open access by the UMSL Graduate Works at IRL @ UMSL. It has been accepted for inclusion in Dissertations by an authorized administrator of IRL @ UMSL. For more information, please contact marvinh@umsl.edu.

Functional Characterization of Non-Specific Phospholipase C (NPC) in *Arabidopsis thaliana*

Carlotta Peters

University of Missouri-St Louis
Department of Biology
Program in Cellular and Molecular Biology

Dissertation presented to the Graduate School of Arts and Sciences at the
University of Missouri-St Louis in partial fulfillment of the requirements of
Doctor of Philosophy

Dissertation Committee

Dr. Xuemin Wang

(Advisor)

Dr. Mark Running

Dr. Bethany Zolman

Dr. Lisa Schechter

Abstract

Phospholipases are enzymes that hydrolyze phospholipids. In terms of the position of bond hydrolysis, phospholipases are classified into four major types: phospholipase C (PLC), phospholipase D (PLD), phospholipase A₁ (PLA₁) and phospholipase A₂ (PLA₂). PLC hydrolyzes phospholipids at the first phosphodiester bond, producing diacylglycerol (DAG) and a phosphorylated head group. Based on substrate specificity, PLC is divided into two distinctively different groups: phosphoinositide-specific phospholipase C (PI-PLC) and non-specific phospholipase C (NPC). PI-PLC has been extensively studied and well characterized in animal systems. There are six members of the NPC family in Arabidopsis, designated NPC1 through 6 that bear sequence homology to bacterial phosphatidylcholine hydrolyzing PLC (PC-PLC). However, their function remains largely unknown. This project was undertaken to study the biochemical properties and the physiological function of this family of enzymes in Arabidopsis.

Histidine (HIS)-tagged NPC1-6 were expressed in *E. coli* and used to study the biochemical properties of these NPCs. All of the NPCs tested hydrolyze phospholipids in a calcium-independent manner. NPC4 hydrolyzes phosphatidic acid (PA), phosphatidylserine (PS), and lysoPC in addition to major membrane lipids such as phosphatidylcholine (PC) and phosphatidylethanolamine (PE). NPC3 has 64.2% amino acid identity to NPC4 and hydrolyzes PC and PE. NPC6 has 52.8% amino acid identity to NPC3 and shows a lower activity than NPC3. The intracellular distribution of the NPCs was examined using NPC fused with green fluorescence protein (GFP). NPC3 predominantly associated with the plasma membrane but a small portion is cytosolic. NPC4 is localized to the plasma membrane, whereas NPC5 and NPC6 are mostly cytosolic.

To study the physiological function of *NPC1-6* in Arabidopsis, T-DNA insertion and overexpression lines were used. Overexpression of *NPC4* increased plant sensitivity to ABA and tolerance to hyperosmotic stress compared to wild-type plants. On the other hand, knock-out of *NPC4* decreased plant sensitivity to ABA, and hyperosmotic stress and also affected lipid composition under phosphate deprivation. NPC5 is highly similar

to NPC4 (84.7% amino acid identity). Loss of *NPC5* decreased lateral root growth under mild salt stress by 90% while overexpression of *NPC5* increased lateral root growth compared to wild-type. Double knockout of *NPC3* and *NPC6* affected response to phosphate deprivation, auxin, seed germination and salt stress. These results indicate that the NPC family plays a pivotal role in sensing and adapting to various types of stress in *Arabidopsis*. Some members of the family have additive effects under certain growth conditions and their cellular functions are distinctly different under some growth conditions.

Acknowledgements

I would like to thank my advisor, Dr. Xuemin (Sam) Wang for his invaluable contribution to my graduate work. His guidance, knowledge, wisdom, understanding and skills have helped my development as a researcher. I would also like to thank my committee members, Dr. Zolman, Dr. Schechter, Dr. Running and Dr. Kellogg for their helpful ideas throughout the course of my graduate studies.

I would also like to thank the members of Dr. Wang's lab, both past and present, for sharing their knowledge with me. These include Dr. Sung Chul Bahn, Dr. Shivakumar Devaiah, Liang Guo, Dr. Geliang Wang, Dr. Xiangqing Pan and Eric Sun. I would like to thank Dr. Maoyin Li for his help with real-time PCR and lipid extraction, and Amanda Tawfall for her help with mutant confirmation. I would also like to thank the green house staff both at the Donald Danforth Plant Science Center and UM-St Louis. I am grateful to Dr. Ruth Welti and Mary Roth at Kansas State University for lipid analysis.

I thank my mentor Dr. Gwendolyn Packnett, my friends and family, my husband, my mother, my sisters and my in-laws for their love and support throughout my graduate years.

Above all I would like to thank the almighty God for giving me strength throughout my graduate study.

Abbreviations

ABA, abscisic acid
DAG, Diacylglycerol
DGDG, Digalactosyldiacylglycerol
DGK, Diacylglycerol kinase
DGPP, Diacylglycerol pyrophosphate
GFP, Green fluorescence protein
HIS, Histidine
IP₃, Inositol tri-phosphate
KO, Knockout
LPC, Lyso phosphatidylcholine
LPE, Lyso phosphatidylethanolamine
LPG, Lyso phosphatidylglycerol
MGDG, Monogalactosyldiacylglycerol
NPC, Non Specific Phospholipase C
OE, Overexpressed
PA, Phosphatidic acid
PAP, Phosphatidic acid phosphatase
PC, Phosphatidylcholine
PE, Phosphatidylethanolamine
PG, Phosphatidylglycerol
PI, Phosphatidylinositol
PI-PLC, Phosphoinositide specific phospholipase C
PKC, Protein kinase C
PS, Phosphatidylserine
PLA, Phospholipase A
PLC, Phospholipase C
PLD, Phospholipase D
PEG, Polyethyleneglycol
SD, Standard deviation
SE, Standard error

T-DNA, Transferred DNA

UTR, Untranslated region

* , P > 0.05

TABLE OF CONTENTS

Chapter 1. Research Background, Goal and Specific Objectives	1
Literature review	1
Goals and Specific Objectives	4
References.....	5
Figures	9
Chapter 2. Initial Characterization of the NPC Gene Family in Arabidopsis.....	11
Introduction	11
Results	11
Discussion	15
Materials and methods	16
References	17
Figure Legends	19
Figures	24
Table 1	39
Table 2	40
Chapter 3. Non-Specific Phospholipase C NPC4 is Involved in Phosphate Deprivation and Promotes Arabidopsis Response to Abscisic Acid and Tolerance to Hyperosmotic Stress	41
Abstract	41
Introduction	41
Results	44
Discussion	52
Materials and methods	56
References	62
Figure Legends	66
Figures	73
Table 1	81
Chapter 4. Double-knockouts of NPC3 and NPC6 are Involved in DAG Production and Accumulation of DGDG under Phosphate Deprived Conditions	86
Abstract	86

Introduction	86
Results	89
Discussion	94
Materials and methods	96
References	100
Figure Legends	104
Figures	108
Chapter 5. Characterization of <i>NPC5</i> in Response to Salt Stress: <i>NPC5</i> and its Lipid Product DAG, Modulate Lateral Root Development Under Mild Salt Stress	116
Abstract	116
Introduction	116
Results	121
Discussion	127
Materials and methods	130
References	134
Figure Legends	140
Figures	145
Chapter 6. Discussion and Conclusions	155

Chapter 1. Background; Goals and Specific Objectives.

Introduction

Phospholipids constitute the major structural component of biological membranes. Phospholipids consist of two fatty acyl chains esterified to a glycerol backbone at the sn-1 and sn-2 positions. A phosphate is attached at the sn-3 position thereby creating the phosphatidyl moiety to which a variable head group is attached (Figure 1). Common glycerolipids in plants include phosphatidylcholine (PC), phosphatidylethanolamine (PE), phosphatidylglycerol (PG), phosphatidylserine (PS), phosphatidylinositol (PI), monoglactosyldiacylglycerol (MGDG) and digalacosyldiacylglycerol (DGDG) (Figure 2). These vital membrane components provide structural support for cell membranes and provide energy for various metabolic processes through their degradation (Wang, 2004). Over recent years, increasing evidence shows that phospholipids can function as second messengers in plant cells (Wang, 2004; Meijer and Munnik et al., 2003). Second messengers are rapidly formed in response to a variety of stimuli (Meijer and Munnik et al., 2003). The lipid signals created can activate enzymes or recruit proteins to membranes via mechanisms such as lipid-protein interaction via lipid binding domains. This can also promote amplification where the local concentration of specific lipids is increased and downstream signaling occurs (Wang, 2004; Meijer and Munnik et al., 2003). Aside from signaling, phospholipids act as mediators in various processes that are crucial for cell survival, growth and differentiation, such as cytoskeleton rearrangement, membrane remodeling, and vesicular trafficking (Wang, 2004).

Phospholipases play important roles in the production of phospholipid-based lipid mediators. These lipid signaling enzymes control the spatial and temporal production of lipid mediators in response to a wide spectrum of biotic and abiotic stress (Wang, 2004).

There are four major classes of phospholipases: phospholipase D (PLD), phospholipase C (PLC) and phospholipase A (PLA), which is divided into PLA₁ and PLA₂. These phospholipases are grouped into different classes based on the site at which they cleave phospholipids (Figure 1). Hydrolysis of phospholipids by PLC gives rise to a

phosphorylated head group and DAG; hydrolysis by PLD produces phosphatidic acid and a free head group; hydrolysis by PLA results in the formation of a lyso-phospholipid and a free fatty acid. PLA₂ specifically hydrolyzes the acyl ester bond at the sn-2 position whereas PLA₁ acts at the sn-1 position (Wang, 2001). In Arabidopsis there are twelve PLDs, and their expression levels tend to increase during stress (Wang, 1999). Members of the PLD family have been implicated in response to wounding, osmotic stress, dehydration, freezing tolerance, nitrogen responses ABA signaling, ethylene signaling and pathogen interaction (Zhang and Wang, 2000; Li et al., 2004; Mishra et al., 2006; Sang et al., 2001, Hong et al., 2008, 2009). On the other hand, plant PLA₂s have been implicated in wounding and jasmonic acid signaling (Viegweger, et al., 2002; Meijer and Munnik et al., 2003).

PLC signaling has been well documented in mammalian systems. In plants there are two types of PLCs: phosphoinositide specific-PLC (PI-PLC) and non-specific phospholipase C (NPC) that hydrolyzes PC and other common membrane lipids (Nakamura et al., 2005). PLC signaling in eukaryotes refers to the hydrolysis of phosphatidylinositol 4,5-bisphosphate [PI(4,5)P₂], releasing second messengers inositol 1,4,5-trisphosphate (IP₃) and DAG. In animals IP₃ diffuses into the cytosol where it activates the release of calcium from intracellular stores (Clapham, 1995). DAG remains in the membrane and activates certain members of the protein kinase C (PKC) family. DAG is removed from the signaling pathway through phosphorylation to PA by DAG kinase (DGK). In plants there is no evidence for the existence of any members of the PKC family; therefore the role of DAG as a signaling molecule remains to be determined (Munnik, 2001). However, there is very convincing evidence that PA is a plant second messenger and PLC can indirectly produce PA (Meijer and Munnik et al., 2003). In plants, several PA targets have been identified. PA has been shown to bind to ABI1, PDK1 and MAPK6 – related protein (Mishra et al., 2006; Anthony et al., 2004; Liu and Zhang, 2004).

Six distinct subfamilies of PI-PLC have been identified in mammalian systems to date. These include PLC beta, gamma, delta, epsilon, zeta and eta (Rebecchi and Pentylala, 2000, Wang 2004; Suh et al., 2008). All of these isoforms are found in animals but only

members of the zeta like subclass have been found in plants (Wang 2004). The *Arabidopsis* genome contains nine putative PI-PLCs that exhibit calcium dependent hydrolysis of PI(4,5)P₂ with the exception of *AtPLC8* and *AtPLC9*. *AtPLC8* and *AtPLC9* are thought to be inactive isoforms because of key amino acid substitutions in their catalytic domain (Mueller-Roeber & Pical, 2002; Tasma et al., 2008). Cloning and characterization of some members of the PI-PLC revealed that *AtPLC2* is associated with the plasma membrane and constitutively expressed in vegetative and floral tissues (Otterhag et al., 2001). Likewise, *AtPLC1f* is constitutively expressed in floral tissues (Hirayama et al., 1997), whereas *AtPLC1S* expression is induced by low temperature, salt and drought stress (Hirayama et al., 1995). *AtPLC4* is highly expressed in mature and developing pollen and *AtPLC5* is expressed in vascular tissues of mature plants (Hunt et al., 2004).

Unlike PI-PLC, NPC has a broader substrate preference. Phosphatidylcholine hydrolyzing PLC (PC-PLC) has been well characterized in microbial systems, and some of these enzymes are toxic to host cells. PC-PLC isolated from *Clostridium perfringens* is a potent toxin; it has an α -toxin domain (Titball, 1993). This enzyme has hemolytic activity (Saint-Joanis et al., 1989), vascular permeabilization (Sugahara et al., 1977) and platelet aggregation properties (Sugahara et al., 1976). Removal of the α -toxin domain from *C. perfringens* PLC greatly reduces its toxic properties, but the enzyme still retains its PC hydrolyzing activity (Titball, 1991). Other non toxic PC-PLCs are also found in bacteria such as *Bacillus cereus* and *Pseudomonas aeruginosa* (Titball, 1993). The *Arabidopsis* genome is predicted to contain six putative NPC genes based on sequence homology with bacterial PC-PLC (Wang 2001). Two cDNAs designated PLCa and PLCd were identified from *Arabidopsis* cDNA libraries based on high sequence homology to bacterial PC-PLC (Ling, 2000). These genes were later referred to as non specific phospholipase C (NPC). These genes encode proteins that are roughly 60-kDa consisting of 514-538 amino acid residues. Multiple alignments of *Arabidopsis* NPCs with *M. tuberculosis* reveal that there are three highly conserved domains among bacteria and plants (Nakamura et al., 2005). However, none of these domains corresponds to any known motifs. AtNPCs lack the X-Y domains (catalytic domain) and the EF-hand motif

(calcium binding domain) of AtPI-PLC. They also lack the C2 (calcium-lipid binding domain) and PX/PH (phosphoinositide binding) domains of AtPLD. Thus, NPCs are likely to be structurally and biochemically distinct from other phospholipases such as PI-PLCs and PLDs. In addition, members of the NPC gene family are differentially expressed in Arabidopsis tissues and under stress. For example, *NPC4* is induced by phosphate limitation in Arabidopsis roots and *NPC5* in leaves (Nakamura et al., 2005; Gaude et al., 2008). At the onset of this study, nothing was known about the biochemical properties and physiological significance of the NPCs in plants. Therefore, the main thrust of this project is to characterize the biochemical properties and physiological function of the NPC gene family in Arabidopsis.

Goals and Objectives

The goal of this project is to determine the biochemical and physiological functions of the NPC family in Arabidopsis with the following specific aims:

I. Isolation of NPC Knockout Mutants to Investigate Their Roles in Plant Stress Response: To determine the potential function of members of the putative NPC family, knockout (KO) mutants were obtained from ARBC (Ohio State University). The mutants were designated *npc1-1-npc6-1*. The mutants were verified to be homozygous and were screened for altered response to a wide variety of stresses. The stress treatments tested were aluminum toxicity, drought stress, light sensitivity, osmotic stress, salt stress, freezing tolerance, ABA response, SA response, IBA and IAA response, ethylene response, cytokinin response, nitrogen deprivation, phosphate deprivation, potassium deprivation and glucose sensitivity. In addition, the phenotype of all mutants under normal growth conditions were compared to wild type to discern changes in germination rate and efficiency, growth defects, changes in flowering time and reproductive viability. The mutants that displayed alterations under the conditions described above were chosen for further characterization.

II. Generation of Double KO and Overexpression Lines to Further Elucidate the Function of NPCs in Arabidopsis: Based on expression pattern, under certain stress conditions several members of the NPC gene family are upregulated as documented by Genevestigator (Figure 4, Chapter 2). However, based on the lack of phenotype of some of these mutants under stress conditions it became evident that some members might be redundant in function. Therefore, the generation of double or possibly triple mutants may be informative in elucidating the pathways that some of these enzymes function in. Hence, double KOs deficient in two selected NPCs were generated. Expression pattern and amino acid identities were taken into consideration when the double mutants were generated. The double mutants generated through genetic crosses were screened under normal and stress conditions as described in Aim I.

III. Determination of the Biochemical Properties and Subcellular Localization of the NPCs: Biochemical characterization of members of the NPC gene family will be instrumental in determining the function of these enzymes. Demonstration of the lipolytic activity of uncharacterized members of the NPC is necessary in order to show that these enzymes are biologically active phospholipases. Additionally, the substrate preferences and subcellular localization among members of this family may help to further elucidate their physiological function in plants.

References

1. **Anthony RG, Henriques R, Helfer A, Meszaros T, Rios G, Testernik C, Deak M, Koncz C, Bogre L.** (2004) A protein kinase target of a PDK1 signaling pathway is involved in root hair growth in Arabidopsis. *EMBO Journal* **23**: 572-581.
2. **Clapham DE.** (1995) Calcium signaling. *Cell* **80**: 259–268.

3. **Gaude N, Nakamura Y, Scheible WR, Ohta H, Dormann P.** (2008) Phospholipase C5 (NPC5) is involved in galactolipids accumulation during phosphate limitation in leaves of *Arabidopsis*. *Plant J* **56**: 28-39.
4. **Hirayama T, Mitsukawa N, Shibata D, Shinozaki K.** (1997) *AtPLC2*, a gene encoding phosphoinositide-specific phospholipase C, is constitutively expressed in vegetative and floral tissues in *Arabidopsis thaliana*. *Plant Mol. Biol* **34**:175–80
5. **Hirayama T, Ohto C, Mizoguchi T, Shinozaki K.** (1995) A gene encoding a phosphatidylinositol-specific phospholipase C is induced by dehydration and salt stress in *Arabidopsis thaliana*. *Proc.Natl. Acad Sci USA* **92**: 3903–3907.
6. **Hong Y, Devaiah SP, Bahn SC, Thamasandra BN, Li M, Welti R, Wang X.** (2009) Phospholipase Dε and phosphatidic acid enhance *Arabidopsis* nitrogen signaling and growth. *Plant J* **58**, 376-387.
7. **Hong Y, PanX, Welti R, Wang X.** (2008) Phospholipase Dα3 is involved in the hyperosmotic response in *Arabidopsis*. *Plant Cell* **20**, 803-816.
8. **Hunt L, Otterhag L, Lee JC, Lasheen T, Hunt J, Seki M, Shinozaki K, Sommarin M, Gilmour DJ, Pical C, and Gray JE.** (2004) Gene-specific expression and calcium activation of *Arabidopsis thaliana* phospholipase C isoforms. *New Phytologist* **162**, 643-654.
9. **Li W, Li M, Zhang W, Welti R, Wang X.** (2004) The plasma membrane – bound Phospholipase Dδ enhanced freeze tolerance in *Arabidopsis thaliana*. *Nature biotechnology* **4**: 427-433.
10. **Ling D.** (2000) Cloning and characterization of a putative phosphatidylcholine-hydrolyzing phospholipase C in *Arabidopsis Thaliana*. MA thesis, Kansas State University.
11. **Liu Y and Zhang S.** (2004) Phosphorylation of 1-aminocyclopropane-1-carboxylic acid synthase by MPK6, a stress responsive mitogen-activated protein kinase, induces ethylene biosynthesis in *Arabidopsis*. *Plant Cell* **16**: 3386-3399.
12. **Meijer HJG and Munnik T.** (2003) Phospholipid-based signaling in plants. *Annual Review Plant Biol.* **54**, 265–306.

13. **Mishra G, Zhang W, Deng F, Zhao J, Wang X.** (2006) A bifurcating pathway directs abscisic acid effects on stomatal closure and opening in *Arabidopsis*. *Science* **312**: 264-266.
14. **Mueller-Roeber B and Pical C.** (2002) Inositol phospholipid metabolism in *Arabidopsis*. Characterized and putative isoforms of inositol phospholipid kinase and phosphoinositide-specific phospholipase C. *Plant Physiology*. **130**: 22–46.
15. **Munnik T.** (2001) Phosphatidic acid: an emerging plant lipid second messenger. *Trends Plant Sci* **6**: 227–33.
16. **Munnik T, Irvine RF, Musgrave A.** (1998) Phospholipid signalling in plants. *Biochim. Biophys. Acta* **1389**: 222–72.
17. **Otterhag L, Sommarin M, Pical C.** (2001) N-terminal EF-hand-like domain is required for phosphoinositide-specific phospholipase C activity in *Arabidopsis thaliana*. *FEBS Lett* **497**,165–70
18. **Rebecchi MJ, Pentylala SN.** (2000) Structure, function, and control of phosphoinositide-specific phospholipaseC. *Physiol. Rev* **80**:1291–335
19. **Saint-Joanis B, Garnier T, Cole S.** (1989) Gene cloning shows the alpha-toxin of *Clostridium perfringens* to contain both sphingomyelinase and lecithinase activities. *Mol Gen Genet* **219**: 453-460.
20. **Sang Y, Zheng S, Li W, Huang B, and Wang X.** (2001) Regulation of plant water loss by manipulating the expression of phospholipase D α . *Plant J* **28**:135-144.
21. **Suh PG, Park JI, Manzoli L, Cocco L, Peak JC, Katan M, Fukami K, Kataoka T, Yun S, Ryu SH.** (2008) Multiple roles of phosphoinositide-specific phospholipase C isozymes. *BMB Rep* **41 (6)**: 415- 434.
22. **Sugahara T, Takahashi T, Yamaya S, Ohsaka A.** (1976) In vitro aggregation of platelets induced by alpha-toxin (phospholipaseC) of *Clostridium perfringens*. *Jpn J Med Sci Biol* **29**: 255-263.
23. **Sugahara T, Takahashi T, Yamaya S, Ohsaka A.** (1977) Vascular permeability increase by α -toxin (phospholipase C) of *Clostridium perfringens*. *Toxicon* **15**: 81-87.

24. **Tasma IM, Brendel V, Whitham SA, Bhattacharyya MK.** (2008) Expression and evolution of the phosphoinositide-specific phospholipase C gene family in *Arabidopsis thaliana*. *Plant Physiol Biochem* **46**: 627-637.
25. **Titball RW, Leslie DL, Harvey S, Kelly DC.** (1991) Haemolytic and sphingomyelinase activities of *Clostridium perfringens* alpha-toxin are dependent on a domain homologous to that of an enzyme from the human arachidonic acid pathway. *Infect Immun* **59**:1872-1874.
26. **Titball RW.** (1993) Bacterial Phospholipases C. *Microbiol Reviews*. **57(2)**: 347-366.
27. **Viehweger K, Dordschbal B, Roos W.** (2002) Elicitor-activated phospholipaseA2 generates lysophosphatidylcholines that mobilize the vacuolar HC Pool for pH signaling via the activation of NaC-dependent proton fluxes. *Plant Cell*. **14**:1509–25.
28. **Wang X.** (2001) **Plant Phospholipases.** *Annu. Rev. Plant Physiol. Plant Mol Biol* **52**: 211-231
29. **Wang X.** (2004) Lipid signaling. *Current opinion in Plant Biology*. **7**: 1- 8.
30. **Wang X.** (2002) Phospholipase D in hormonal and stress signaling. *Current opinion in Plant Biology* **5**: 408- 414
31. **Wang X.** The role of Phospholipase D in signal cascades. *Plant physiology*. **120**: 645- 651.
32. **Wang X, Devaiah SP, Zhang W, Welti R.** (2006) Signaling functions of phosphatidic acid. *Prog Lipid Res* **45**: 250-278.
33. **Zhang W and Wang X.** (2000) Phospholipid metabolism and signal transduction in plants. *Chinese Bulletin of Life Sciences*. **12**:100-104.

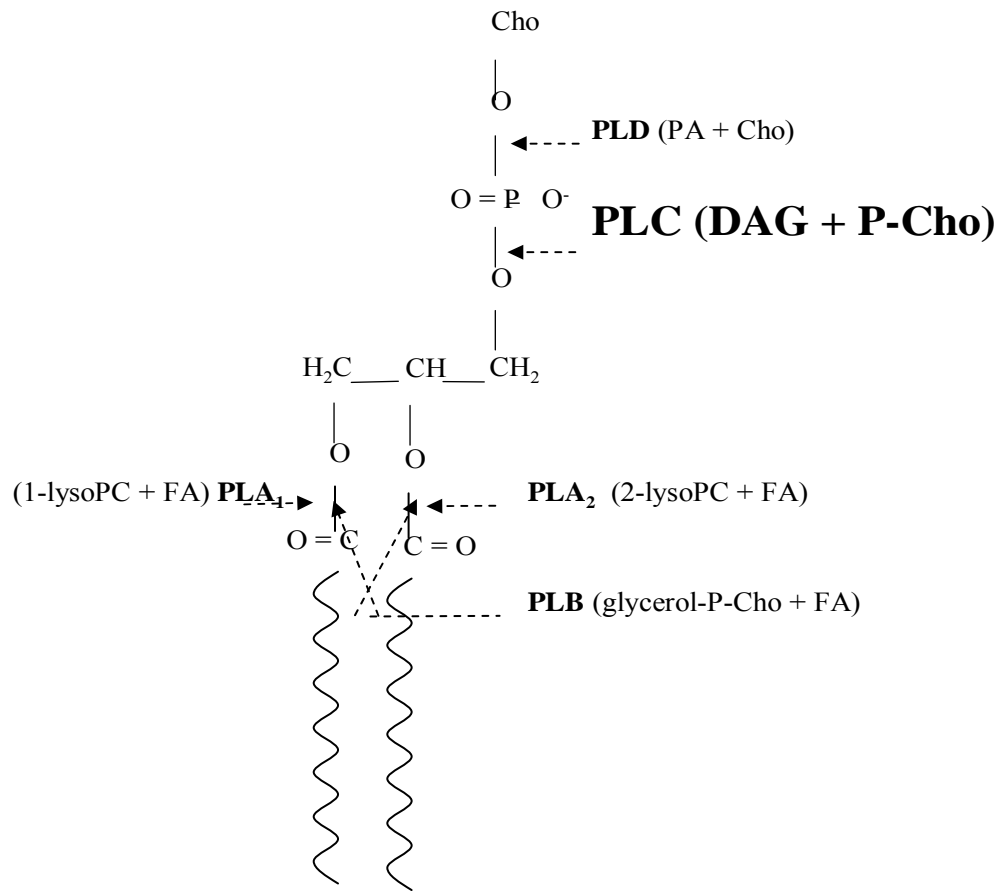


Figure 1. Hydrolysis sites of phospholipases

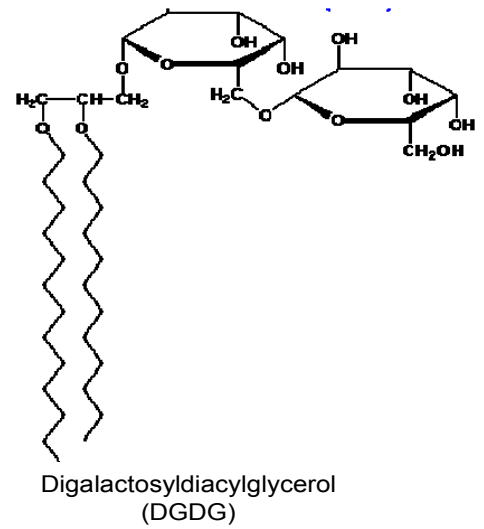
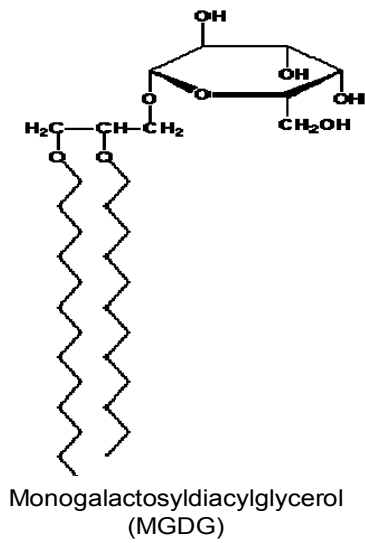
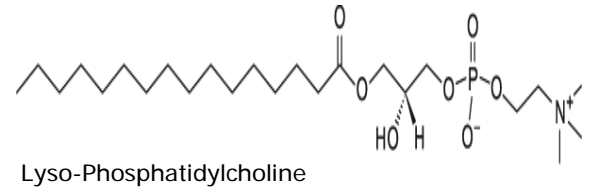
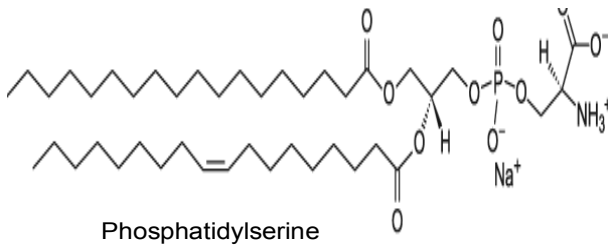
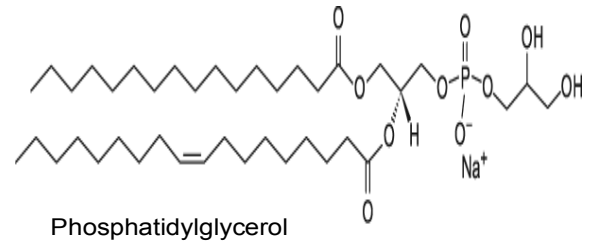
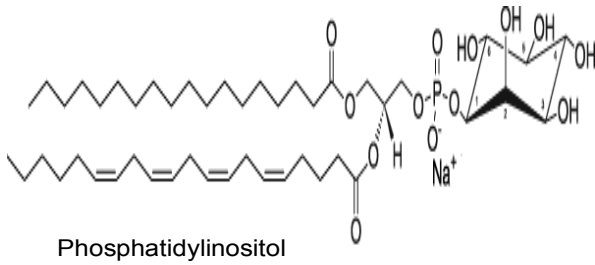
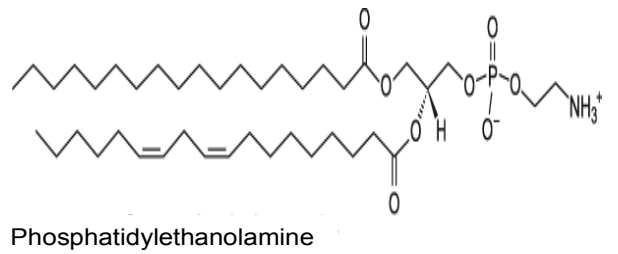
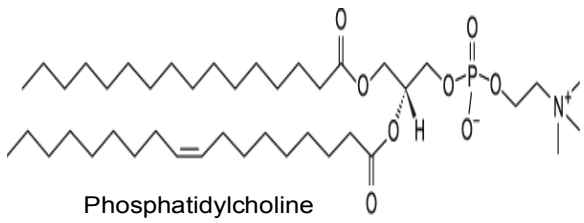


Figure 2. Common types of glycerolipids found in plants

Chapter 2. Initial Characterization of the *NPC* Gene Family in Arabidopsis

Introduction

In plants, there are two types of Phospholipase Cs (PLCs): phosphoinositide specific PLC (PI-PLC) and non-specific PLC (NPC). The hydrolysis of phosphatidylinositol 4,5-bisphosphate [PI(4,5)P₂] by PI-PLC, produces second messengers inositol 1,4,5-triphosphate (IP₃) and diacylglycerol (DAG). In animals IP₃ diffuses into the cytosol where it activates the release of calcium from intracellular stores (Clapham, 1995). DAG remains in the membrane, recruiting and activating certain members of the protein kinase C (PKC) family (Munnik, 2001; Munnik and Testerink, 2009). In plants, PKC, the target of DAG is absent (Munnik and Testerink, 2009). PI-PLC has been studied more extensively in plants and animals than NPC. Phosphatidylcholine hydrolyzing activity by NPC has been reported in rice (Chrastil et al., 1987), spinach leaves (Oursel et al., 1990), brassica seedlings (Nola et al., 1986), oats (Andersson et al. 2005), and ripening tomato (Rouet-Mayer et al., 1995). A signaling role for NPC in plants was first reported by Scherer et al., (2002).

The Arabidopsis genome is predicted to contain six putative NPCs. In order to characterize the NPC gene family, database searches were performed and T-DNA mutant lines were obtained from the Arabidopsis Biological Resource Center (Columbus, OH). The NPC mutant lines were screened under various growth conditions as described below. The mutants showing alterations under defined growth conditions were selected for further characterization.

Results

Chromosomal Location, Predicted Subcellular Localization, and Expression Pattern of the NPCs in Arabidopsis

In Arabidopsis, there are six putative NPC genes that were numerically named *NPC 1-6*, based upon chromosomal location (Figure 1). *NPC1* is located on chromosome I and *NPC2* is located on chromosome II. *NPC3* – *NPC6* are located on chromosome III. *NPC3*, *NPC4* and *NPC5* are located in tandem (Figure 1). These NPCs encode proteins

that are ~60 kDa with 514 – 538 amino acid residues. Amino acid identities between *NPC4* and *NPC5* are 84.7%, *NPC3* and *NPC4* 64.2% and *NPC6* and *NPC3* 52.8%.

Based on prediction using PSORT (<http://wolfsort.org/>), *NPC1* is predicted to be localized in the mitochondria, vacuole and chloroplast. *NPC2* in the vacuole and *NPC3* to the chloroplast and cytosol. *NPC4* and *NPC5* are predicted in the nucleus and cytosol, whereas *NPC6* is in the chloroplast and vacuole. No apparent trans-membrane domains were observed for *NPC1* – *NPC6* using hydropathy plots, suggesting that *NPC1* – *NPC6* are soluble or membrane associated proteins (www.arabidopsis.org/).

Expression patterns of the NPCs using www.genevestigator.com, showed that *NPC1* and *NPC6* were highly expressed in inflorescence, flower, siliques, and leaf tissues. The highest level of expression of *NPC4* was in old leaves followed by roots, callus, and siliques. *NPC3* was highly expressed in roots followed by *NPC1* and *NPC6*. For *NPC2* the highest level of expression was in siliques and inflorescences and the lowest level of expression in old leaves (Figure 2). The expression pattern of *NPC5* was not found in this database possibly due to the high level of sequence identity between *NPC4* and *NPC5*. Expression patterns documented by the Massively Parallel Signature Sequencing Data base (www.mpss.udel.edu/at/GeneAnalysis.php/) showed that *NPC3* and *NPC4* were highly expressed in roots, and *NPC1* and *NPC6* had relatively high expression in floral organs. Relative expression levels of *NPC2* and *NPC5* were too low to garner comparative data. To verify the expression profile obtained from Genevestigator and MPSS, quantitative real-time PCR was performed using tissue from 6-week old Arabidopsis plants. Similar to the genevestigator expression profile, *NPC1* and *NPC6* had the highest level of expression in siliques of the NPCs and *NPC4* highest level of expression was observed in old leaves followed by roots (Figure 3). *NPC3* was also the highest expressed NPC in roots. Of the NPCs, the expression level of *NPC5* was the lowest, with the highest expression observed in inflorescence and old leaves (Figure 3). The *NPC* genes may be functionally distinct, based on the differential patterns of expression in Arabidopsis tissues.

Determination of the Physiological Function of the NPC Gene Family in Arabidopsis

To study the function of the *NPC* gene family in Arabidopsis, T-DNA insertion mutants were obtained from ARBC (Ohio State University). The mutants designated *npc1-1–npc6-1* were confirmed to be homozygous by PCR. The expression pattern of *NPC1–NPC6* under stress conditions was determined by using the Genevestigator database. *NPC4* was highly expressed under phosphate deprivation, drought, low nitrate, heat and late osmotic stress (Figure 4). No induction was observed for the other NPCs under long term phosphate deprivation, but a slight induction of *NPC1*, *NPC2*, and *NPC3* was observed under medium-term (24 and 48h) phosphate deprivation. *NPC1* and *NPC3* were slightly induced by low nitrate and drought (Figure 4). *NPC4*, *NPC2* and *NPC6* were responsive to high light intensity. *NPC4* was the most responsive of the NPCs when subjected to cold stress and treatment with 10 μM ABA for 1h and 3h (Figure 4). Slight induction of *NPC4* and *NPC6* was observed when treated with 5 μM IAA for 2 h. *NPC2* and *NPC6* were sucrose responsive whereas *NPC3* and *NPC4* were slightly responsive to late salt stress in roots (Figure 4).

The *npc* mutants were screened using germination assays and root elongation assays on $\frac{1}{2}$ MS agar plates. All of the NPC mutants germinated at wild-type levels and no differences in the rate of root elongation were observed under normal growth conditions (Figure 5). Based upon the expression data obtained from Genevestigator, the expression of the NPCs was determined by quantitative real-time PCR. Three-day old wild-type seedlings were transferred to plates containing 0 μM or 500 μM phosphate for ten days. Similar to the results obtained from Genevestigator, *NPC4* was the most induced NPC both in roots and shoots under phosphate deprivation. *NPC1* and *NPC3* were induced in shoots whereas *NPC2*, *NPC5*, and *NPC6* were not induced by phosphate deprivation (Figure 6A). Seedlings of wild-type and *npc1-1–npc6-1* were grown on plates containing 0 μM phosphate for 12 days. *npc4-1* and *npc1-1* root elongation and length were similar to wild-type, whereas *npc6-1* was slightly longer and *npc2-1*, *npc3-1* and *npc5-1* were shorter (Figure 6B). For ABA experiments, five-day old NPC mutants and wild type were transferred to agar plates containing 25 μM ABA and the rate of root elongation was

monitored over a twelve-day period. *npc4-1* elongated faster than wild-type and had longer roots than wild-type and the other NPCs. All the other NPCs displayed wild-type sensitivity to ABA treatment (Figure 7).

Gene expression data obtained from Genevestigator showed that *NPC4*, *NPC1* and *NPC3* were responsive to low nitrate and osmotic stress. The NPCs were tested on ½ MS containing 100 mM NaCl and 0.5 mM nitrogen. On plates containing salt, *npc5-1* and *npc1-1* had longer primary roots than wild-type, whereas *npc4-1* and *npc2-1* were more sensitive (Figure 8A). *npc5-1* also had fewer lateral roots than wild-type under salt stress. On 0.5mM nitrogen *npc5-1* grew slightly shorter roots than wild-type and the other NPCs were similar to wild-type (Figure 8B). *NPC4* and *NPC3* were slightly induced after treatment with 5 µM IAA according to Genevestigator, thus the NPCs response was tested using IBA and IAA. Five-day old seedlings were transferred to plates containing 10 µM IBA or 1µM IAA and the primary root length was measured after seven days. All of the *NPCs* showed wild-type sensitivity in response to IBA (Figure 9A), whereas *npc5-1* grew slightly longer roots than wild-type on 1 µM IAA (Figure 9B).

Generation and Screening of Double Mutants

Several double mutants have been generated and screened (Table1). *NPC3*, *NPC4*, and *NPC5* are located in tandem on chromosome III, and thus crosses between those genes are difficult and require extensive screening to generate homozygous lines. The double mutants generated include, *npc2-1npc5-1*, *npc2-1npc3-1*, *npc1-1npc5-1*, *npc3-1npc6-1*, and *npc2-1npc4-1* (Table1). These mutants were tested for their response to cold stress. *npc1-1*, *npc2-1*, *npc6-1*, *npc2-1npc3-1*, and *npc2-1npc4-1* were more sensitive to cold stress than wild-type (Figure 10). Double mutants of *npc1-1npc5-1* and *npc3-1npc6-1* show alterations when subjected to 100 mM NaCl. *npc1-1npc5-1* showed increased primary root growth compared to wild type, whereas the root growth of *npc3-1npc6-1* was inhibited (Figure 11).

The double mutant displaying the most overt phenotype is *npc3-1npc6-1*. Under normal growth conditions, *npc3-1npc6-1* displays distinct morphological differences from wild-

type plants. Seed germination is impaired by 15% compared to wild-type plants; tri-cotyledons or deformed cotyledons occur at a frequency of 10-15% (Figures 12A and 12B); apical dominance is lost earlier than wild-type plants (Figure 12C); and the primary root growth is shorter than wild-type when treated with 1 μ M IAA (Figure 12D). Some aspects of the phenotype described above such as loss of apical dominance might be associated with auxin signaling. Therefore, *npc3-1npc6-1* plants were transformed using DR5-GUS construct in order to determine if there are changes in auxin accumulation. In addition, *npc3-1npc6-1* was complemented using genomic *NPC6*. The phenotype of these plants is yet to be determined.

The effect of ablation of *NPC3* and *NPC6* on lipid content was determined. In rosettes no differences in glycerolipid and phospholipid content was seen for *npc6-1* and *npc3-1npc6-1* compared to wild-type under control and treatment conditions (Figure 13A). However, lower levels of MGDG and DGDG were observed in *npc3-1* rosettes. In roots, under control conditions *npc6-1* contained higher levels of PC compared to wild-type (Figure 13B). Under salt stress conditions in rosettes, the lysophospholipid content was the comparable among wild-type, *npc3-1* and *npc3-1npc6-1*. LysoPC content in *npc6-1* was lower than wild-type levels (Figure 4A). In roots, under salt stress the lysoPC content was higher in *npc3-1npc6-1* compared to wild type. The DAG content was also determined for *npc3-1npc6-1* under salt stress and normal conditions. The level of DAG in *npc3-1npc6-1* rosettes is significantly lower than wild-type under normal growth conditions (Figure 15A). Also of interest is the fact that DAG levels in *npc3-1npc6-1* roots are significantly lower than wild-type plants treated with 100mM NaCl (Figure 15B).

Discussion

Based on the results obtained from the initial characterization of the NPC gene family, the mutants that displayed the most overt phenotypes were selected for further characterization. *NPC4* was selected for characterization in ABA responses and phosphate deprivation since it was highly induced by phosphate deprivation and less sensitive to ABA than the other NPCs. *NPC3* was selected for characterization in

phosphate responses because the roots of *npc3-1* were shorter than wild-type on phosphate-deficient media. *NPC5* was selected for characterization in response to salt stress.

Materials and Methods

Plant Growth and treatment

Seeds were germinated on $\frac{1}{2}$ MS medium supplemented with 1.5% sucrose. Seeds were sterilized in 70% ethanol for 5 min followed by 20% bleach for 3 min and then rinsed three times with sterile distilled water. Sterilized seeds were sown on agar plates and stratified at 4°C for 48 h. Germination was scored after 4 days. For root elongation assays, 5-day old seedlings were transferred to medium containing 25 μ M ABA and grown under cool white fluorescent light of 100 \sim mol $\text{m}^{-1}\text{s}^{-1}$ under 16-h light/ 8-h dark and 23°C/22°C cycles for 2 weeks. For salt stress, nitrogen, phosphorous, IAA, and IBA treatments, plants were grown under cool white fluorescent light of 100 \sim mol $\text{m}^{-1}\text{s}^{-1}$ under 12-h light/ 12-h dark and 23°C/22°C cycles. For cold stress experiments, four-week old plants grown under cool white fluorescent light of 120 \sim mol $\text{m}^{-1}\text{s}^{-1}$ under 12-h light/12-h dark and 23°C/22°C cycles were cold acclimated at 4°C for 48h. Non-acclimated plants were not placed at 4°C for 48h. The temperature was decreased from 23°C at 1°C per hour to -2°C. The temperature of -2°C was maintained for 2h. Ice crystals were placed on the soil to prevent supercooling and the final temperature of -10°C was maintained for 2h. The plants were thawed overnight at 4°C and allowed to recover for 7 days.

Quantitative Real Time PCR

Total RNA was isolated from 6-week old soil grown plants or 2-week old Arabidopsis tissues grown on agar plates containing 0.5 mM or 0 mM phosphate using a rapid CTAB method (Stewart and Via, 1993; Li et al., 2006), and RNA was precipitated using 2M LiCl at 4°C. RNA integrity was checked on 1% (w/v) agarose gel. Eight μ g of total RNA was digested with DNaseI according to manufacturer's instructions (Ambion, Inc.) to remove DNA contamination. The RNA was reverse transcribed using iScript cDNA Synthesis Kit (BIO-Rad, CA). The efficiency of

cDNA synthesis was analyzed by real time PCR amplification of *UBQ10* (At4g05320). The level of gene expression was normalized to that of *UBQ10*. PCR was performed with MyiQ Sequence Detection System (Bio-Rad, CA) using SYBR Green to monitor dsDNA synthesis. Reaction mix contained 7.5 μ l 2xSYBR Green Master Mix reagent Kit (BIO-Rad, CA), 1.0 ng cDNA, and 200 nM of each gene specific primer in a final volume of 15 μ l. The qRT-PCR cycling conditions comprised 90 sec denaturation at 95°C and 50 cycles at 95°C for 30 sec, 55°C for 30 sec, and 72°C for 30 sec, with the final cycle being terminated at 72°C for an additional 10 min. The primers used are *NPC1* -*NPC6* (Table 2).

Lipid Extraction and Phospholipid and DAG Profiling:

The process of lipid extraction, lipid analysis and quantification was performed as described by Welti et al. (2002). Rosettes and roots were excised from 2-week old *Arabidopsis* plants and immersed immediately in 3 mL hot isopropanol containing 0.01% butylated hydroxytoluene at 75°C. Samples were kept at 75°C for 15 min and 1.5 mL of chloroform and 0.6 mL water were added. Samples were placed on a shaker for 1 h, and the solvent was transferred to a new tube. The samples were reextracted using chloroform:methanol (2:1) for at least 4 times for 30 min each on a shaker. The lipid extracts were combined and washed with 1 M KCl followed by washing with 1 mL water. The solvent was dried under a stream of nitrogen gas and the remaining tissue was oven dried at 100°C and weighed. Lipids composition was analyzed by an electrospray ionization triple quadrupole mass spectrometer (API4000). Data was analyzed using Q-test to remove aberrant data points followed by student's t-test to determine significance.

References

1. **Andersson MX, Larsson KE, Tjellstrom H, Liljenberg, Sandelius AS** (2005) the plasma membrane and the tonoplast as major targets for phospholipid to glycolipid replacement and stimulation of phospholipases in the plasma membrane. *JBC* **280**, 27578- 27586.

2. **Chrastil J, Parrish FW.** (1987) Phospholipase C and D in rice grains. *J. Agric. Food Chem.* **35**, 624-627.
3. **Clapham DE.** (1995) Calcium signaling. *Cell* **80**: 259–268.
4. **Scherer GFE, Paul RU, Holk A, Martinec J** (2002) Down-regulation by elicitors of phosphatidylcholine-hydrolyzing phospholipase C and up-regulation of phospholipase A in plants cells. *Biochem. and Biophysical Research Communications.* **293**, 766-770.
5. **Stewart CN Jr, Via LE** (1993) A rapid CTAB DNA isolation technique useful for RAPD fingerprinting and other PCR applications. *Biotechniques* **14**, 748-758
6. **Li M, Qin C, Welti R, Wang X** (2006) Double Knockouts of Phospholipases D ζ 1 and D ζ 2 in Arabidopsis Affect Root Elongation during Phosphate-Limited Growth But Do Not Affect Root Hair Patterning. *Plant Physiol.* **140**, 761-770.
7. **Munnik T.** (2001) Phosphatidic acid: an emerging plant lipid second messenger. *Trends Plant Sci* **6**, 227–33.
8. **Munnik T, Testerink C** (2009) Plant phospholipid signaling: “in a nutshell”. *J Lipid Res* **50**, S260-S265.
9. **Nola L, Mayer AM** (1986) Effect of temperature on glycerol metabolism in membranes and on phospholipase C and D of germinating pea embryos. *Phytochemistry* **25**, 2255-2259.
10. **Oursel A, Grenier G, Tremolieres A** (1990) Isolation and assays of purification of one soluble phospholipase C from spinach. *Plant Lipid Biochem, Structure and Utilization*, Quinn, P.J. and Harwood, J.L., EDs, Portland Press, London, 316-318.
11. **Rouet-Mayer MA, Valentova O, Simond-Cote E, Daussan J, Thevenot C** (1995) Critical analysis of phospholipid hydrolyzing activities in ripening tomato fruits. Study by spectrofluorimetry and high-performance liquid chromatography. *Lipids* **30**, 739-746.
12. **Welti R, Li W, Li M, Sang Y, Biesiada H, Zhou HE, Rajashekar CB, Williams TD, Wang X** (2002) Profiling membrane lipids in plant stress response. Role of phospholipase D in freezing-induced lipid changes in Arabidopsis. *J Biol Chem* **277**, 31994-32002

Database or websites used:

www.mpss.udel.edu/at/GeneAnalysis.php/

www.genevestigator.com

<http://wolfpsort.org/>

www.arabidopsis.org

www.ncbi.nlm.nih.gov

Figure Legends

Figure 1. Chromosomal location of the NPCs in Arabidopsis.

Figure 2. Expression patterns of *NPC1*, *NPC2*, *NPC3*, *NPC4* and *NPC6* in Arabidopsis tissues as documented by Genevestigator (www.genevestigator.com).

Figure 3. Expression patterns of *NPC1-NPC6* using q-RT-PCR.

Tissues from six-week old Arabidopsis plants were harvested and level of expression was quantified based on the expression level of *UBQ10*. Values are means \pm SD, n = 3 discrete samples.

Figure 4. Expression pattern of *NPC1*, *NPC2*, *NPC3*, *NPC4* and *NPC6* in Arabidopsis tissues in response to stimuli from Genevestigator (www.genevestigator.com).

Figure 5. Germination and root elongation of the NPC mutants.

(A) Germination of the NPC mutants on $\frac{1}{2}$ MS media. Seeds were sown on $\frac{1}{2}$ MS plates and stratified at 4°C for 48 h. Germination was scored four days later. 100 seeds per genotype were sown. Values are means \pm SD (n=3).

(B) Root elongation of the *npc* mutants on ½ MS media. Five-day old seedlings were transferred to vertical plates and the rate of root elongation was monitored for 8 days. Values are means ± SD (n=15).

Figure 6. Expression and root elongation of the NPCs under phosphate starvation.

(A) Expression level of the *NPCs* under phosphate starvation. Tissues from two-week old Arabidopsis plants were harvested and level of expression was quantified based on the expression level of *UBQ10*. Values are means ± SD, n = 3 discrete samples.

(B) Root elongation of the *NPCs* under phosphate starvation. Five-day old seedlings were transferred to plates containing 0 µM phosphate. Values are means ± SD (n=15).

Figure 7. Response of the *NPCs* to ABA.

(A) The rate of root elongation of wild-type and *npc1-1* to *npc6-1* on 25 µM ABA. Five-day old seedlings were transferred to ABA media and the primary root growth was monitored for 12 days. Values are means ± SD (n=15).

(B) Pictures of wild-type and *npc1-1-npc6-1* on 25 µM ABA. Pictures were taken at the end of the experiment.

Figure 8. Response of the *NPCs* to salt stress and low nitrogen.

(A) Root length of wild-type and *npc1-1* to *npc6-1* on 100 mM NaCl. Five-day old seedlings were transferred to 100 mM NaCl and the primary root was measured after 10 days. Values are means ± SD (n=15).

(B) The rate of root elongation of wild-type and *npc1-1* to *npc6-1* on 500 µM nitrogen. Five-day old seedlings were transferred to low nitrogen media and the primary root growth was monitored for 8 days. Values are means ± SD (n=15).

Figure 9. Response of the *NPCs* to IBA and IAA.

(A) Root length of wild-type and *npc1-1-npc6-1* on 10 μ M IBA. Five-day old seedlings were transferred to IBA plates and the primary root was measured after 7 days. Values are means \pm SD (n=15).

(B) Root length of wild-type and *npc1-1-npc6-1* on 1 μ M IAA. Five-day old seedlings were transferred to IAA media and the primary root growth was measured on day 7. Values are means \pm SD (n=15).

Figure 10. Freezing tolerance of double mutants and corresponding single mutants.

Four-week old plants were cold acclimated at 4°C for 48h. Non-acclimated plants were not placed at 4°C for 48h. The temperature was decreased from 23°C at 1°C per hour to -2°C. The temperature was maintained at -2°C for 2h. Ice crystals were placed on the soil to prevent supercooling and the final temperature of -10°C was maintained for 2h. The plants were thawed overnight at 4°C and allowed to recover for 7 days. Pictures were taken after recovery.

Figure 11. Response of *npc1-1npc5-1* and *npc3-1npc6-1* to salt stress.

(A) Picture of wild-type, *npc3-1*, *npc6-1* and *npc3-1npc6-1* on $\frac{1}{2}$ MS media. Picture was taken ten days after seedlings were transferred.

(B) Picture of wild-type, *npc3-1*, *npc6-1* and *npc3-1npc6-1* on 100 mM NaCl. Picture was taken ten days after seedlings were transferred.

(C) Picture of wild-type, *npc1-1*, *npc5-1* and *npc1-1npc5-1* on $\frac{1}{2}$ MS media. Picture was taken ten days after seedlings were transferred.

(D) Picture of wild-type, *npc1-1*, *npc5-1* and *npc1-1npc5-1* on 100 mM NaCl. Picture was taken ten days after seedlings were transferred.

Figure 12. Germination and growth phenotype of *npc3-1npc6-1*.

(A) Seedling phenotype of *npc3-1npc6-1*. Seeds of wild-type, *npc3-1*, *npc6-1* and *npc3-1npc6-1* were germinated on $\frac{1}{2}$ MS. Pictures were taken five days after sowing the seeds.

(B) Quantification of germination of wild-type, *npc3-1*, *npc6-1* and *npc3-1npc6-1*. Seeds were sown on ½ MS plates and stratified at 4°C for 48 h. Germination was scored four days later. 100 seeds per genotype were sown. Values are means ± SD (n=3).

(C) The apical dominance phenotype of *npc3-1npc6-1*. Wild-type and *npc3-1npc6-1* plants were grown under cool white fluorescent light of 120 ~mol m⁻¹s⁻¹ under 12-h light/12-h dark and 23°C/22°C cycles. Plants were six weeks old when the picture was taken.

(D) Root growth of wild-type, *npc3-1*, *npc6-1*, *npc3-1npc6-1*, *NPC3-OE*, and *NPC6-OE*. Five-day old seedlings were transferred to media containing 50 nM IAA and pictures were taken two weeks later.

Figure 13. Lipid changes in *NPC3* and *NPC6* altered plants.

(A) Lipid composition in rosettes in the presence of 0 mM or 100 mM NaCl. Five-day old seedlings were transferred to media containing 0 mM or 100 mM NaCl and rosettes were harvested after 10 days. Lipids were extracted and analyzed by ESI/MS/MS. Values are means ± SE (n=5).

(B) Lipid composition in roots in the presence of 0 mM or 100 mM NaCl. Five-day old seedlings were transferred to media containing 0 mM or 100 mM NaCl and roots were harvested after 10 days. Lipids were extracted and analyzed by ESI/MS/MS. Values are means ± SE (n=5).

Figure 14. Total lysophospholipid content of wild-type, *npc3-1*, *npc6-1*, and *npc3-1npc6-1* under control and treatment conditions.

(A) Lysophospholipid composition in rosettes in the presence of 0 mM or 100 mM NaCl. Five-day old seedlings were transferred to media containing 0 mM or 100 mM NaCl and rosettes were harvested after 10 days. Lipids were extracted and analyzed by ESI/MS/MS. Values are means ± SE (n=5).

(B) Lysophospholipid composition in roots in the presence of 0 mM or 100 mM NaCl. Five-day old seedlings were transferred to media containing 0 mM or 100 mM NaCl and roots were harvested after 10 days. Lipids were extracted and analyzed by ESI/MS/MS.

Values are means \pm SE (n=5). * Indicates that the difference between wild type and mutant is significant ($p < 0.05$) as determined by student's t- test.

Figure 15. DAG content in *NPC3* and *NPC6* altered plants.

(A) DAG content in rosettes in the presence of 0 mM or 100 mM NaCl. Five-day old seedlings were transferred to media containing 0 mM or 100 mM NaCl and rosettes were harvested after 10 days. Lipids were extracted and analyzed by ESI/MS/MS. Values are means \pm SE (n=5).

(B) DAG content in roots in the presence of 0 mM or 100 mM NaCl. Five-day old seedlings were transferred to media containing 0 mM or 100 mM NaCl and roots were harvested after 10 days. Lipids were extracted and analyzed by ESI/MS/MS. Values are means \pm SE (n=5). * Indicates that the difference between wild type and mutant is significant ($p < 0.05$) as determined by student's t- test.

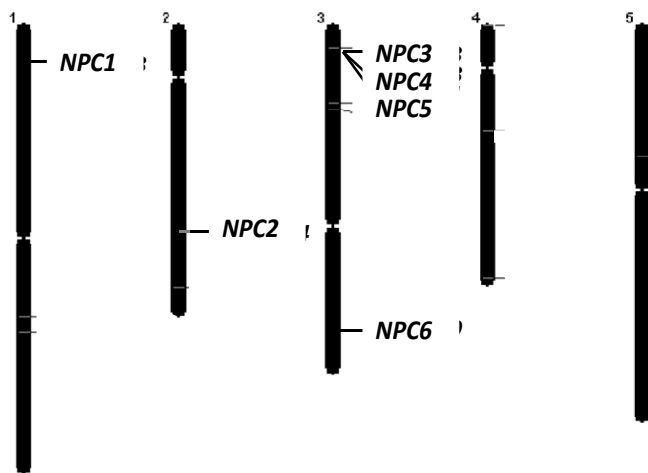


Figure 1

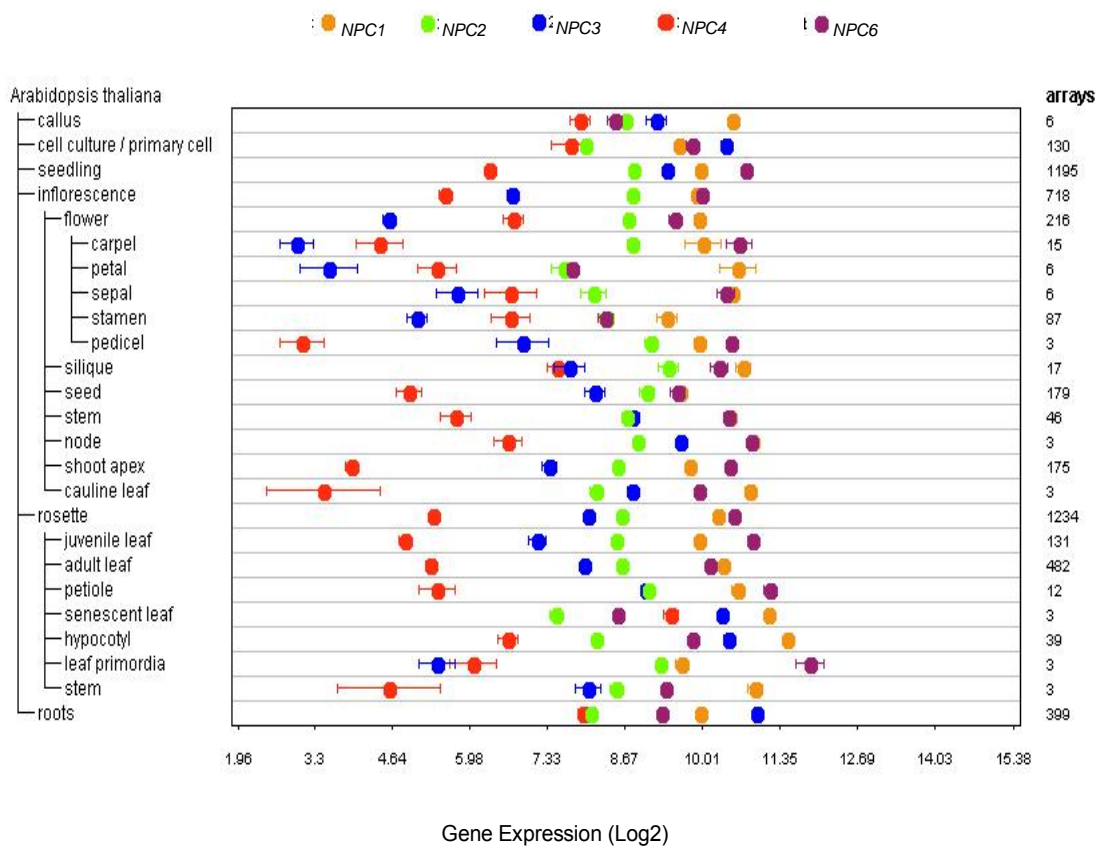


Figure 2

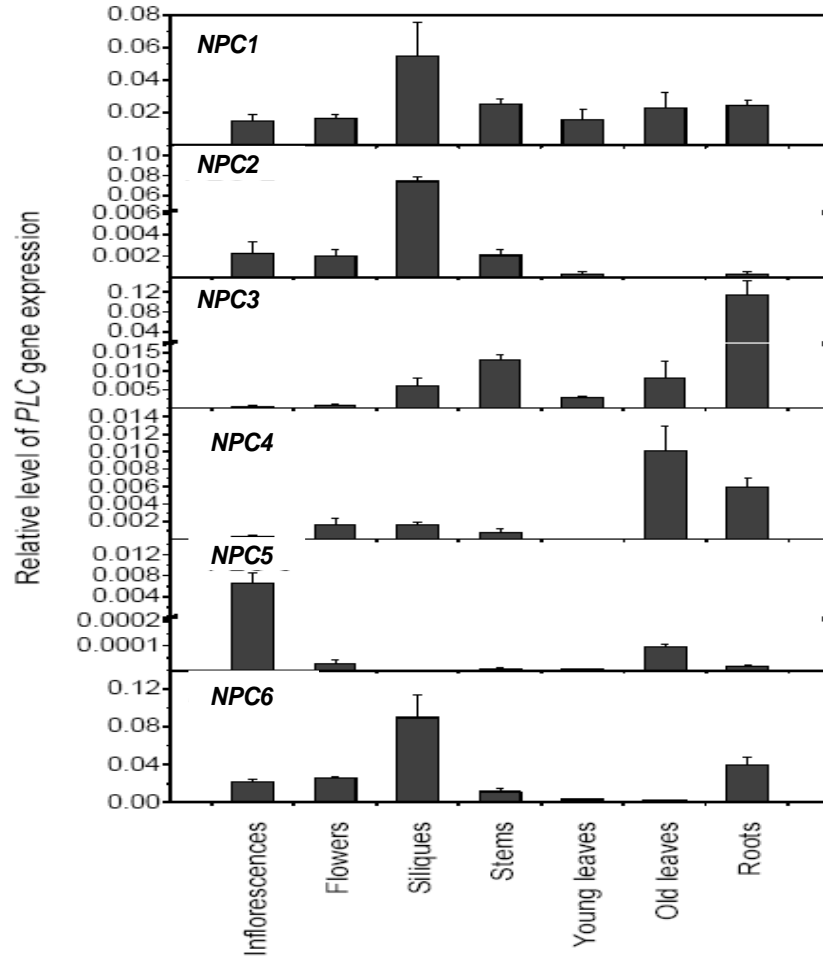


Figure 3

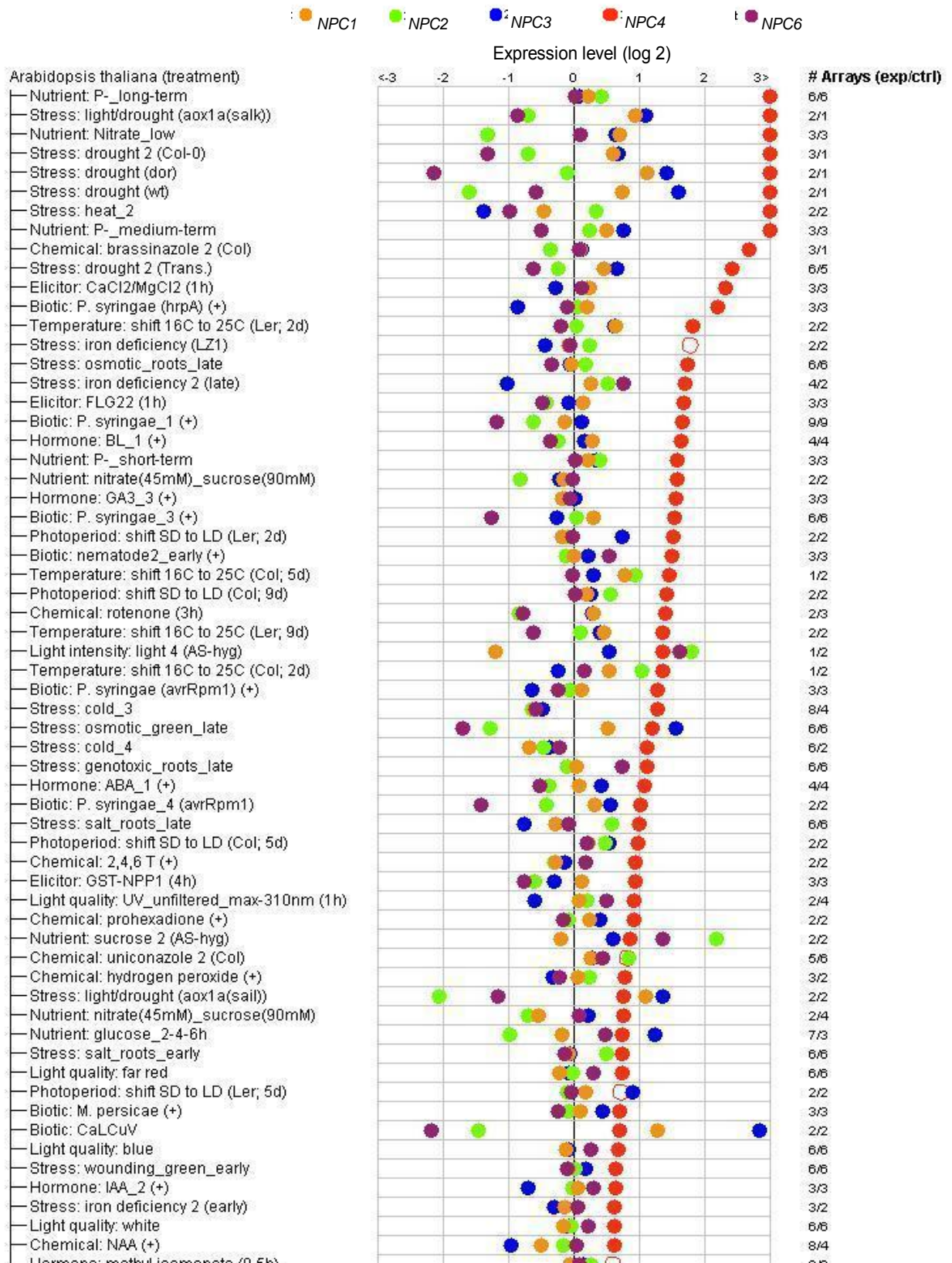


Figure 4

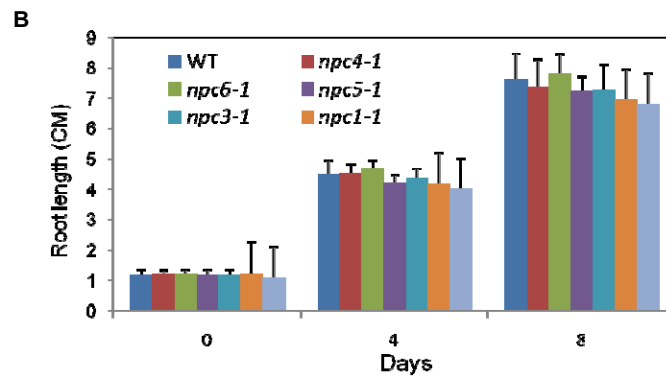
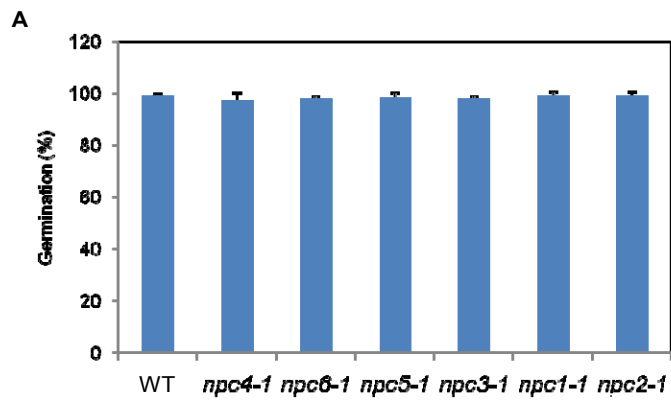


Figure 5

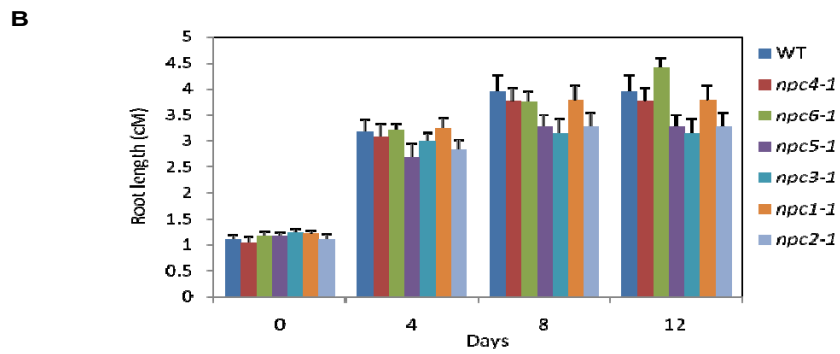
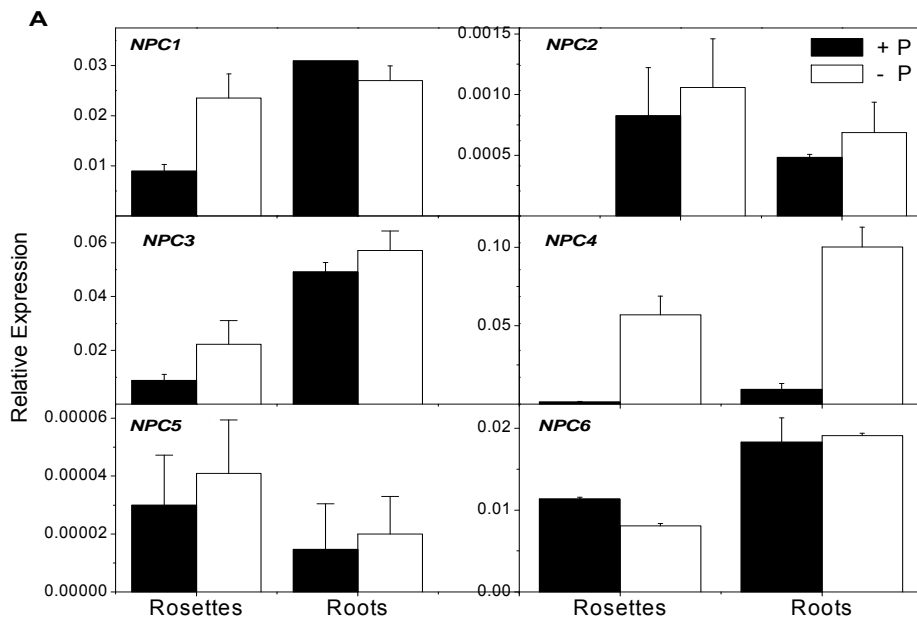
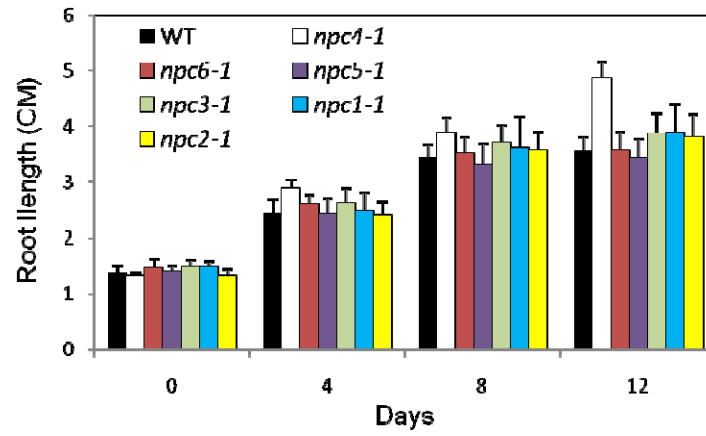


Figure 6

A



B

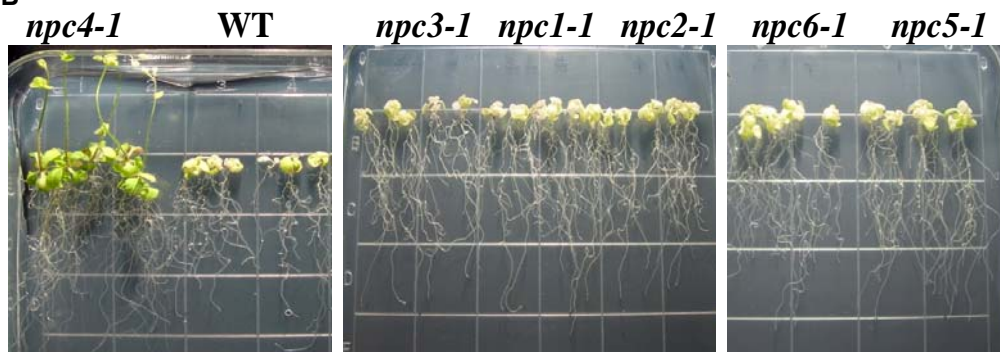


Figure 7

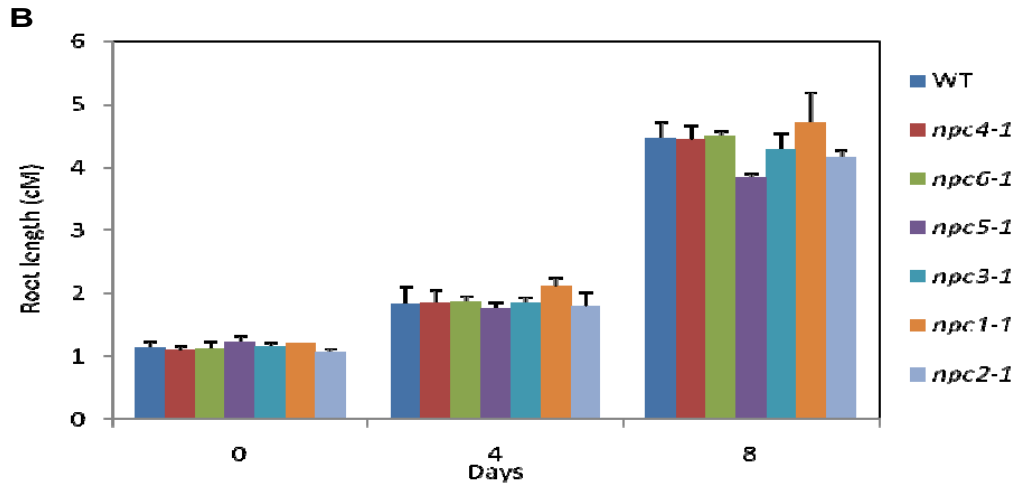
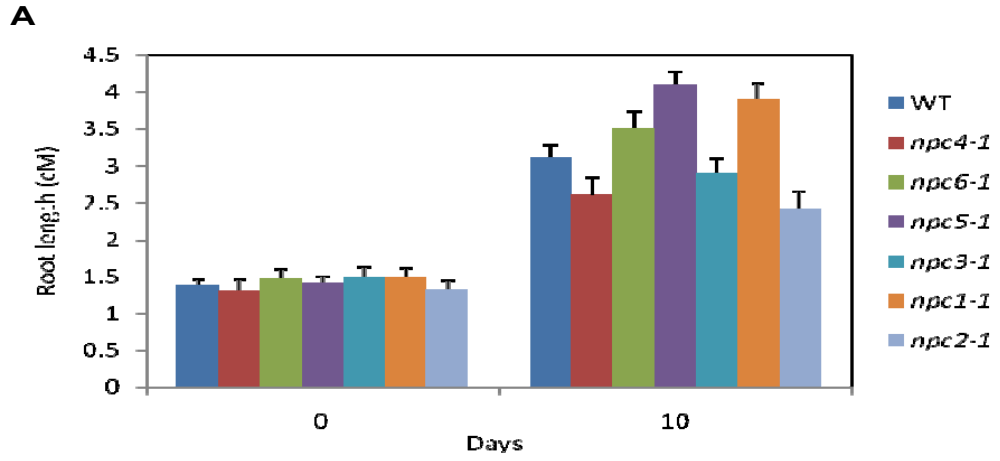
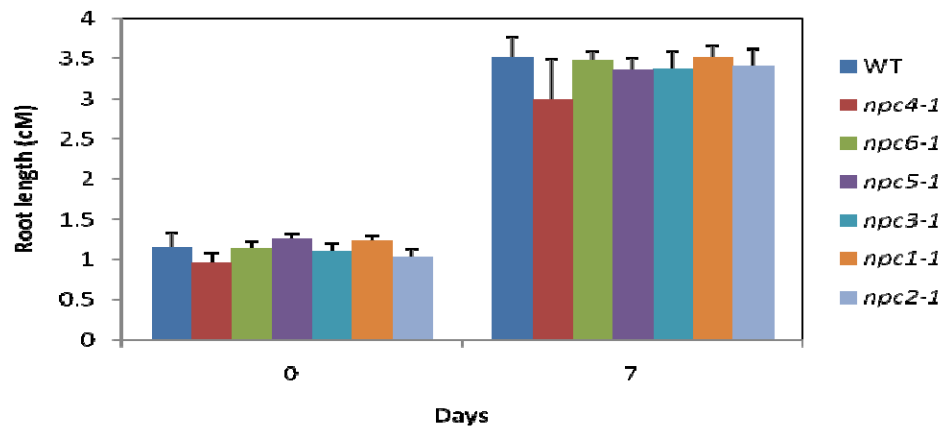


Figure 8

A



B

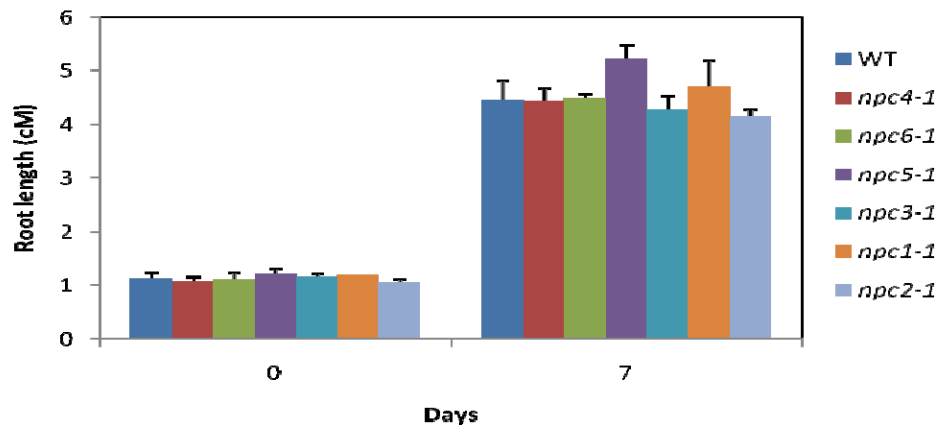


Figure 9

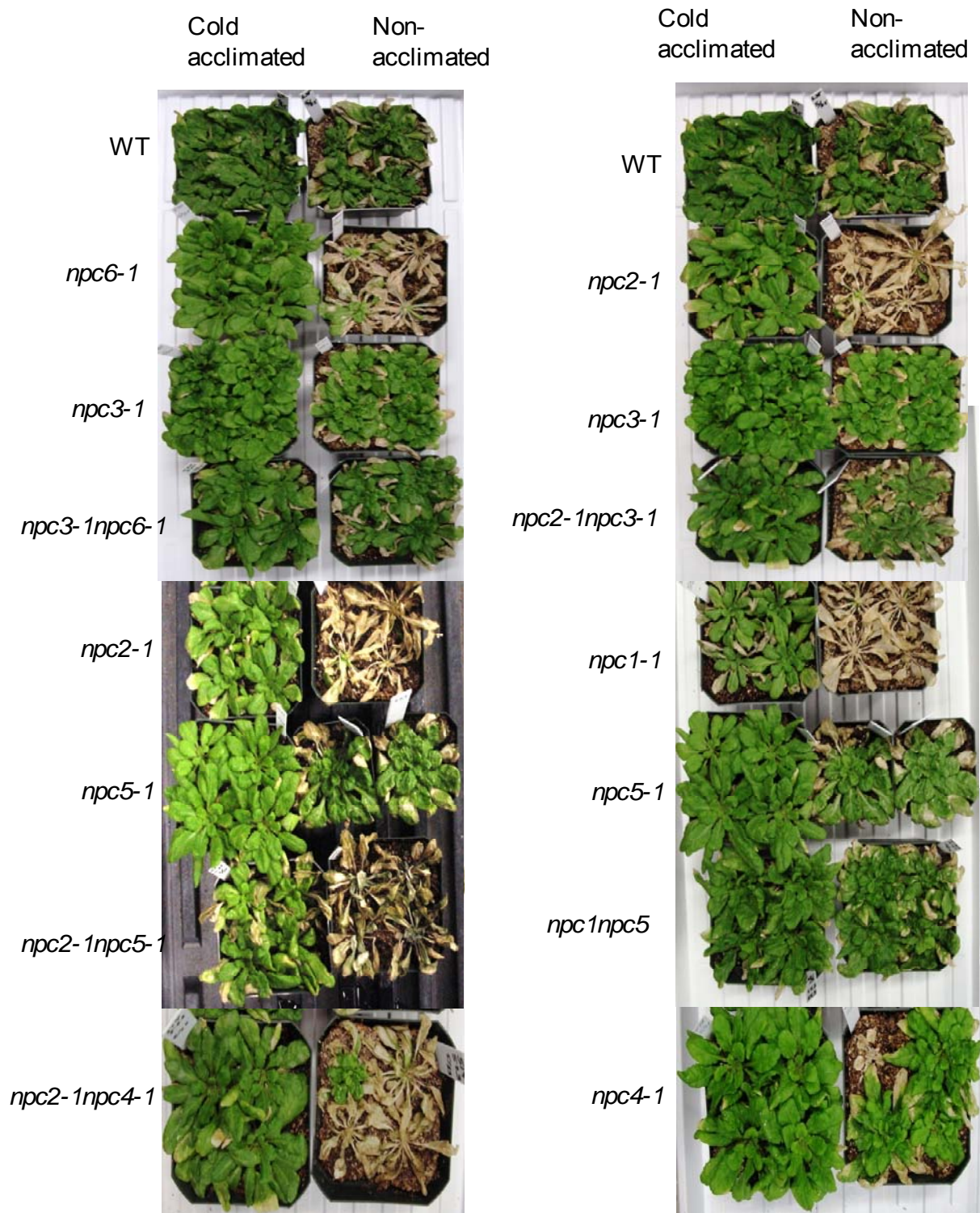


Figure 10

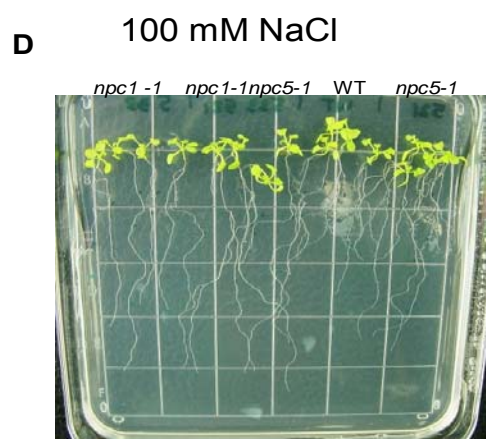
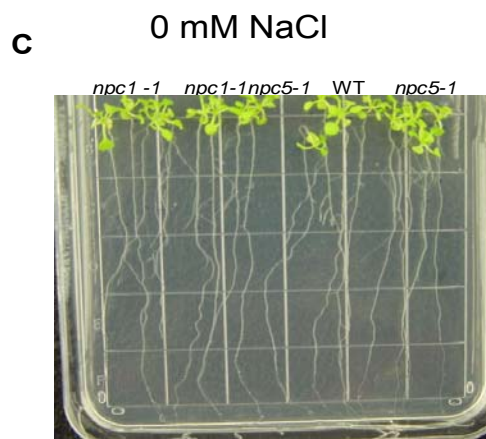
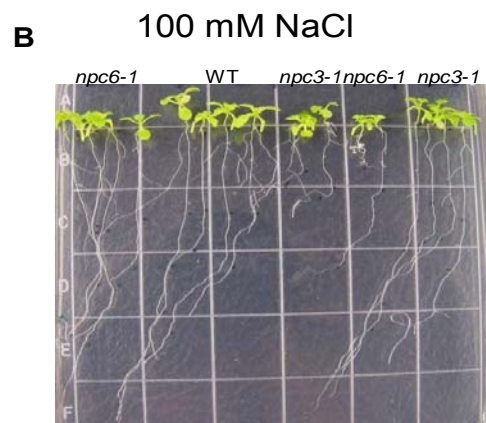
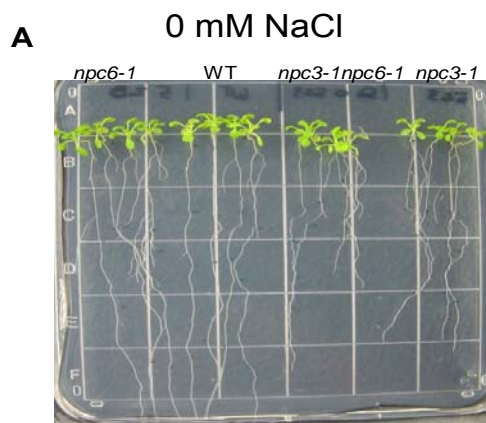


Figure 11

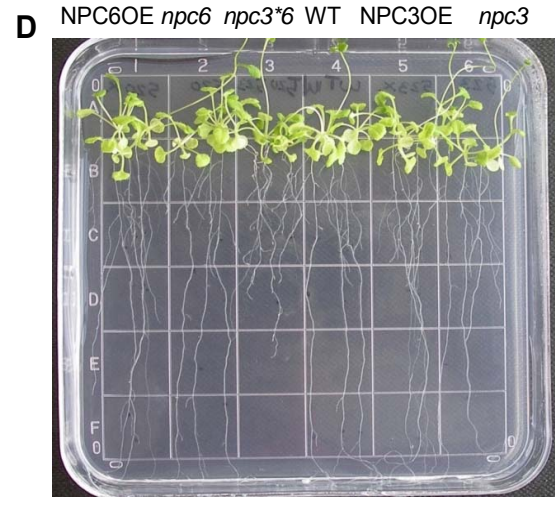
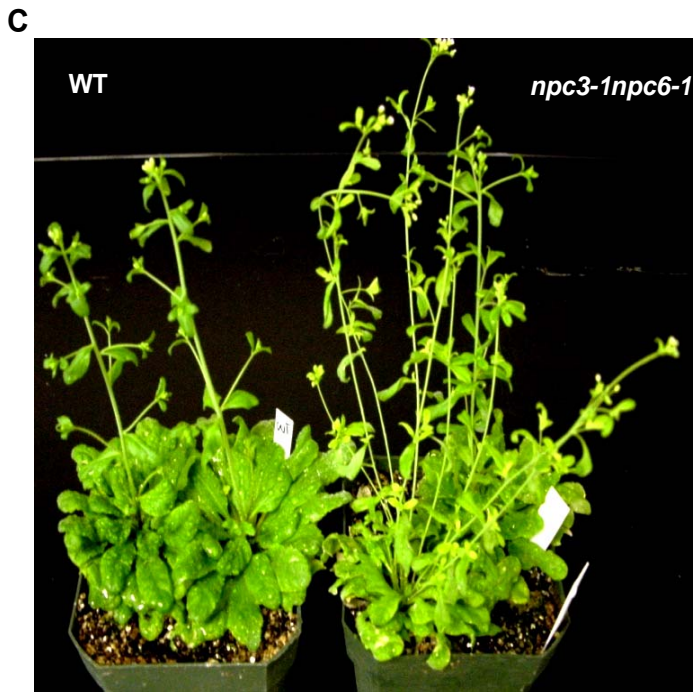
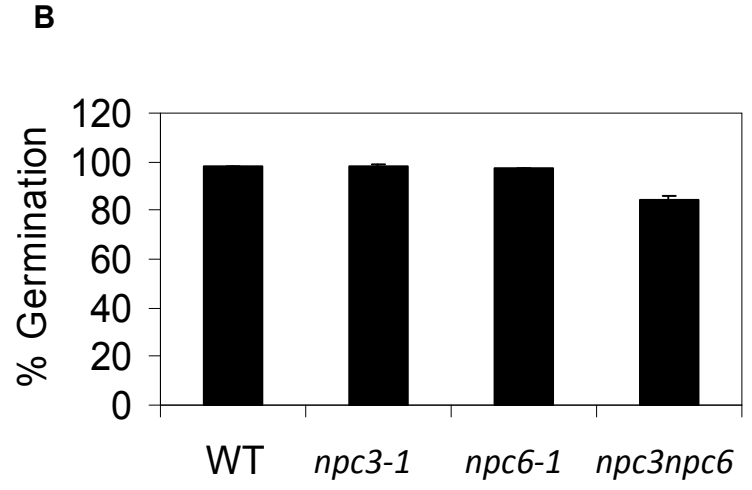
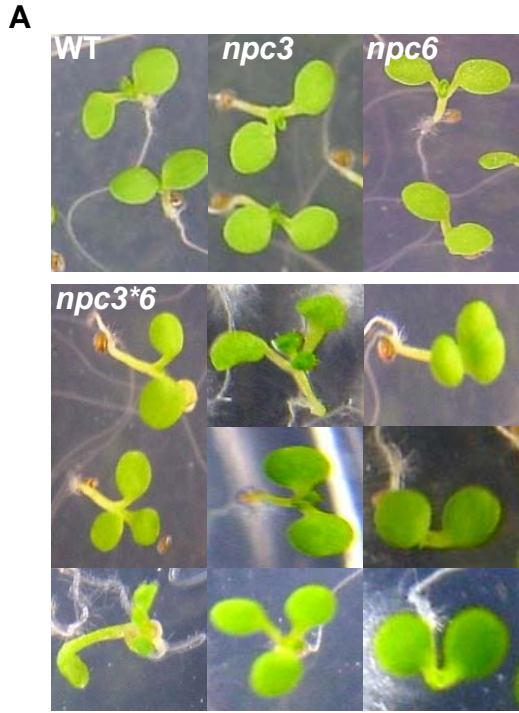


Figure 12

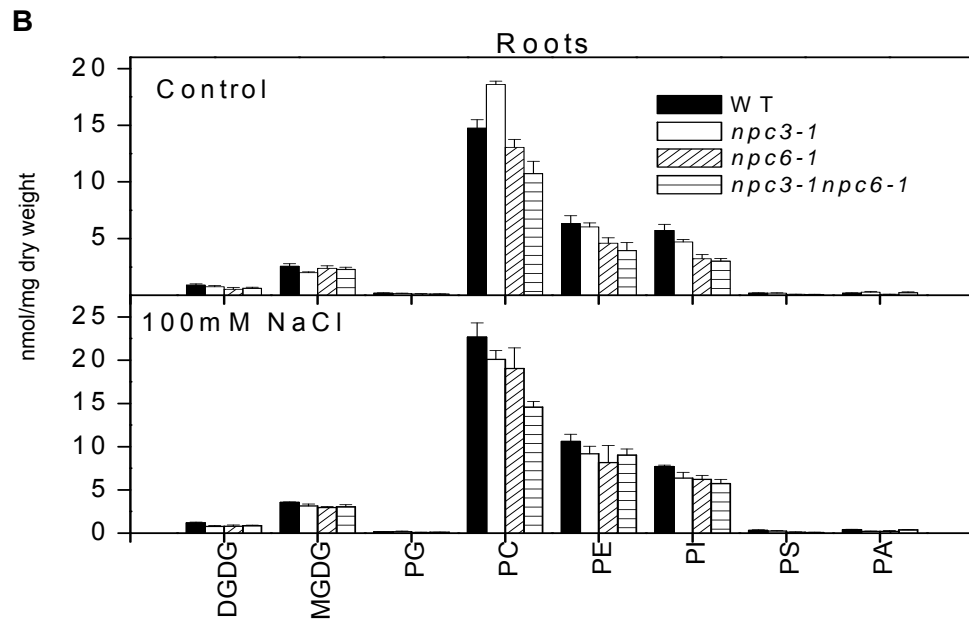
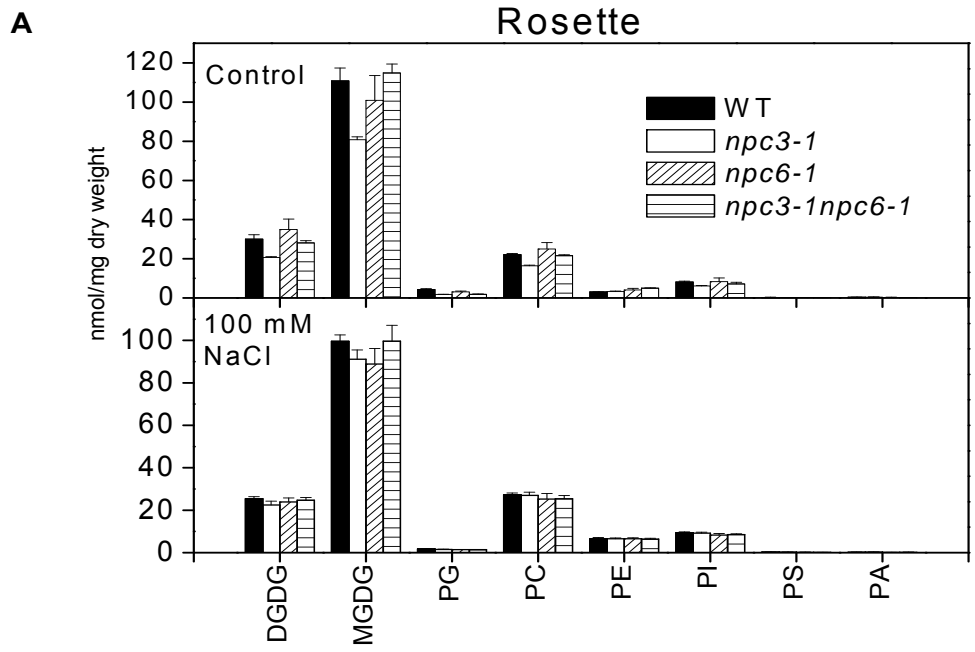


Figure 13

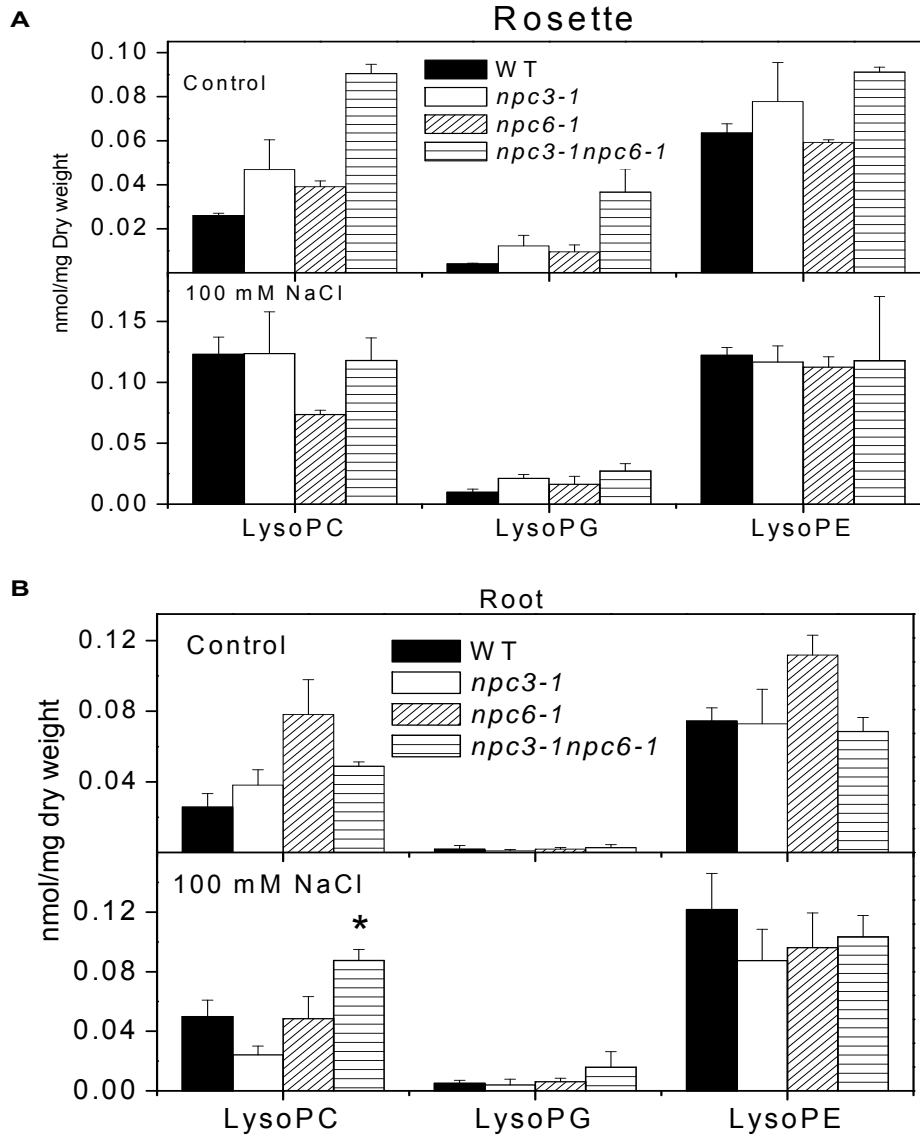


Figure 14

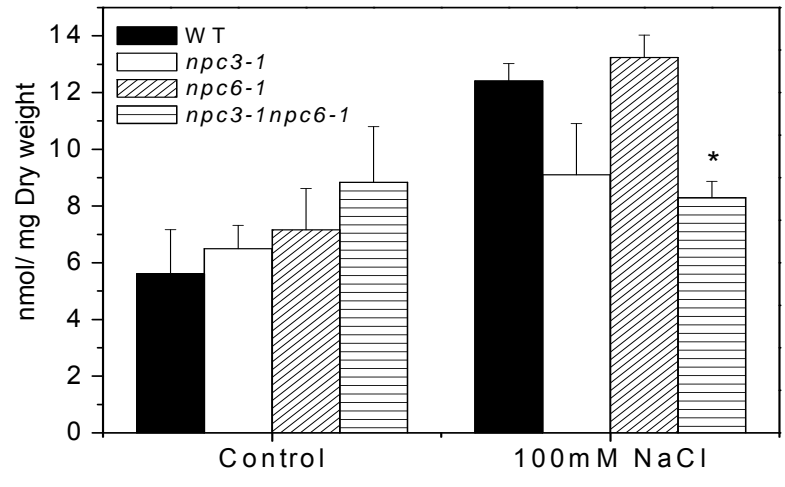
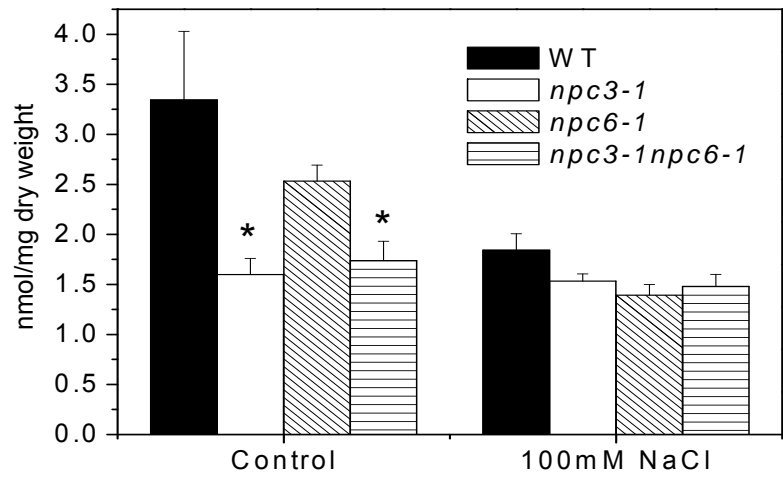


Figure 15

Table 1. Genetic alterations and phenotypes of the NPC mutants

<i>Gene</i>	<i>Gene locus</i>	Designated Name	Stress Phenotype	Lipid Change
NPCs	At1g07230	<i>NPC1</i>	Less freeze tolerant	
	At2g26870	<i>NPC2</i>	Less freeze tolerant, increase of lateral roots under salt stress	
	At3g03520	<i>NPC3</i>	Increased sensitivity of primary roots to NaCl, decreased germination on 200mM NaCl	Lower levels of DAG in rosette
	At3g03530	<i>NPC4</i>	Decreased sensitivity to ABA, increased sensitivity to NaCl (Germination and primary root) and drought	Higher levels of PA, lysoPC, PS
	At3g03540	<i>NPC5</i>	No lateral roots under 75 mM NaCl in KO, but OE increases lateral roots. Reduced germination under 200mM salt.	more PC; less DAG
	At3g48610	NPC6	Reduced lateral root under salt stress, less freeze tolerance	Lower DGDG in rosettes and DAG in roots under phosphate starvation.
		<i>NPC6*<i>NPC3</i></i>	Loss of apical dominance, reduced seed germination, defective seedling growth, increased sensitivity to salt stress.	Less DAG in rosettes, less DAG in roots under salt stress and phosphate deprivation. Reduced DGDG in roots under phosphate starvation.
		<i>NPC2*<i>NPC5</i></i>	Less freeze tolerant	
		<i>NPC2*<i>NPC6</i></i>	Less freeze tolerant	
		<i>NPC6*<i>NPC5</i></i>	Reduced lateral root under salt stress and increased tolerance of primary root under salt stress	
		<i>NPC1*<i>NPC5</i></i>	Reduced sensitivity to auxin and increased salt tolerance	
		<i>NPC2*<i>NPC4</i></i>	Less freeze tolerant	

Table 2. List of Primers

	Gene	Primer Sequence
Real time PCR	<i>NPC1</i>	Forward 5'-ATATGTGCCCTCTGCATGTACCCA-3' Reverse 5'-ATGGAGGCCATACCCGACAATCAT-3'
	<i>NPC2</i>	Forward 5'-AGAGCTTGTACAACCTAGCTGCGGT-3' Reverse 5'-AGCCATACGACCAGCCTCTAAGAA-3'
	<i>NPC3</i>	Forward 5'-CTGATTCAAGCAGCGGCTGTACTA-3' Reverse 5'-AGCCTTCTTGGACTCACCATGGAA-3'
	<i>NPC4</i>	Forward 5'-AGCATCAAATGCTGCTGCTCAACC-3' Reverse 5'-TCCACCCACACACAAGAGAAGTGA-3'
	<i>NPC5</i>	Forward 5'-GGAGACTACAAAAACGAAGAATTGCTAT-3' Reverse 5'-GTGATGGTGGTGGTTTCACAACATTAT-3'
	<i>NPC6</i>	Forward 5'-GCGGTTCTCAATGGTGATCACTTCCT-3' Reverse 5'-GGCACCAAGCTTCATTGCCTCTTTAC-3'

Chapter 3. Non-Specific Phospholipase C NPC4 is Involved in Phosphate Deprivation and Promotes Arabidopsis Response to Abscisic Acid and Tolerance to Hyperosmotic Stress

ABSTRACT

Diacylglycerol (DAG) is an important class of lipid messengers in animal systems, but its function in plants remains elusive. Here we show that knockout of the non-specific phospholipase C (NPC), NPC4, results in a decrease in DAG levels and compromises plant response to abscisic acid (ABA) and hyperosmotic stress response. *NPC4* is also highly induced by phosphate deprivation, but does not affect the metabolism of major membrane phospholipids. NPC4 hydrolyzes common membrane in a calcium-independent manner with distinguishable substrate preferences, producing DAG and a phosphorylated head group. *NPC4-KO* plants display reduced sensitivity to ABA-mediated stomata movement, seed germination, and root elongation, whereas *NPC4-OE* plants have increased sensitivities. In contrast, *NPC4-KO* plants display increased sensitivities to salinity and water deficiency, whereas *NPC4-OE* plants display increased tolerance and biomass production. The expression of ABA responsive genes is lower in *NPC4-KO* than wild-type plants. The addition of DAG or PA restores the ABA response of *NPC4-KO* to that of wild-type, and the addition of a DAG kinase inhibitor (DGK11) does not rescue *npc4-1* phenotype. These data suggest that *NPC4* positively modulates ABA signaling through its lipid product DAG that is converted to PA and *NPC4* promotes plant growth under osmotic stress.

INTRODUCTION

Drought and salinity are the two crucial environmental factors that limit plant growth, productivity, and geographic distribution. In many regions drought is the limiting factor for crop harvest, and nearly one-fifth of irrigated land worldwide is affected by high salinity stress (Szaboles, 1997). Drought and salinity both cause hyperosmotic stress and limit water availability. Great progress is being made towards understanding the abiotic stress signaling pathways, but little is known about the process by which hyperosmotic

stress is sensed at cell membranes and transduced into physiological responses (Chinnusamy et al., 2004; Fujita et al., 2006).

Cell membranes play key roles in stress perception and signal transduction. In addition to being the initial site of cellular encounter of the stress cues, many subsequent steps in signaling cascades, such as activation of effector proteins, generation of second messengers, and alteration in cellular metabolism, are associated with membranes. Whereas proteins have been the focus of most research on membrane-associated signaling events, recent advances have made it evident that membrane lipids and their derivatives are important players in the signaling network of plant responses to stress, including drought and salinity. Increasing evidence indicate that membrane lipids are rich sources for signaling messengers in plant response to hyperosmotic stresses (Wang, 2004; Testerink and Munnik 2005; Wang et al., 2006). Specifically, phosphatidic acid (PA) is produced rapidly in response to hyperosmotic stress.

Cellular PA may be produced by multiple enzymes, and available data suggest that two principal routes that produce signaling PA are by phospholipase D (PLD) and by phospholipase C (PLC) followed by diacylglycerol kinase (DGK). Multiple PLDs have been described in various plant species and several of them, PLD α 3, ϵ , δ , and, α 1, have been shown recently to contribute to hyperosmotic stress-induced PA production and affect plant response to hyperosmotic stress (Hong et al., 2008). In addition to PLD, PLC, which hydrolyzes phospholipids to produce DAG and a phosphorylated head group, has also been found to contribute to PA formation. In several cases, PLD and PLC/DGK reactions are activated differentially in response to different stimuli (den Hartog et al., 2003; Zonia and Munnik, 2004).

There are two distinctly different families of PLC: PI-PLC that uses primarily phosphoinositides, and nonspecific PLC (NPC) uses common membrane phospholipids, such as phosphatidylcholine (PC) and phosphatidylethanolamine (PE). The signaling function of PI-PLC has been well established in animals. PLC hydrolysis of phosphatidylinositol 4,5-bisphosphate (PI $_4$,5)P $_2$ releases two potent second messengers,

inositol 1,4,5-trisphosphate (IP₃) and DAG. DAG remains in the membrane and activates certain members of the protein kinase C (PKC) family. DAG is removed from the signaling pathway through phosphorylation to phosphatidic acid (PA) by DAG kinase (DGK). The Arabidopsis genome contains nine putative PI-PLCs that exhibit calcium dependent hydrolysis of PI(4,5)P₂ with the exception of AtPLC8 and AtPLC9. Members of the PI-PLC family have been implicated in ABA signaling, salt and drought stress (Hirayama et al., 1995). In plants, there is no evidence for the existence of any members of the PKC family; therefore the role of DAG as a signaling molecule remains to be determined (Munnik, 2001). An earlier study indicated that addition of DAG activates ion pumping in patch-clamped guard cell protoplasts and opening of intact stomata in *Vicia faba* (Lee and Assmann, 1991). Later studies suggest that DAG produced via the PLC pathway is rapidly converted to PA (Munnik et al., 1998b), and it has been proposed that PLC-derived DAG makes a strong contribution to PA synthesis during osmotic stress (Munnik et al., 2000).

Unlike PI-PLC, NPCs hydrolyze common membrane lipids such as PC and PE in a calcium-independent manner (Nakamura et al., 2005). NPCs share sequence similarity with bacterial PC-PLC and the Arabidopsis genome is predicted to contain six putative NPC genes designated *NPC-1-6*. Genome wide transcriptional analysis showed that *NPC4* is greatly induced by phosphate deprivation (Mission et al., 2005). Cloning and characterization of *NPC4* in Arabidopsis confirmed that *NPC4* is a functional phospholipase. However, it is not a major player in supplying phosphate to roots during times of low phosphate availability (Nakamura et al., 2005). *NPC5* is also induced by phosphate deprivation and is critical for phospholipid degradation and DGDG accumulation in Arabidopsis leaves (Gauze et al., 2008). Based on the high level of induction of *NPC4* under phosphate deprived conditions, we quantitatively profiled the membrane lipids of *npc4-1* under phosphate limited conditions. We found that minor phospholipids such as PA, PS and lysoPC were altered in KO Plants. Additionally, there are still no reports of the participation of NPCs in response to other abiotic stresses and hormone signaling. Hence, we tested the mutant under various abiotic and hormone stresses. We found that *NPC4* is involved in ABA mediated responses.

RESULTS

Expression Pattern and Subcellular Localization of NPC4

The tissue expression of *NPC4* was determined by quantitative real-time PCR using RNA from 6-week old Arabidopsis plants. The highest level of expression was detected in mature leaves and roots. The expression level between flowers and siliques was similar and expression levels between stems and buds were similar. No expression was detected in young leaves (Figure 1A). To measure *NPC4* expression in response to phosphate deprivation, three-day old seedlings were transferred from ½ MS to media containing 500 or 0 µM phosphate and grown for 10 days. The basal level of *NPC4* expression was low both in the roots and shoots under phosphate sufficient conditions; the expression level in roots was ~6 fold greater than shoots under control conditions. Phosphate deprivation resulted in strong induction of *NPC4* both in roots and shoots; ~40 fold induction in shoots and a ~10 fold induction in roots were observed under phosphate deprivation (Figure 1B). These data are consistent with earlier reports that *NPC4* expression was strongly induced by phosphate deficiency (Mission et al., 2005; Nakamura et al., 2005).

To determine the subcellular localization of NPC4, the cDNA of *NPC4* was C-terminally and N-terminally fused with green fluorescence protein (GFP) and transiently expressed in tobacco leaves. After 48 h, the tobacco leaves were analyzed by confocal microscopy. NPC4 localized to the plasma membrane (Figure 1C) (Nakamura et al., 2005; Gaude et al., 2008). Localization of NPC4 differed from NPC2-GFP. A diffuse intracellular fluorescence pattern for NPC2 is in agreement with its predicted cytosolic localization.

NPC4 Hydrolyzes Minor Membrane Phospholipids under Phosphate Deprivation

A T-DNA insertion mutant of *NPC4*, *npc4-1* (SALK_046713), was obtained from the Arabidopsis Biological Resource Center (Columbus, OH) and homozygous *npc4-1* was isolated (Figures 2A, 2B). The T-DNA insert ablated *NPC4* expression as verified by real-time PCR (Figure 2C). The *npc4-1* seedlings grew and developed normally under control and phosphate deprived growth conditions. Since *NPC4* is greatly induced by phosphate deprivation we quantitatively profiled the glycerophospholipids and

galactolipids of wild-type and *npc4-1* using ESI-MS/MS. Under control conditions and phosphate deprivation no significant differences were seen among the lipid composition of major phospholipids and galactolipids between wild-type and *npc4-1* roots and rosettes (Figures 2D and 2E). These results are consistent with previous studies showing that NPC4 is not a major player in phospholipid degradation and DGDG accumulation under phosphate starved conditions (Nakamura et al., 2005; Gaude et al., 2008). However, under control conditions *npc4-1* had higher levels of total PA than wild-type roots (Figure 2F). Under phosphate deprived conditions *npc4-1* had higher levels of PA, PS, and lysoPC compared to wild-type roots (Figure 2F). Molecular species 34:2, 36:4 and 36:5 PA were higher in *npc4-1* compared to wild-type roots under phosphate starved conditions. LysoPC molecular species 16:0, 18:1, and 18:3 and PS 34:3 and 42:3 were also higher in *npc4-1* roots than wild-type (Figure 2F).

The elevated levels of lysoPC, PA, and PS in *npc4-1* roots prompted us to investigate whether NPC4 uses these phospholipids as substrates *in vitro*. To test this, the coding region of *NPC4* was fused with a histidine (His)-tag at the C terminus and expressed in *E. coli* (Figure 3A). PLC activity was assayed in a calcium-independent manner under conditions previously defined (Nakamura et al., 2005). NPC4 hydrolyzed common membrane lipids such as phosphatidylcholine (PC), phosphatidylethanolamine (PE), phosphatidylserine (PS) and phosphatidylglycerol (PG) (Figures 3B and 3C). The use of crude bacterial lysates to assay NPC4 activity towards PA and lysoPC resulted in high background activity (Figure 3D). Therefore, NPC4-His tagged protein was purified to test whether lysoPC and PA are substrates of NPC4 (Figure 3E). Both PA and lysoPC were hydrolyzed by NPC4 (Figures 3F-3H). Purified NPC4 hydrolyzes PA but the activity is quite low compared to substrates like PC, PE and lysoPC (Figures 3C, 3F and 3G).

Knockout of *NPC4* Decreases Plant Sensitivity to ABA

We then tested whether *npc4-1* was altered in response to other abiotic stresses and hormones. No apparent differences in growth and development were observed when seedlings of these plants were grown under nitrogen deficiency, potassium deficiency or

on media containing the growth regulators indole acetic acid (IAA), cytokinin or 1-aminocyclopropane-1-carboxylic acid (ACC). However, *npc4-1* seedlings were less sensitive to ABA than wild-type.

ABA inhibits the elongation of primary roots by limiting cell extensibility and causing cell division to arrest in the G1 phase (Kutschera and Schopfer, 1986; Liu et al., 1994). The seedlings of *npc4-1* exhibited longer root length than wild-type seedlings (Figures 4A and 4B). In addition, the seedlings of *npc4-1* were able to produce inflorescences at 25 μ M ABA, a concentration that inhibits flowering in wild-type plants (Figure 4A). *npc4-1* plants produced more biomass than wild-type plants treated with ABA. The dry weight of *npc4-1* rosettes was \sim 4 fold greater than wild-type rosettes grown on 20 and 25 μ M ABA and two fold greater than wild-type at 35 μ M ABA (Figure 4C). The ABA-resistant root elongation and flowering phenotype of *npc4-1* is dosage dependent, since at higher concentration of ABA (35-50 μ M) the root length of *npc4-1* decreased and was comparable to wild-type. The *npc4-1* plants complemented with wild-type *NPC4* behaved like wild-type (Figures 4D and 4E). These results indicate that loss of *NPC4* is responsible for the reduced sensitivity towards ABA.

One of the best known effects of ABA is to induce seed dormancy and inhibit seed germination (Lopez-Molina et al., 2001). In the absence of ABA, nearly 100% of seeds of wild-type and *npc4-1* germinated within 4 days (Figure 5A). In the presence of 1 μ M ABA, *npc4-1* seeds broke dormancy earlier than wild-type seeds and exhibited \sim 20% more germination than wild-type seeds (Figure 5B). When the concentration of ABA was increased to 3 μ M, the percentage germination was greatly reduced in *npc4-1* and wild-type seeds, but *npc4-1* germination was \sim 25% greater than wild-type seeds. The percentage germination of *npc4-1* seeds on 5 μ M ABA was \sim 10%, and wild-type seeds failed to germinate. On higher concentrations of ABA wild-type and *npc4-1* seed germination was similarly inhibited (Figure 5C). Additionally, none of the genotypes developed green cotyledons but exhibited an etiolated phenotype after germination on concentrations in excess of 3 μ M ABA.

Another well documented function of ABA is to promote stomata closure (Mishra et al 2006). To test whether *npc4-1* is altered in ABA-mediated stomata movement, stomata peels of wild-type and *npc4-1* plants were incubated with 50 μ M ABA. In wild-type plants treated with ABA, stomata closure was promoted and stomata opening was inhibited (Figures 5D and 5E). In the presence of ABA, *npc4-1* did not exhibit ABA-promoted stomata closure or ABA-inhibition of stomata opening (Figures 5D and 5E). Since stomata closure reduces transpirational water loss, the water loss was measured in 4-week old detached rosette leaves of wild-type and *npc4-1* plants. Water loss in *npc4-1* was not significantly different than wild-type plants (Figure 5F). Therefore, *npc4-1* plants were tested for desiccation tolerance. Water was withheld for 10 days from 4-week old soil grown wild-type and *npc4-1* plants. The phenotype of *npc4-1* plants under these conditions is not quite distinct from wild-type plants. However, the signs of drought stress like anthocyanin accumulation begin to appear earlier in *npc4-1* plants than wild-type plants (Figure 5G).

ABA Content and the Expression of ABA Responsive Genes

To investigate whether alterations of *NPC4* changed ABA content, ABA content was measured in *npc4-1* and wild-type fresh picked and desiccated seeds and leaf tissue. The level of ABA in freshly picked *npc4-1* seeds was about 20% higher than wild-type seeds, and the difference was significant (Figure 5H). Desiccated *npc4-1* seeds showed still slightly higher ABA content than wild-type seeds (Figure 5I). To determine whether the increase in ABA content in *npc4-1* is tissue-specific, the ABA content of *npc4-1* and wild-type rosettes was assayed. The level of ABA in *npc4-1* rosettes was similar to wild-type (Figure 5J). These results indicate that the decreased sensitivity of *npc4-1* towards ABA is not attributed to a lower ABA content than wild-type tissue, rather *NPC4* is involved in plant response to ABA.

We then tested whether the expression of ABA-responsive genes is altered in *npc4-1*. Several known ABA-responsive and stress-inducible genes such as *ABI1*, *ABI2*, *RD29B*, *OST1*, *KAT1*, *KAT2* and *RCN1* were selected (Figure 5). Four-week old soil grown Arabidopsis plants were sprayed with 50 μ M ABA and total RNA was extracted at

several time intervals. RNA was reversed transcribed and gene expression of the selected ABA and stress inducible genes were analyzed by quantitative real time PCR. The data obtained revealed that *NPC4* is ABA responsive, with the highest level of expression at 12 hours. The basal level of expression of the selected ABA responsive genes was similar in wild-type and *npc4-1*. After treatment with 50 μ M ABA, *ABI1*, *ABI2*, *RAB18*, *OST1*, *ERA1* and *RD29B* expression were induced in wild-type and *npc4-1*, but the expression levels were 1.5-3.5 fold less than wild-type. *KAT1* and *KAT2* were not induced at wild-type levels in *npc4-1*. A general pattern emerged in which the ABA responsive genes were expressed at a lower level in *npc4-1* than in wild-type with the exception of *RCN1* (Figure 6).

Overexpression of NPC4 Increases ABA Sensitivity

To further investigate the effect of *NPC4* alterations on ABA responses, we generated transgenic Arabidopsis lines overexpressing STREP-tagged *NPC4* (*NPC4-OE*) under the control of the cauliflower mosaic virus 35S promoter. The plants harboring *NPC4*-STREP were confirmed by immunoblotting using STREP antibodies (Figure 7A). Several independent lines were tested for their stress responses, and two representative transgenic lines were used in these experiments. Wild-type, OE, and *npc4-1* plants were tested for their response to ABA in seed germination. In contrast to *npc4-1* seeds that showed ~12% higher germination and broke dormancy earlier than wild-type seeds, OE seeds germinated at ~80% of wild-type levels on media containing 1 μ M ABA (Figures 7B and 7C). *NPC4-OE* seeds were more sensitive to ABA-inhibition of germination than wild-type and *npc4-1*, and some of the seedlings did not develop green cotyledons but exhibited an etiolated phenotype after germination (Figure 7B).

ABA maintains seed dormancy and prevents precocious germination. Genetic studies in Arabidopsis revealed that the first ABA peak occurs maternally right before the maturation phase of the offspring and the second ABA peak occurs in the embryo itself and is essential for the induction of dormancy (Karssen et al., 1983). To test precocious germination in these genotypes, freshly picked wild-type, *npc4-1*, and OE seeds were germinated on filter paper. Freshly harvested *npc4-1* seeds germinated at significantly

higher levels than wild-type seeds (~2 fold higher germination), while OE seed germination was ~75% of wild-type level (Figures 7D and 7E). These results suggest that NPC4 promotes ABA action and seed dormancy.

Knockout and Overexpression of *NPC4* Lead to Opposite Effects on Sensitivity to Hyperosmotic Stress

ABA plays an important role in sensing and adapting to abiotic stresses such as drought and salinity (Yamaguchi-Shinozaki and Shinozaki, 1994). Since *npc4-1* exhibited reduced ABA sensitivity in both germination and vegetative growth, we investigated the effect of *NPC4* alterations on plant tolerance to salinity and hyperosmotic stress. Wild-type and *npc4-1* seeds were sown on 200 mM NaCl and the emergence of a radicle was scored as total germination, and seedlings with green cotyledons were scored as viable seedlings. Total germination was slightly lower in wild-type than *npc4-1* and OE seeds. However, *npc4-1* is hypersensitive to NaCl in seed germination; only $22.6\% \pm 5.2$ *npc4-1* seedlings were viable compared to wild-type ($47\% \pm 4.9$) (Figures 8A and 8B). *NPC4-OE* seedlings had 80% viability (Figure 8B).

To test whether *NPC4* alterations affect root growth responses to NaCl, 5-day old wild-type, *NPC4-OE* and *npc4-1* seedlings grown on $\frac{1}{2}$ MS were transferred to plates containing 100 or 150 mM NaCl. Ten days after transfer to MS plates containing 100 mM NaCl, *npc4-1* primary roots were significantly shorter than wild-type, and OE roots were significantly longer than wild-type. On plates containing 150 mM NaCl, the primary root growth of *npc4-1* was inhibited; *npc4-1* roots were ~79% the length of wild-type primary roots (Figures 8C and 8D). Biomass accumulation in *npc4-1* seedlings was similar to wild-type in the absence of NaCl, but in the presence of NaCl, biomass accumulation of *npc4-1* seedlings was ~70% of wild-type (Figure 8E).

To determine whether the response was specific to salt stress, *npc4-1* and wild-type seedlings were tested for their responses to other hyperosmotic stresses. $\frac{1}{2}$ MS plates were infused with polyethylene glycol (PEG) to a water potential of -0.25 or -0.45 MPa.

The growth of *npc4-1* primary roots was ~10% shorter than wild-type roots on -0.25 MPa whereas on -0.45 MPa, *npc4-1* displayed 18% shorter primary roots than wild-type (Figures 8C and 8F). Compared with wild-type seedlings, *npc4-1* seedlings accumulated ~18% and ~5% less biomass on -0.25 MPa and -0.45 MPa, respectively (Figure 8G). In contrast, *NPC4-OE* seedlings accumulated ~34% and ~30% more biomass than wild-type seedlings on -0.25 MPa and -0.45 MPa, respectively (Figure 8G).

NPC4 affects DAG Content and Lipid Composition

To determine the effect of NPC4 on lipid composition during hyperosmotic stresses, total lipids were analyzed by ESI/MS/MS from four-week old drought-stressed wild-type and *npc4-1* plants and plants treated with 50 μ M ABA. Under control growth conditions, the DAG level in *npc4-1* plants was ~80% of wild-type, indicating that NPC4 is involved in the production of basal DAG (Figure 9A). DAG content was substantially reduced in response to water deficit. The DAG level in drought-stressed wild-type plants was ~26% of control plants, whereas the stress-induced reduction was ~48% between *npc4-1* control and treated plants. DAG content in water stressed *npc4-1* plants was only ~52% of wild-type plants, suggesting that NPC4 may contribute to nearly 50% of the DAG pool during drought stress. Treatment with ABA caused ~25% reduction of DAG in wild-type plants compared to ~47% reduction in *npc4-1* plants. Moreover, DAG levels were significantly lower in *npc4-1*, which had only ~83% of the wild-type levels (Figures 9A and 9B).

Under control growth conditions, the levels of DGDG, PG, PI, PS, and lyso-PE were similar in *npc4-1* and wild-type leaves. However PC, PE, lyso-PC and MGDG levels were slightly higher in *npc4-1* plants, but significantly different from wild-type leaves (Figure 10A). PA levels were reduced by ~45 % in *npc4-1* leaves under control conditions compared to wild-type. After drought treatment, the levels of PC, PS, PA, PI, MGDG, and DGDG were similar between wild-type and *npc4-1*. However, lyso-PE and PE were significantly higher in *npc4-1* plants than wild-type plants (Figures 10A and 10B). ABA treatment caused a reduction in the content of both phospholipids and galactolipids, but the reduction was similar in wild-type and *npc4-1* plants. Compared with wild-type plants, *npc4-1* had higher levels of DGDG, MGDG, PC, PG, PE, and PS

(Figure 10A). However, PA content of *npc4-1* was ~38% of the wild-type levels.

The difference in DAG level between *npc4-1* and wild-type plants was due primarily to differences in levels of 34:2, 34:3, 36:4, 36:5 and 36:6 molecular species (Figure 9B). The *npc4-1* plants had higher levels of 34:2 PS and PE; 34:3 PS and PE; 36:4 PC; 36:5 PC; 36:6 PE, MGDG and DGDG; therefore these represent potential substrates for *npc4-1* (Figure 9B). Consistent with these results are the *in vitro* phospholipid substrates of NPC4, but DGDG and MGDG were not tested. Conversely, the difference in PA between wild-type and *npc4-1* was due primarily to differences in levels of 34:2, 34:3 and 36:4 PA molecular species (Figure 9B). The molecular species of DAG that are likely substrates for DAG kinases (DGK) are 34:2, 34:3 and 36:4 DAG, since these were also significantly reduced in *npc4-1* plants compared to wild-type plants (Figure 8B). These results indicate that NPC4 is involved in the modification of membrane lipid composition under control, drought and ABA treatment.

PA Derived from the NPC/DGK Pathway is Involved in ABA and Hyperosmotic Stress Response

In recent years, PA has emerged as an important lipid signaling molecule (Wang, 2005). PA can be produced by the action of phospholipase D (PLD), de novo synthesis or through the PLC/DGK pathway. *PLD α 1* derived PA binds to ABI1, a negative regulator of ABA signaling removing ABI1 inhibition, promoting ABA signaling (Zhang et al., 2004, Mishra et al., 2006). Since NPC4 produces DAG that can be converted to PA, we tested whether the addition of PA or DAG can restore ABA sensitivity in *npc4-1* to wild-type levels. The addition of 8:0 DAG and PA were able to rescue the *npc4-1* phenotype (Figure 11A). To further dissect the role of NPC4 in the ABA signaling pathway, we used DAG kinase inhibitor 1 (DGKI1) (Gomez-Merino et al., 2005) to differentiate the lipid that is responsible for *npc4-1* phenotype. In the presence of 100 μ M DGKI1 and ABA, the roots of *npc4-1* remained longer than wild-type, thus DGKI1 had no effect on the root growth of *npc4-1* (Figure 11B). When DAG and DGKI1 were added in the presence of ABA, DAG was no longer able to rescue *npc4-1*. On the other hand, when PA and DGKI1 were added in the presence of ABA, *npc4-1* was reverted to wild-type

phenotype. These results indicate that the DAG produced by NPC4 is converted to PA and the NPC4/DGK pathway plays a role in ABA signaling events.

To further test the role of PA produced by the NPC4/DGK pathway in ABA signaling and hyperosmotic stress, the PA content of *npc4-1*, *NPC4-OE* and wild-type roots was quantitatively profiled. Plants were grown under treatment conditions for 10 days, then the roots were excised and the lipids were extracted. Under control conditions *npc4-1* roots had higher levels of PA than wild-type roots (Figure 2F and 12A), whereas *NPC4-OE* was not significantly different than wild-type (Figure 12A). Upon treatment with ABA there was a slight increase in PA levels in wild-type roots, but a drastic decrease in PA was seen in *npc4-1* roots (Figure 12A). Treatment with DGKI caused a further decrease in PA in both wild-type and *npc4-1* roots, whereas *NPC4-OE* showed higher levels of PA. Salt stress resulted in higher PA levels in wild-type compared to *npc4-1*; *NPC4-OE* PA level was comparable to wild-type roots. After treatment with DGKI in the presence of NaCl the PA levels of wild-type and *npc4-1* were comparable while *NPC4-OE* had higher levels of PA.

DISCUSSION

NPC4 is activated in response to phosphate deficiency but had little effect on membrane lipid composition of major phospholipids and galactolipids. This study shows that PA levels were higher in *npc4-1* roots than wild-type roots under control conditions and phosphate-starved conditions, indicating that NPC4 hydrolyzes PA under both of these conditions. Recent studies show that PLD activity correlates with the increase of PA in the plasma membrane, but PA phosphatase (PAP) activity does not match the rate of removal of PA from the membrane (Tjellstrom et al., 2008). Since *NPC4* is greatly induced by phosphate deprivation and hydrolyzes PA, it may also be responsible for removing PA from the membrane. Also, lysoPC and PS are significantly higher only under phosphate deprivation in *npc4-1* roots compared to wild-type. *NPC4* encodes a functionally active phospholipase C with a broad substrate preference. Previous reports showed that NPC4 hydrolyzes PC and PE but not PA (Nakumara et al., 2005). When *E. coli* extract is incubated with PA as substrate, high levels of DAG are produced, possibly

due to the presence of a phosphatase that dephosphorylates PA (Figure 2D). In addition, *E. coli* extracts contain phospholipase A (PLA) activity producing monoacylglycerol (MAG) and free fatty acid (Gaude et al., 2008). To circumvent this problem, NPC4 was purified in order to test whether NPC4 uses PA and lysoPC as substrates *in vitro*. Our results indicate that NPC4 uses PA and lysoPC as substrates but the activity towards PA is ~10 fold lower compared to lysoPC and ~100 fold lower compared to PC (Figure 2F).

The results suggest that NPC4 is not a major player in providing inorganic phosphate in times of low phosphate availability. So, we investigated whether NPC4 affects plant responses to abiotic stresses and hormones. The effect of *NPC4-KO* and *NPC4-OE* on lipid composition, ABA responses, and hyperosmotic responses was analyzed. Several lines of evidence suggest that NPC4 functions specifically in ABA signaling to modulate root growth, stomatal movement, and seed dormancy (Figures 3 and 4). Firstly, *npc4-1* responded to auxin, ethylene and cytokinin similarly to wild-type. These hormones have all been implicated in the ABA signaling cascade (Tanaka et al., 2006). Notably the ethylene signaling cascade inhibits ABA signaling in seeds (Beaudoin et al., 2000; Cheng and Fedoroff, 2000). Secondly, *npc4-1* exhibits strong insensitivity in ABA inhibition of root growth as compared to ABA inhibition of seed germination (Figures 4 and 5). This phenomenon is not uncommon, as PPC2A acts as a strong negative regulator of ABA both in seed germination and vegetative growth (Kuhn et al., 2006). Additionally, positive regulators of ABA signaling, such as *ABI4* (Finkelstein et al., 1998), *ABI5* (Finkelstein et al., 2002) and *OST1* (Mustilli et al., 2002), affect different aspects of ABA signaling. The *abi4-2* mutant allele was reported to germinate on 30 μ m ABA (Finkelstein et al., 2002). Thirdly, fresh seeds of *npc4-1* exhibit precocious germination, 100% more than of wild-type seeds and OE germination was ~75% of wild-type levels (Figures 7D and 7E). Taken together these results suggest that NPC4 may play a more pivotal role in vegetative growth than in seed germination, since the root growth response to ABA is stronger compared to the weak ABA insensitivity seen in seeds.

The results presented suggest that NPC4 acts as a positive regulator of ABA responses

in *Arabidopsis*. The *NPC4-KO* showed reduced sensitivity in seed germination, decreased seed dormancy and ABA resistant root growth, while *NPC4-OE* showed increased sensitivity. ABA-mediated stomata movement was also affected in *npc4-1*, in both the opening and closing in the presence of ABA. However, water loss experiments revealed that *npc4-1* does not lose less water than wild-type plants despite reduced sensitivity to ABA mediated stomata movement. This might be due to the finding that excised leaf transpiration experiments reflect the differences in stomata aperture that may vary between genotypes at the beginning of the experiment (Kuhn et al., 2006). ABA accumulation in *npc4-1* fresh and desiccated seeds was slightly higher than wild-type, but the levels were similar in leaves; indicating that *NPC4* is most likely involved in ABA responses opposed to ABA accumulation. Additionally, stress responsive and ABA inducible genes such as *RD29B*, *ABI1*, *ABI2*, *RAB18*, *KAT2*, *KAT1* and *OST1* were down-regulated in *npc4-1* (Figure 6). These genes were induced by ABA but their transcript levels in *npc4-1* were lower than wild-type plants.

The physiological response of *npc4-1* to drought and salt stress was assessed, because ABA is involved in sensing and adaptation to abiotic stress such as drought, freezing and salinity (Finkelstein et al., 2002). Based on reduced sensitivity to ABA in *npc4-1* mutants, we hypothesized that *npc4-1* plants may be reduced in tolerance to abiotic stress. Consistent with this, *npc4-1* displayed hypersensitivity under salt stress both in root elongation and seed germination while OE plants were more tolerant and produced more biomass. In addition, *npc4-1* grown on PEG infused media were slightly less tolerant than wild-type plants while OE grew better and accumulated more biomass (Figures 8F and 8G). The altered stress responses exhibited in *npc4-1* may be caused by alterations in lipid metabolism. The lipid changes observed between *npc4-1* and wild-type rosettes in response to ABA were more drastic than those observed under drought stress. Additionally, PA levels in *npc4-1* were the same as wild-type rosettes under drought stress, compared to ~60% less than wild-type rosettes after ABA treatment.

Lipid signaling and second messengers produced by lipases are an important aspect of the ABA signaling cascade. IP_3 produced by the action of PI-PLC increases calcium fluxes

affecting ABA signaling in guard cells (Hunt et al., 2003). PLD α 1 derived PA has been shown to regulate ABI2 function by binding to ABI1 and sequestering it to the plasma membrane, ultimately removing ABI1 inhibition promoting stomata closure (Mishra et al., 2006). Under normal growth conditions, galactolipid and phospholipid levels were higher in KO mutants than in wild-type plants. Even though the differences were small, they were significant and consistent with the in vitro substrate preferences of NPC4. No changes were seen in DGDG, PI, PS and PG, but PA levels in the leaves of *npc4-1* mutants were lower than wild-type plants. In roots the PA levels were higher in *npc4-1* than wild-type plants, indicating that the PA content of root and shoot is affected differently in *npc4-1* plants. DAG content in *npc4-1* was lower than wild-type plants. On the induction of drought treatment, the glycerolipid content of *npc4-1* was similar to wild-type, except PS, PE, and lyso-PE which were elevated in *npc4-1* plants. The DAG content of *npc4-1* was lower than wild-type levels after treatment. Following ABA treatment almost all the phospholipids were altered in *npc4-1*. DAG and PA content were lower in the *npc4-1* compared to wild-type plants. The levels of 34C and 36C-PA and DAG were lower in *npc4-1* plants; this is significant since DAG can be converted to PA through the action of DAG kinases. These results could mean that DAG produced by NPC4 contributes to the pool of signaling PA present in plants. This PA derived from this pathway is important in ABA-mediated root growth. This is supported by the reversion of *npc4-1* to wild-type sensitivity in the presence of ABA when PA or DAG is added. However, blocking the DAG/DGK pathway in *npc4-1* does not revert ABA sensitivity of *npc4-1* to that of wild-type (Figure 11). The PA content of roots is higher in *npc4-1* than wild-type but lower in rosettes under control conditions, suggesting that PA is regulated differently between roots and shoots. When treated with ABA the PA content in both root and shoot of *npc4-1* plants is lower than wild-type plants. These results suggest that since PA level is decreased in *npc4-1* plants, sensitivity to ABA and hyperosmotic stress is altered.

Results from this work provide new information and insights about the metabolic and physiological functions of the non-specific phospholipase C, NPC4 and its derived DAG. Under phosphate deprived conditions, NPC4 hydrolyzes minor phospholipids PS, PA and

lysoPC. The hydrolysis seems to be more related to cellular regulation than providing inorganic phosphate and an acyl backbone for DGDG synthesis.

Materials and Methods

Plant material and growth

Seeds of *npc4-1* and wild-type *Arabidopsis* (ecotype Columbia) were sown in soil and kept at 4°C for 2 days. Plants were grown in a growth chamber with cool white fluorescent light of 100 $\mu\text{mol m}^{-2}\text{s}^{-1}$ under 16-h light/ 8-h dark and 23°C/22°C cycles. For water deficit experiments, plants were withheld water for 10 days.

Seed germination was performed on ½ MS medium supplemented with 1.5% sucrose. Seeds were sterilized in 70% ethanol for 5 min followed by 20% bleach for 3 min and then rinsed three times with sterile distilled water. Sterilized seeds were sown on medium containing 0-10 μM ABA. Germination was scored at two-day intervals for 10 days. For root elongation assays, 5-day old seedlings were transferred to 0- 50 μM ABA and grown under cool white fluorescent light of 100 $\mu\text{mol m}^{-2}\text{s}^{-1}$ under 16-h light/ 8-h dark and 23°C/22°C cycles for 2 weeks. For rescue experiments, 8:0 DAG and PA (Avanti Polar Lipids) were prepared by drying the chloroform under a stream of nitrogen gas and resuspending the dried lipid in water followed by sonication. The DGK11 (Calbiochem) was dissolved in DMSO. These solutions were added to the surface of 20 μM agar plates (200 μl of 100 μM). For NaCl (0-150 mM) and PEG (-0.25 and -0.45 MPa) experiments, 5-day old seedlings were transferred and grown under cool white fluorescent light of 100 $\mu\text{mol m}^{-2}\text{s}^{-1}$ under 12-h light/ 12-h dark and 23°C/22°C cycles for 10 days.

Isolation of NPC4 Knockout Mutant

A T-DNA-insertional mutant of *NPC4* (*At3g05340*) was identified as SALK_046713. Seeds were obtained from the *Arabidopsis* Biological Resource Center (Columbus, OH). *NPC4* homozygous T-DNA insertion mutant was isolated by PCR using *NPC4* specific primers: *NPC4*: 5'-AGCTACCCA ACTA CGTCGTGGTTCG-3' (forward), 5'-GGTTGAGCAGCATTGATGCTTC-3' (reverse) and a TDNA left border primer: 5'TGGTTCACGTAGTGGGCCATC3'. A

single T-DNA insert was verified by cosegregation of the mutant allele with kanamycin resistance in a 3:1 ratio. The loss of transcription of *NPC4* was confirmed using primers 5'-AGCATCAAATGCTGCTGCTCAACC-3' (Forward) and 5'-TCCACCCACACACAAGAGAAGTGA-3' (Reverse) by quantitative real time PCR as described below.

ABA Gene Expression using Quantitative Real Time PCR

Total RNA was isolated from 4-week leaves sprayed with 50 μ M ABA, using a rapid CTAB method (Stewart and Via, 1993; Li et al, 2006), and RNA was precipitated using 2 M LiCl at 4°C. RNA integrity was checked on 1% (w/v) agarose gel. 8 μ g of total RNA was digested with DNaseI according to manufacturer's instructions (Ambion, Inc.) RNA was reverse transcribed using iScript cDNA Synthesis Kit (BIO-Rad, CA). The efficiency of cDNA synthesis was analyzed by real time PCR amplification of *UBQ10* (At4g05320). The level of gene expression was normalized to that of *UBQ10*. qRT-PCR was performed with MyiQ Sequence Detection System (Bio-Rad, CA) using SYBR Green to monitor dsDNA synthesis. Reaction mix contained 7.5 μ l 2xSYBR Green Master Mix reagent Kit (BIO-Rad, CA), 1.0 ng cDNA, and 200 nM of each gene specific primer in a final volume of 15 μ l. The primer sequences used to amplify the selected ABA responsive genes are listed in Table 1.

Measurement of Stomata Movement and Water Loss

Epidermal peelings from six-week-old plants were floated in a solution of 5mM MES-KOH (pH 6.15), 30mM KCl and 1mM CaCl. After incubation for 3 hours under dark to ensure the closure of stomata, 50 μ M of ABA was added and incubated under cool white light (150 mol m⁻¹s⁻¹) at room temperature for 3h to induce stomatal opening. To test the effect of ABA on stomatal closure, epidermal peelings were incubated in 5mM MES-KOH (pH 6.15), 30mM KCl and 1mM CaCl for 3 hours under cool white light(150 mol m⁻¹s⁻¹) at room temperature to ensure the opening of stomata. After incubation 50 μ M of ABA was added and incubated under cool white light (150 mol m⁻¹s⁻¹) at room temperature for 3h. Epidermal peelings were observed

under microscope and stomatal aperture was recorded using digital camera and analyzed by using IMAGEPRO software (Media Cybernetics, Silver Spring, MD).

For water loss experiments, detached leaves of six-week-old plants were exposed to cool white light ($125 \text{ mol m}^{-1}\text{s}^{-1}$) at 23°C . Leaves were weighed at various time intervals, and loss of fresh weight (%) was used to indicate water loss.

Precocious Germination

Fresh seeds of WT, *npc4-1*, and *NPC4-OE* were collected directly from the plants at the same time from the plants grown under the same conditions. Seeds were placed on moistened Whatman filter paper for germination and germination percentage was calculated after five days of plating.

Plant transformation and complementation test

NPC4 genomic DNA containing the entire ORF was amplified from wild-type Arabidopsis and cloned into *AscI* sites of pEC291 under its native promoter. The primers used for amplification are -5'-ATGGCGCGCCGACAGGGTTTGTGATGCTACAATG3'(forward) and 5'-ATGGCGCGCCGGCGCGACTTTGTATTCTATTC-3' (reverse). The construct was introduced into JM109 strain, to test for positive clones. The resulting positive clone was transformed in Agrobacterium C58 and was used to transform *npc4-1* mutants plants by floral dip (Clough, and Bent 1998). Hygromycin resistant T3 transgenic plants were screened for homozygous lines. Homozygous lines did not segregate when placed on hygromycin. These seeds were collected and subjected to complementation tests on MS agar medium supplemented with ABA.

Lipid Extraction and Profiling:

The process of lipid extraction, lipid analysis and quantification was performed as described by Welti et al. (2002). Rosettes and roots were excised from 2-week old Arabidopsis plants and immersed immediately in 3 mL hot isopropanol containing 0.01% butylated hydroxytoluene at 75°C . Samples were kept at 75°C for 15 min and

1.5 mL of chloroform and 0.6 mL water of were added. Samples were place on a shaker for 1 h, and the solvent was transferred to a new tube. The samples were reextracted using chloroform:methanol (2:1) for at least 4 times for 30 min each on a shaker. The lipid extracts were combined and washed with 1 M KCl followed by washing with 1 mL water. The solvent was dried under a stream of nitrogen gas and the remaining tissue was oven dried at 100°C and weighed. Lipids composition was analyzed by an electrospray ionization triple quadrupole mass spectrometer (API4000). Data was analyzed using Q-test to remove aberrant data points followed by student's t-test to determine significance.

Enzyme Activity Assay of NPC4 Expressed in *E.coli*

The *NPC4* cDNA was amplified from 5'RACE pollen cDNA library using Phusion high fidelity Taq polymerase. The PCR product was cloned into pCR® 2.1-TOPO® (Invitrogen) vector to screen for a positive clone. A positive clone was selected, purified and cloned into pET28a(+) expression vector with a His tag under the T7 promoter and transformed into *E. coli* Rosetta (DE3). To induce the expression of *NPC4*, 0.1 mM of isopropyl β -D-thiogalactopyranoside was added when the culture had an A_{600} of ~0.4. Culture was incubated for 36 h at 12 °C. Cells were harvested by centrifugation (12,000 rpm, 2 min) and resuspended in extraction buffer containing 50 mM Tris-HCl (pH 7.3), 50 mM NaCl, 5% glycerol, 1 mM DTT, and 0.5 mM PMSF. Cells were lysed by sonication and centrifuged (1,500 rpm, 10 min) to remove cell debris. The supernatant was used for the enzyme activity as described below.

Protein concentration in the supernatant was quantified using Bradford reagent (BIO-Rad, CA) with BSA as a standard according to manufacturer's instructions. The activity assay was carried out using previously defined conditions (Nakamura et al., 2005). Briefly, the reaction mixture contained 100 μ L of enzyme, 100 μ L of substrate and 300 μ L of assay buffer (50 mM Tris-HCl (pH 7.3), 50 mM NaCl, and 5% glycerol). The substrate was prepared as follows: 0.5% of 18:1 PC (Avanti Polar lipids), 0.5% egg transphosphatidylated PE (Avanti Polar lipids), 0.5% egg LysoPC (Sigma), 0.5% 16:0 PA (Matreya LLC) and 0.5% 18:1 PA (Avanti Polar lipids) was dried under a stream of nitrogen gas and resuspended in 250 mM Tris-HCl (pH 7.3)

and 0.25% deoxycholate. The samples were incubated for 1 hour at 37°C. The reaction was stopped by the addition of 0.75 ml ethyl acetate followed by vigorous vortex and the addition 0.75 ml of NaCl. The upper phase was dried under a stream of nitrogen gas and dissolved in 20 µL of chloroform methanol (2:1, v/v) and separated on a TLC plate. The solvents used to separate the product are petroleum ether/ethyl ether/acetic acid (50:50:1, v/v/v). DAG was scraped from the TLC plates and transmethylated. The solvent for transmethylation contained methanol and 1% H₂SO₄. 5 µL of 5.4 µM/mL 17:0 TAG was added to the samples as an internal standard. Samples were heated for 1 h at 90°C. 1 ml of hexane and 1 ml of water was added and the upper phase was removed for GC analysis. The fatty acid methyl esters were separated on a SHIMADZU GC-17A supplied with a hydrogen flame ionization detector and a capillary column DB-5MS (30 m; 0.25mm i.d.) with helium carrier at 11 ml/min. The oven temperature was maintained at 170°C for 3 min and then increased linearly to 210°C (5°C min⁻¹). Fatty acid methyl esters (FAMES) were identified by comparison of their retention times with known standards (37-component FAME mix, Supelco 47885-U).

ABA Content

Seeds or leaf tissues were ground in liquid nitrogen and 0.5 ml of 1-propanol:H₂O:HCL (2:1:0.002 v/v) was added to the homogenate and vortexed well. 1 ml of dichloromethane and ABA internal standards was added. The samples were vortexed and centrifuged at 11300g for 1 min. The lower phase was transferred and ABA was quantified by mass spectrometry.

Subcellular Localization of GFP Fusion Proteins

For generation of NPC4-GFP, *NPC4* cDNA was cloned into pMDC43 and pMDC83 vectors (Curtis & Grossniklaus, 2003). The primers used to clone *NPC4* into pMDC43 are: 5'-TTGGCGCGCCTATGATCGAGACGACCAAAGGC-3' and 5'-CCCTTAATTAATCAATCATGGCGAATAAAGCAAGAGAATAAC-3'. The primers used to clone *NPC4* into pMDC83 are: 5'-GGGTTAATTAATGATCGAGACGACCAAAGGCG-3' and 5'-TTGGCGCGCCCATCATGGCGAATAAAGCAAGAGAATAACTTATTG-3'.

C-terminally fused NPC4-GFP was generated from pMDC83 construct and N-terminally fused NPC4-GFP was generated from pMDC43. Constructs were transformed into *Agrobacterium* C58 and grown at 30°C in LB broth supplemented with 50 µg ml⁻¹ kanamycin. The cells were harvested by centrifugation at 5000 g for 10 min at room temperature and resuspended in 10 mM MgCl₂ and 150 µg ml⁻¹ acetosyringone. Cells were left for 3 h at room temperature and then infiltrated into 3-week old tobacco leaves. After 48 h the specimens were analyzed using a Zeiss 510 confocal fluorescence microscope.

Immunoblotting, Detection, and Purification of NPC4-His

Bacterial cells expressing NPC4 were harvested by centrifugation (10,000 rpm, 2 min) and resuspended in an extraction buffer (50 mM Tris-HCl (pH 7.3), 50 mM NaCl, 5% glycerol, 1 mM DTT, and 0.5 mM PMSF). Cells were lysed by sonication and centrifuged at 1,500 rpm for 5 min. The supernatant and total cell lysates were separated by 10% SDS-PAGE. After electrophoresis, proteins were transferred to a polyvinylidene difluoride membrane. The membrane was blotted with anti-His antibody (1:10,000) conjugated with alkaline phosphatase for two hours. The protein bands were visualized by alkaline phosphatase reaction. For purification of NPC4-His, Ni-NTA agarose (Qiagen) was used according to manufacturer's instructions. Briefly, 3 mL supernatant containing NPC4-His or empty vector control were added to 0.5 mL of Ni-NTA agarose and incubated for 1 h with gentle agitation at 4°C. Samples were washed four times and Ni-NTA agarose was resuspended in 1 mL assay buffer (50 mM Tris-HCl (pH 7.3), 50 mM NaCl, and 5% glycerol). Samples were used for immunoblotting and phospholipase C activity.

Immunoblotting and Detection of NPC4-STREP

Total proteins were extracted from 4-week old *Arabidopsis* leaves using buffer A (50 mM Tris-HCl, pH 7.5, 10 mM KCl, 1 mM EDTA, 1 mM DTT, and 0.5 mM PMSF). After centrifugation at 12,000 rpm for 5 min, the supernatant proteins were separated by 10% SDS-PAGE. The proteins were transferred to a polyvinylidene difluoride membrane and the membrane was blotted with anti-STREP antibody (1:10,000)

conjugated with horseradish peroxidase for 1 h. The membrane was washed four times for 10 min with PBS/T buffer (1x phosphate saline buffer and 0.05% Tween 20). The membrane was incubated with LumiGLO substrate for 1 min and then exposed to x-ray film.

References

1. **Barrero JM, Piqueras P, Gonzalez-Guzman M, Serrano R, Rodriguez PL, Ponce MR, Micol JL.** (2005) A mutational analysis of the ABA1 gene of *Arabidopsis thaliana* highlights the involvement of ABA in vegetative development. *Journal of Experimental Botany* **56**, 2071-2083.
2. **Beudoin N, Serizet C, Gosti F, Giraudat J.** (2000) Interactions between abscisic acid and ethylene signaling cascades. *Plant Cell* **12**, 1103-1115.
3. **Burnette RN, Gunsekera BM, Gillaspay GE.** (2003) An *Arabidopsis* Inositol 5-phosphate gain of function alters abscisic acid signaling. *Plant Physiology* **132**, 1011-1019.
4. **Clough SJ and Bent AF.** (1998) Floral dip: a simplified method for *Agrobacterium*-mediated transformation of *Arabidopsis thaliana*. *The Plant Journal* **16**, 735-743.
5. **Cornforth JW, Miborrow BV, Ryback PF, Wareing PF.** (1965) Identity of Sycamore dormin with abscisin II. *Nature* **205**, 1296.
6. **Cutler S, Ghassemian M, Bonetta D, Cooney S, McCourt P.** (1996) A protein farnesyl transferase involved in abscisic acid signal transduction in *Arabidopsis*. *Science* **273**, 1239-1241.
7. **Finkelstein RR.** (1994) Mutations at two new *Arabidopsis* response loci are similar to *abi3* mutations. *Plant Journal* **5**, 765-771.
8. **Finkelstein R, Reeves W, Ariizumi T, Steber C.** (2008) Molecular aspects of seed dormancy. *Annu. Rev. Plant Biol.* **59**, 387-415.
9. **Finkelstein RR, and Somerville CR.** (1990) Three classes of abscisic acid (ABA)-insensitive mutations of *Arabidopsis* define genes that control overlapping subsets of ABA responses. *Plant Physiology* **94**, 1172-1179.

- 10. Finkelstein RR, Gampala SS, Rock CD.** (2002) Abscisic acid signaling in seeds and seedlings. *Plant Cell*, S15-S45.
- 11. Gaude N, Nakamura Y, Scheible WR, Ohta H, Dormann P.** (2008) Phospholipase C5 (NPC5) is involved in galactolipids accumulation during phosphate limitation in leaves of Arabidopsis. *Plant J* **56**: 28-39.
- 12. Gifford IB, Lynch TJ, Garcia ME, Malhotra B, Finkelstein RR.** (2004). The Arabidopsis thaliana ABSCISIC ACID- INSENSITIVE8 locus encodes a novel protein mediating abscisic acid and sugar responses essential for growth. *Plant Cell* **16**, 406-421.
- 13. Gomez-Merino FC, Arana-Ceballos FA, Trejo-Tellez LI, Skirycz A, Bearly CA, Dormann P, Muller-Roeber B.** (2005) Arabidopsis AtDGK7, the smallest member of plant diacylglycerol kinases (DGKs), displays unique biochemical features and saturates at low substrate concentration. The DGK inhibitor R59022 differentially affects AtDGK2 and AtDGK7 activity in vitro and alters plant growth and development. *J Biol Chem* **280(44)**, 34888-34899.
- 14. Gosti F, Beaudoin N, Serizet C, Webb AAR, Vartanian N, Giraudat J.** (1999) ABI1 protein phosphatase2C is a negative regulator of abscisic acid signaling. *Plant Cell* **11**, 1897-1909.
- 15. Hong Y, Devaiah SP, Bahn SC, Thamasandra BN, Li M, Welti R, Wang X.** (2009) Phospholipase D ϵ and phosphatidic acid enhance Arabidopsis nitrogen signaling and growth. *Plant J* **58**, 376-387.
- 16. Hong Y, PanX, Welti R, Wang X.** (2008) Phospholipase D α 3 is involved in the hyperosmotic response in Arabidopsis. *Plant Cell* **20**, 803-816.
- 17. Hugouvieux V, Kwak JM, and Schroeder JI.** (2001) An mRNA cap binding protein, ABH1, modulates early abscisic acid signal transduction in Arabidopsis. *Cell* **106**, 477-487.
- 18. Jang YH, Lee JH, Kim J-K.** (2008) Abscisic acid does not disrupt either the Arabidopsis FCA-FY interaction or its rice counterpart in vitro. *Plant Cell Physiol* **49(12)**, 1898-1901.
- 19. Kuhn JM, Biosson-Dernier A, Dizon MB, Maktabi MH.** (2005) The

- Protein Phosphatase AtPP2CA Negatively Regulates Abscisic Acid Signal Transduction in Arabidopsis, and Effects of *abh1* on AtPP2CA mRNA. *Plant Physiol* **140**, 127-139.
- 20. Leung J, Merlot S, Giraudat J.** (1997) The Arabidopsis ABSCISIC ACID-INSENSITIVE (ABI2) and ABI1 genes encode homologous protein phosphatases 2C involved in abscisic acid signal transduction. *Plant Cell* **9**, 759-771.
- 21. Liu Y, Bergervoet JHW, Ric De Vos CH, Hilhorst HWM, Kraak HL, Karssen CM, Bino, RJ.** (1994) Nuclear replication activities during imbibition of abscisic acid- and gibberellin-deficient tomato (*Lycopersicon esculentum* Mill.) seeds. *Planta* **194**, 368-373.
- 22. Lopez-Molina L, Mongrand S, Chua NH.** (2001) A postgermination developmental arrest checkpoint is mediated by abscisic acid and requires the ABI5 transcription factor in Arabidopsis. *Proc Natl Acad Sci USA* **98**, 4782–4787
- 23. Lu C and Fedoroff N.** (2000) A mutation in the Arabidopsis HYL1 gene encoding a dsRNA binding protein affects responses to abscisic acid, auxin, and cytokinin. *Plant Cell* **12**, 2351-2365.
- 24. Mishra G, Zhang W, Deng F, Zhao J, Wang X.** (2006) A bifurcating pathway directs abscisic acid effects on stomatal closure and opening in Arabidopsis. *Science* **312**, 264-266.
- 25. Mustilli A, Merlot S, Vavasseur A, Fenzi F, Giraudat J.** (2002) Arabidopsis OST1 protein kinase mediates the regulation of stomatal aperture of abscisic acid and acts upstream of reactive oxygen species production. *Plant Cell* **14**, 3089-3099.
- 26. Nakamura Y, Awai K, Masuda T, Yoshioka Y, Takamiya K, Ohta H.** (2005) A novel phosphatidylcholine-hydrolyzing phospholipase C induced by phosphate starvation in Arabidopsis. *J Biological Chemistry* **280**, 7469-7476.
- 27. Ohkuma K, Lyon JL, Addicott FT, Smith OE.** (1963) Abscisin II, an abscission- accelerating substance from young cotton fruit. *Science* **142**, 1592-1593.

- 28. Seki M, Ishida J, Narusaka M, Fujita M, Nanjo T, Umezawa T, Kamiya, A, Nakajima M, Enju A, Sakurai T, Satou M, Akiyama K, Yamaguchi-Shinozaki K, Carninci P, Kawai J, Hayashizaki Y, Shinozaki K.** (2002) Monitoring the expression of around 7,000 Arabidopsis genes under ABA treatments using a full length cDNA microarray. *Funct Interg Genomics* **2**, 282-291.
- 29. Schroeder JI, Kuhn J.M.** (2006) Plant biology: abscisic acid in bloom. *Nature* **439**, 277–278.
- 30. Soderman EM, Brocard IM, Lynch TJ, Finkelstein RR.** (2000) Regulation and function of Arabidopsis ABA-insensitive Gene in seed and abscisic acid response signaling networks. *Plant Physiology* **124**, 1752-1765.
- 31. Stewart CN Jr, Via LE** (1993) A rapid CTAB DNA isolation technique useful for RAPD fingerprinting and other PCR applications. *Biotechniques* **14**, 748-758
- 32. Szaboles I.** (1997) The global problems of salt-affected soils. *Acta Agron. Hung.* **36**: 159–172.
- 33. Tanaka Y, Sano T, Tamaoki M, Nakajima N, Kondo N, Hasezawa S.** (2006) Cytokinin and auxin inhibit abscisic acid-induced stomatal closure by enhancing ethylene production in Arabidopsis. *J Exp Botany* **57(10)**, 2259-2266.
- 34. Wang KLC, Li H, Ecker JR.** (2002) Ethylene biosynthesis and signaling networks. *Plant Cell*, S131-S151.
- 35. Welti R, Li W, Li M, Sang Y, Biesiada H, Zhou H, Rajashekar CB, Williams TD, Wang X.** (2002) Profiling membrane lipids in plant stress responses: role of phospholipase D α in freezing- induced lipid changes in Arabidopsis. *J. Biol. Chem.* **277**, 31994-32002.
- 36. Xiong L and Zhu JK.** (2003) Regulation of abscisic acid biosynthesis. *Plant Physiology* **133**, 29-36.
- 37. Xiong L, Gong Z, Rock CD, Subramanian S, Guo Y, Xu W, Galbraith D, Zhu JK.** (2001a) Modulation of abscisic acid signal transduction and biosynthesis by an Sm-like protein in Arabidopsis. *Dev. Cell* **1**, 771-781.
- 38. Xiong L, Lee B, Ishitani M, Lee,H, Zhang C, Zhu JK.** (2001b) FIERY1

- encoding and inositol polyphosphate 1-phosphatase is a negative regulator of abscisic acid and stress signaling in Arabidopsis. *Genes Dev.* **15**, 1971-1984.
- 39. Yamaguchi-Shinozaki K and Shinozaki K.** (1994) A novel cis-acting element in an Arabidopsis gene is involved in responsiveness to drought, low- temperature, or high salt stress. *Plant Cell* **6**, 251-264.
- 40. Zheng ZL, Nafisi M, Tam A, Li H, Crowell DN, Chary SN, Schroeder JI, Shen J, Yang Z.** (2002) Plasma membrane-associated ROP10 small GTPase is a specific negative regulator of abscisic acid responses in Arabidopsis. *The Plant Cell* **14**, 2787-2797.

Figure Legends

Figure 1. *NPC4* expression and localization.

(A) Expression level of *NPC4* in Arabidopsis tissues. Expression level was determined using real-time PCR and level of expression was quantified based on the expression level of *UBQ10*. Values are means \pm SD, n = 3 discrete samples.

(B) Expression level of *NPC4* in response to phosphate deprivation. Seedlings were grown on media containing 500 μ M or 0 μ M of phosphate for 10 days. Level of expression was determined by quantitative real-time PCR and expression level was quantified based on *UBQ10*.

(C) Subcellular localization of NPC4. Fusion proteins of NPC2 and NPC4 with GFP under the control of the 35S promoter were transiently expressed in tobacco leaves. Localization was analyzed by confocal microscopy of GFP and chlorophyll fluorescence (red). i. NPC2, the positive control, ii. C-terminus fused NPC4-GFP, iii. N-terminus fused NPC4-GFP.

Figure 2. The T-DNA insertion mutant of NPC4 and effects of NPC4-KO on lipid composition under phosphate deprivation in Arabidopsis roots

(A) Location of the TDNA insert. Diagram showing the position of the T-DNA insert in *NPC4* genomic sequence and primers used to identify the *npc4-1* knockout mutant. A single T-DNA is inserted in the 2nd intron of *NPC4*.

(B) PCR confirmation of the T-DNA insertion in *npc4-1*. i, product obtained using LBa1 primer and P2; ii, product obtained using primers P1 and P2. The mutation in *npc4-1* is homozygous.

(C) Level of expression of *NPC4* in wild-type plants and *npc4-1* plants. Gene specific primer pair P3 and P4 failed to amplify the product in *npc4-1*, hence *npc4-1* is a null mutant.

(D) Phospholipid composition in wild type and *npc4-1* under phosphate sufficient and replete conditions. Phospholipid content was determined by electrospray ionization/tandem mass spectrometry. Values are means \pm SE (n=5). * indicate significant changes between wild type and *npc4-1* before and after treatment. Statistical analysis was performed using student's t-test.

(E) Galactolipid changes under phosphate starvation. Values are means \pm SE (n=5).

(F) *npc4-1* effect on minor lipid composition. NPC4 affects PA, lysoPC and PS content under phosphate deprivation. Values are means \pm SE (n=5). * indicate significant changes between wild-type and *npc4-1*, ($p < 0.05$) as determined by student's t-test.

Figure 3. Protein expression and enzyme activity

(A) Production of His-tag NPC4 in *E. coli*. Proteins were extracted from *E. coli* cells harboring *NPC4* gene expression cassette and separated by 10% SDS-PAGE then transferred to a polyvinylidene difluoride membrane. NPC4 was detected in the soluble fraction by immunoblotting, using His conjugated alkaline phosphatase antibody.

(B) NPC4 activity using thin layer chromatography (TLC). *NPC4* expression was induced in *E. coli* cells for 36h at 12°C. Proteins were harvested from the soluble fraction and incubated with 0.5% PC, PE, PG, PS, PA and Lyso-PC for 90 min at 37°C. The lipid product was separated by TLC and visualized using iodine vapor. Enzyme blank (EB)

represent samples that NPC4 extract were not added. Control (C) samples are bacterial extracts harboring pET28a(+) empty vector. FFA, free fatty acid.

(C) Quantification of PLC hydrolyzing activity towards PC, PE, PG, and PS. Values are means \pm (n=3).

(D) NPC4 activity towards PA using TLC plates. High background activity is seen when 18:1 PA and 16:0 PA are used as substrate but not when 18:1 PC is used as substrate. Enzyme blank (EB) represent samples that NPC4 extract were not added. Control (C) samples are bacterial extracts harboring pET28a(+) empty vector.

(E) Purification of HIS-tagged NPC4 protein. NPC4-His was purified using Ni-NTA agarose. NPC4-His bound to the Ni-NTA agarose was detected by immunoblotting with anti-His antibody conjugated with AP. Lane 1, NPC4 bound to Ni-NTA was denatured by SDS and heating, beads were removed by centrifugation and supernatant was loaded on the gel. Lane 2, NPC4 bound to Ni-NTA beads. Lane 3, empty vector control bound to Ni-NTA was denatured by SDS and heating, beads were removed by centrifugation and supernatant was loaded on the gel. Lane 4, empty vector control bound to Ni-NTA agarose. Arrow indicates NPC4 protein.

(F) NPC4 activity towards 16:0 PA. DAG formed from the reaction was removed from TLC plate and transmethylated and quantified by GC analysis. Values are means \pm (n=3).

(G) NPC4 activity towards lysoPC. MAG formed from the reaction was removed from TLC plate and transmethylated and quantified by GC analysis. Values are means \pm (n=3).

(H) TLC plate showing MAG formed from NPC4 activity towards lysoPC. Arrow indicates formation of MAG. Enzyme blank (EB) represent samples that NPC4 extract were not added. Control (C) samples are bacterial extracts harboring pET28a(+) empty vector. Arrow indicates the formation of MAG.

Figure 4. The effects of *NPC4* alterations on root elongation in response to ABA.

(A) Seedlings on $\frac{1}{2}$ MS media containing 0-25 μ M ABA. Five-day old seedlings were transferred to vertical plates containing 0-25 μ M ABA. Pictures were taken two weeks later.

(B) Root elongation on $\frac{1}{2}$ MS media supplemented with 0-50 μ M ABA. Values are means \pm SD, (n=15).

(C) Dry weight of seedlings grown medium containing 0-50 μ M ABA. Values are means \pm SD, (n=15).

(D) Wild type *NPC4* complements the reduced sensitivity phenotype of *npc4-1*. Root elongation on $\frac{1}{2}$ MS media supplemented with 0 or 25 μ M ABA. Values are means \pm SD, (n = 15).

(E) Seedlings on $\frac{1}{2}$ MS media containing 25 μ M ABA. Wild-type *NPC4* was introduced into *npc4-1* plants and homozygous *npc4-1* complemented plants were tested. Pictures were taken two weeks after transfer.

Figure 5. ABA effect on and content in *NPC4*-KO and wild-type plants.

(A) (B) and (C) Effect of ABA on seed germination. One hundred seeds per genotype were measured in each experiment. Values are means \pm SD (n=3) (A) Seeds were germinated in the absence of ABA. (B) Seeds were germinated on $\frac{1}{2}$ MS containing 1 μ M ABA (C) Seeds were germinated on 0-10 μ M ABA.

(D) Opening of stomata in the presence of 50 μ M ABA. WT and mutant epidermal peels were incubated in the dark without ABA to close stomata. These peels were then placed under light for 3 hours in the presence of ABA. Stomata aperture was imaged using a light microscope. The images obtained were measured using Image Pro software.

(E) Closure of stomata in the presence of ABA. To fully open stomata of both mutant and wild-type, stomata peels were placed under light for three hours. Then plants were treated with ABA. Stomata aperture was imaged using a light microscope. The images obtained were measured using Image Pro software. At least 40 stomata were measured.

(F) Water loss was measured from detached leaves of four-week old Arabidopsis plants.

(G) Desiccation tolerance of *npc4-1* plants. Four-week old soil grown plants were withheld water for ten days. Pictures were taken 4 hours after rehydration.

(H) ABA content of freshly picked seeds. ABA was extracted from tissue using 1-propanol:H₂O:Concentrated HCl (2:1:0.002 v/v) and internal standard d₅ABA was added. ABA content was analyzed by the use of LC/MS/MS. Values are means \pm SD (n=5).

(I) ABA content in desiccated seeds. Values are means \pm SD (n=5).

(J) ABA content of four week old Arabidopsis plants. Values are means \pm SD (n=5).

Figure 6. Expression level of ABA responsive genes in *npc4-1*.

Several ABA responsive genes are down regulated in *npc4-1*. Four week old Arabidopsis plants were treated with 50 μ M ABA and samples were harvested at four intervals. RNA was extracted and quantitative real time PCR was performed. Relative expression is based on the expression of *UBQ10*. Values are means \pm SD (n=3). The experiment was repeated three times under the same conditions with similar results.

Figure 7. Overexpression of *NPC4* and the effects of *NPC4* alteration on seed germination in response to ABA.

(A) Production of Strep-tagged NPC4 in Arabidopsis tissue. Eight over-expression lines were obtained and NPC4-STREP expression was verified by immunoblotting using STREP antibody conjugated with horse radish peroxidase.

(B) Germination of wild-type, *npc4-1*, and *NPC4-OE* in the presence of 1 μ M ABA. Pictures were taken five days after seeds were sown. Values are means \pm SD, (n=3).

(C) Percentage germination on $\frac{1}{2}$ MS and 1 μ M ABA. One hundred seeds were measured. Values are means \pm SD, (n = 3), experiments were repeated three times to ensure reproducibility.

(D) Precocious germination. Freshly picked seeds were germinated on whatmann filter paper and the germination was quantified after seven days. One hundred seeds were measured.

(E) Precocious germination in wild-type, *npc4-1* and *NPC4-OE*. Pictures were taken seven days after seeds were sown.

Figure 8. Growth of wild-Type, *NPC4-KO*, and *NPC4-OE* plants under hyperosmotic stress.

(A) (B) Seed germination on 200 mM NaCl. Fifty seeds per genotype were measured. Values are means \pm SD (n=3). Total germination represents the percentage of radicle

emergence and viable seedlings withstood bleaching and remained green after germination.

(C) Root elongation under hyperosmotic stress. Four day old seedlings were transferred to media containing 0, 100, or 150 mM NaCl or PEG infused plates to -0.25 MPa or -0.45 MPa. Pictures were taken 10 days after transfer.

(D) Root elongation on 0, 100, and 150mM NaCl. On 0mM NaCl no differences were observed between the genotypes. On 100 and 150 mM NaCl OE lines grew better than KO and wild-type.

(E) Biomass production under salt stress. The rosettes from wild-type, *npc4-1* and *NPC4-OE* were harvested on day 10 from plants subjected to salt stress and oven dried for 2 days at 60°C. Dry weight was measured. Values are means \pm SD (n=10).

(F) Root elongation on 1/2MS and PEG plates. PEG plates were prepared by infusing PEG (8000) into solidified agar plates to yield an Mpa of -0.25 and -0.45. Four day old Arabidopsis seedling were transferred from 1/2 MS plates and allowed to grow for 10 days.

(G) Biomass production under drought stress. Values are means \pm SD (n=10).

Figure 9. DAG changes in response to ABA and drought treatment.

(A) Total DAG changes in response to ABA and drought. Four week old soil grown Arabidopsis plants were treated with 50 μ M ABA for one and drought stress was induced by withholding water for ten days. Total lipids were extracted and profiled using tandem ESI/MS/MS. * Denotes that the difference between wild-type and mutant is significant with $P < 0.05$ based on student's t-test. Values are means \pm SE (n=5).

(B) DAG molecular species changes in response to ABA and Drought treatment. * Denotes that the difference between wild-type and mutant is significant with $P < 0.05$ based on student's t-test. Values are means \pm SE (n=5).

Figure 10. Lipid changes in response to ABA and Drought in Arabidopsis leaf tissue.

(A) Four week old soil grown Arabidopsis plants were not watered for 10 days or treated with 50 μ M ABA for one hour and total lipids were extracted and profiled using tandem

ESI/MS/MS. * Denotes that the difference between wild-type and mutant is significant with $P < 0.05$ based on student's t-test. Values are means \pm SE (n=5).

(B) Molecular species of lipids extracted under drought and ABA treatment. * Denotes that the difference between wild-type and mutant is significant with $P < 0.05$ based on student's t-test. Values are means \pm SE (n=5).

Figure 11. DAG and PA attenuate *npc4-1* reduced sensitivity to ABA but DAG kinase inhibitor (DGKI1) does not abrogate *npc4-1* reduced sensitivity to ABA.

(A) Root length of wild-type, *npc4-1*, *NPC4-OE3* and *NPC4*-complemented (COM) plants in response to $\frac{1}{2}$ MS supplemented with 20 μ M ABA in the presence of DAG or PA. 200 μ L of 100 μ M DAG or PA was spread evenly on solidified agar plates. Five-day old seedlings were transferred to agar plates and root length was recorded 12 days after transfer. Values are means \pm SD (n=15).

(B) Root length of wild-type, *npc4-1*, *NPC4-OE3* and *NPC4*-complemented (COM) plants in the presence of 20 μ M ABA and DGKI1 with DAG or PA. 200 μ L of 100 μ M DAG, DGKI1 or PA was spread evenly on solidified agar plates. Five-day old seedlings were transferred to agar plates and root length was recorded 12 days after transfer. Values are means \pm SD (n=15).

(C) Pictures of rescue experiments using DAG, PA, and DGKI1 in the presence of ABA. Pictures were taken 12 days after transfer.

Figure 12. The effect of DGKI1 on PA levels in roots under ABA and Salt Stress

(A) PA content in *NPC4* altered plants and wild-type plants under control and treatment conditions. 200 μ L of 100 μ M DGKI1 was spread evenly on solidified agar plates containing 20 μ M or 100 mM NaCl. Five-day old seedlings were transferred to agar plates and roots were harvested 10 days after transfer. Total lipids were extracted and analysed by ESI/MS/MS. Values are means \pm SD (n=5).

(B) Pictures of wild-type and *NPC4* altered plants under control and treatment conditions. Pictures were taken 10 days after transfer.

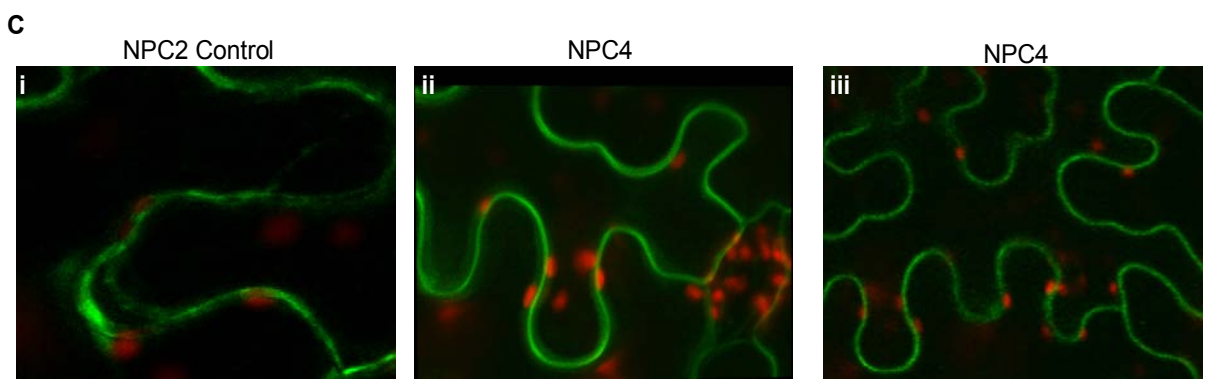
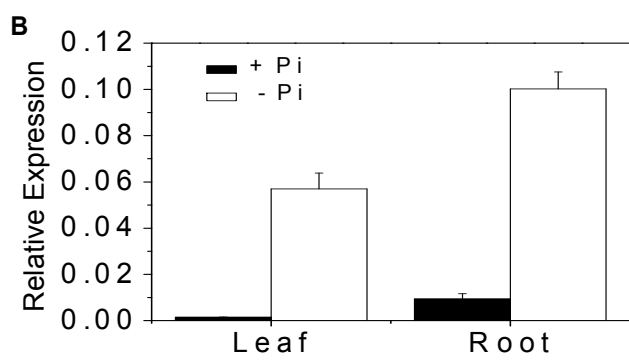
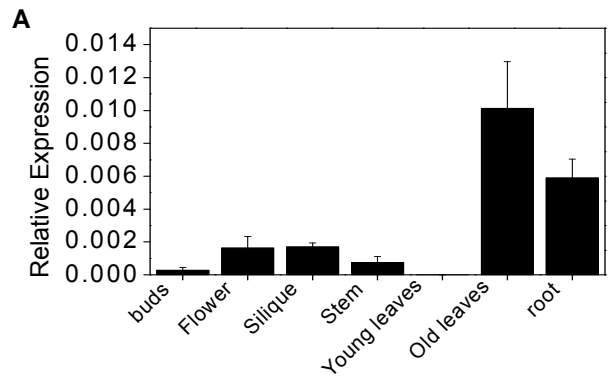


Figure 1

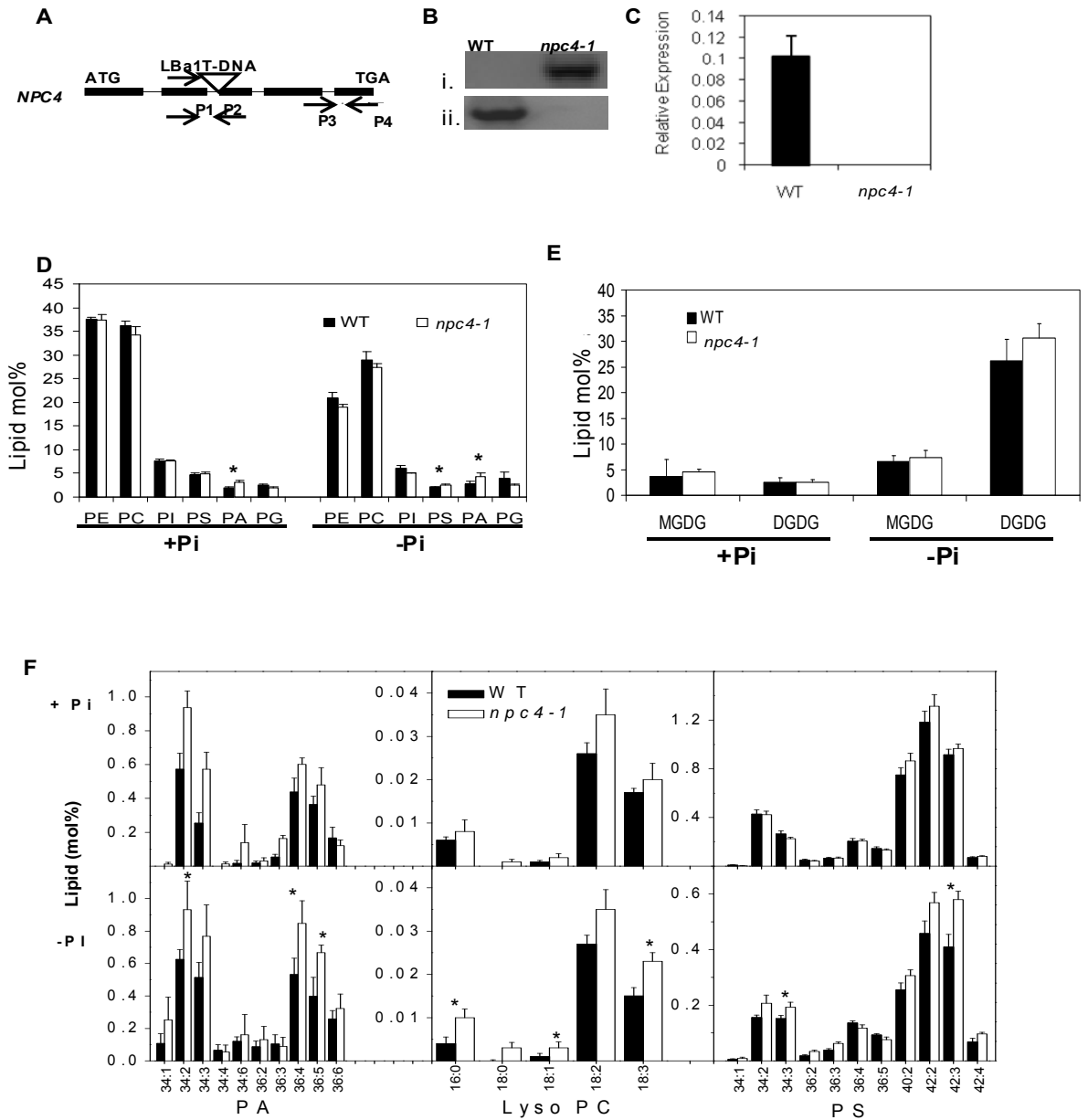


Figure 2

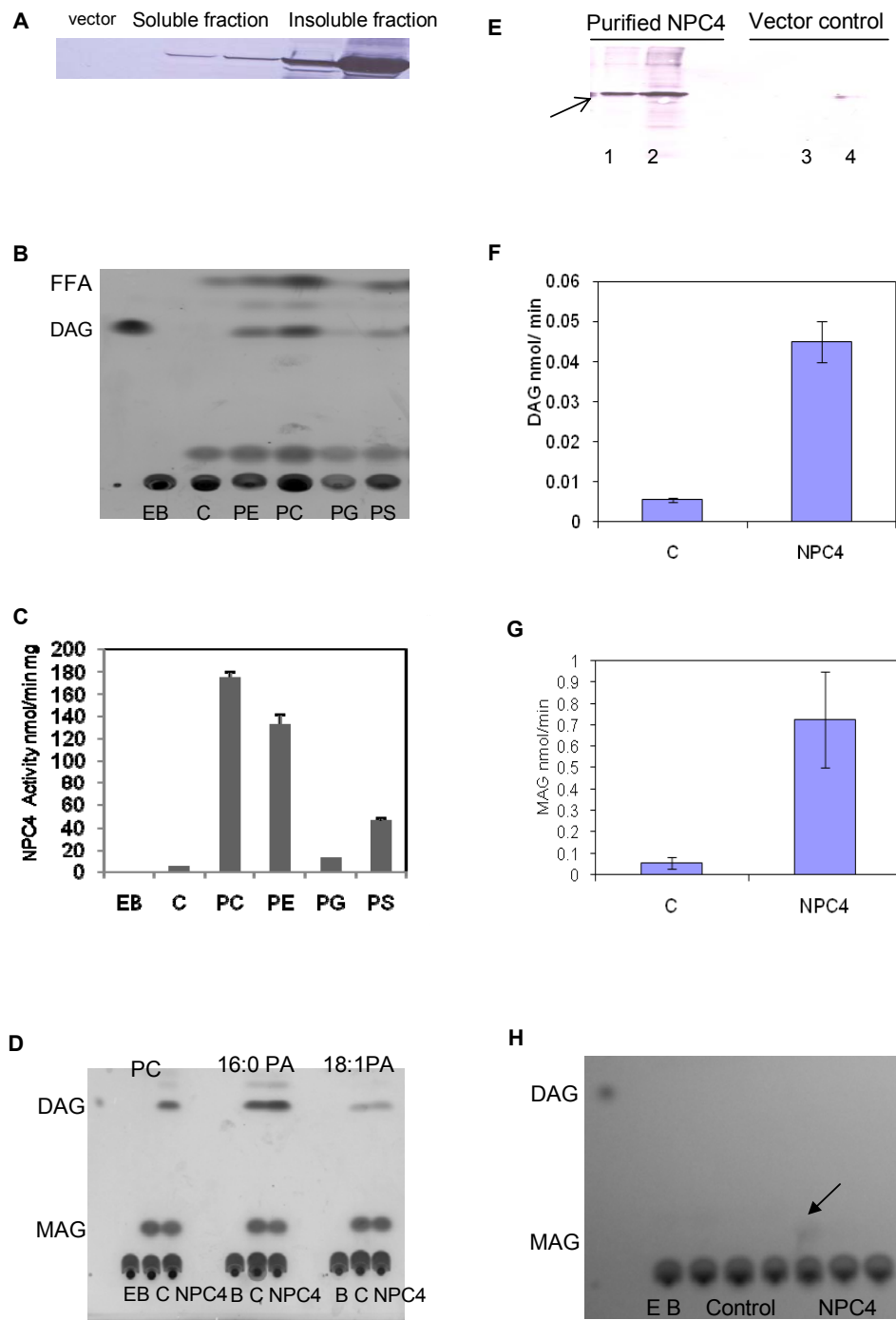


Figure 3

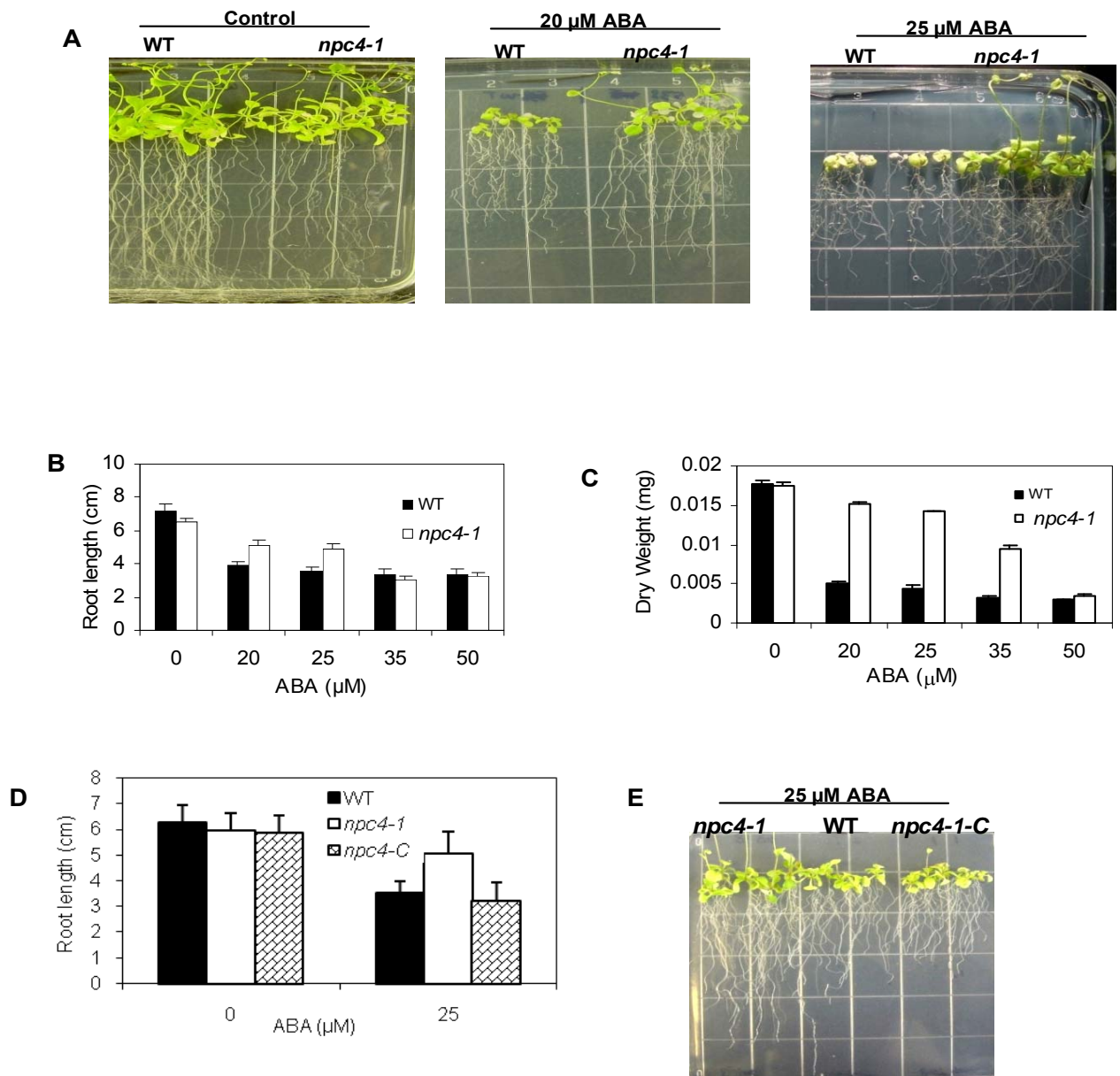


Figure 4

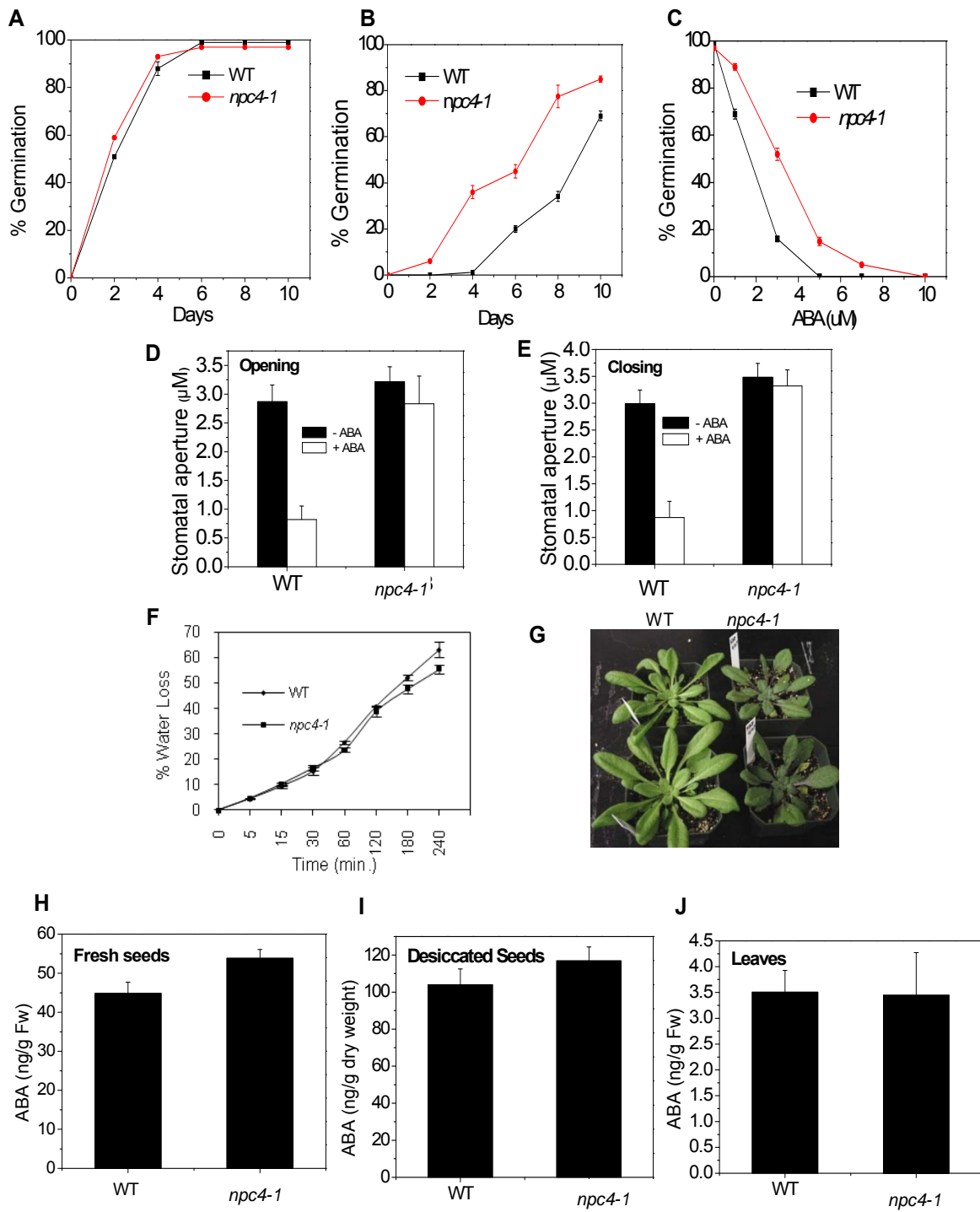


Figure 5

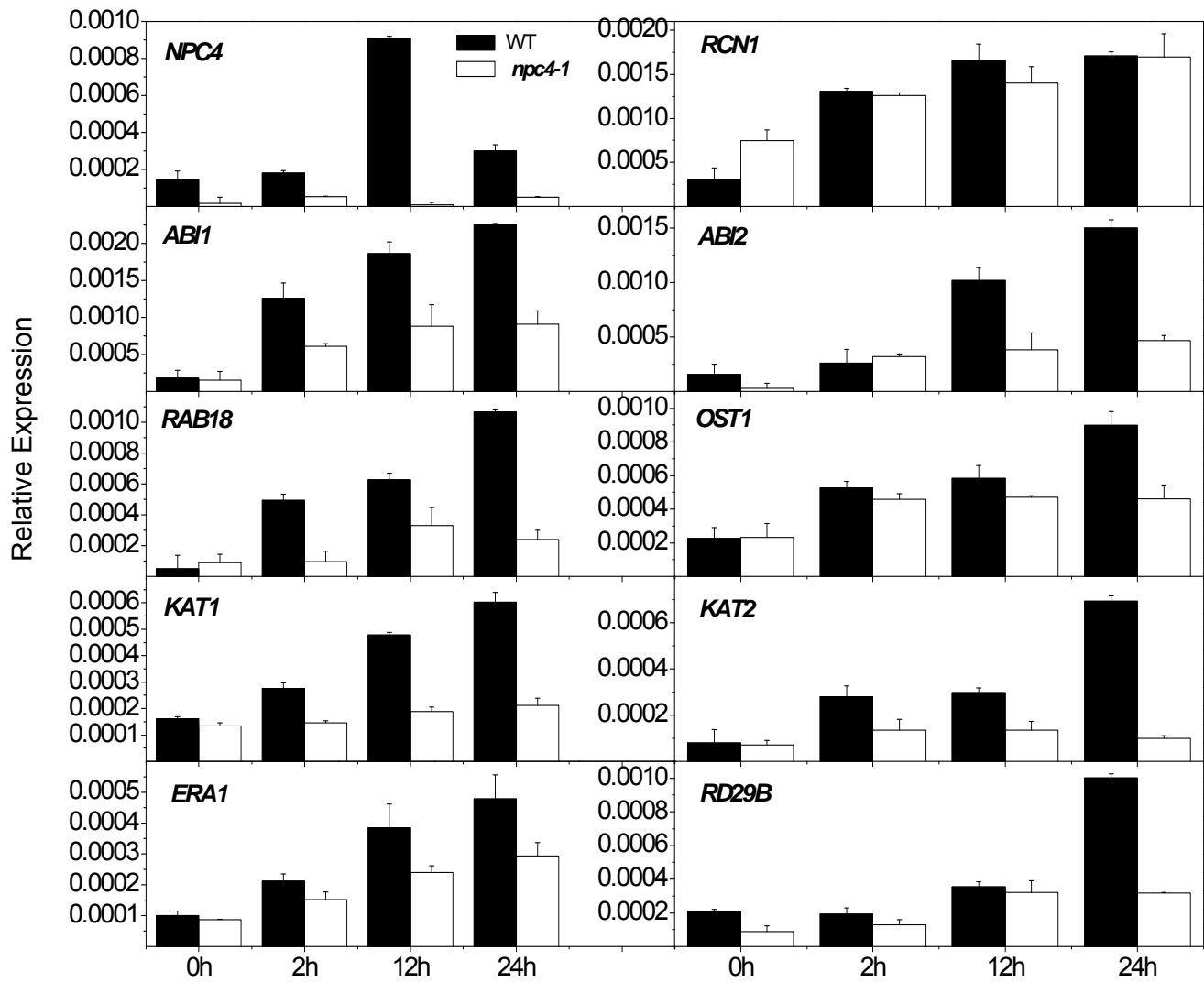


Figure 6

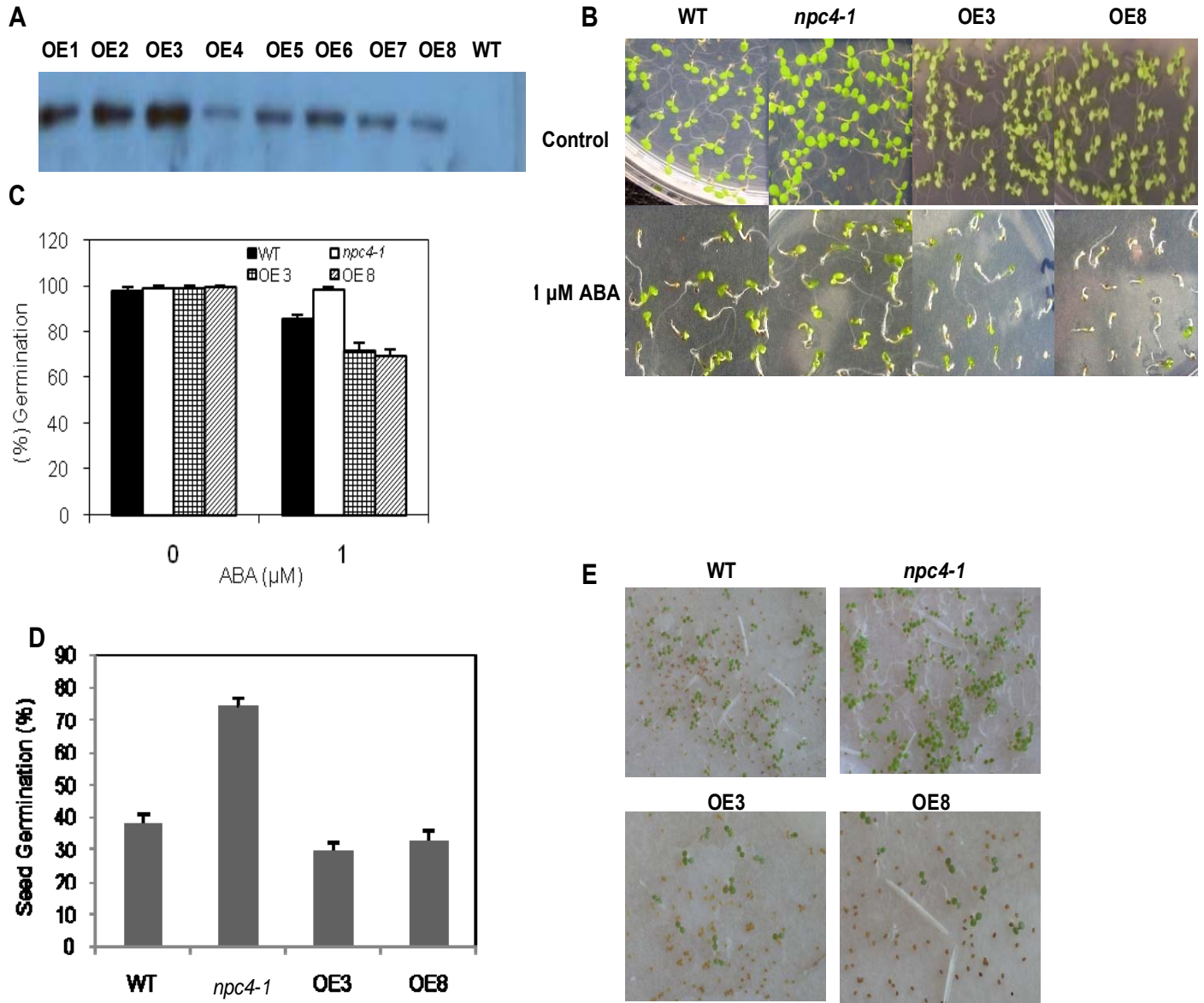


Figure 7

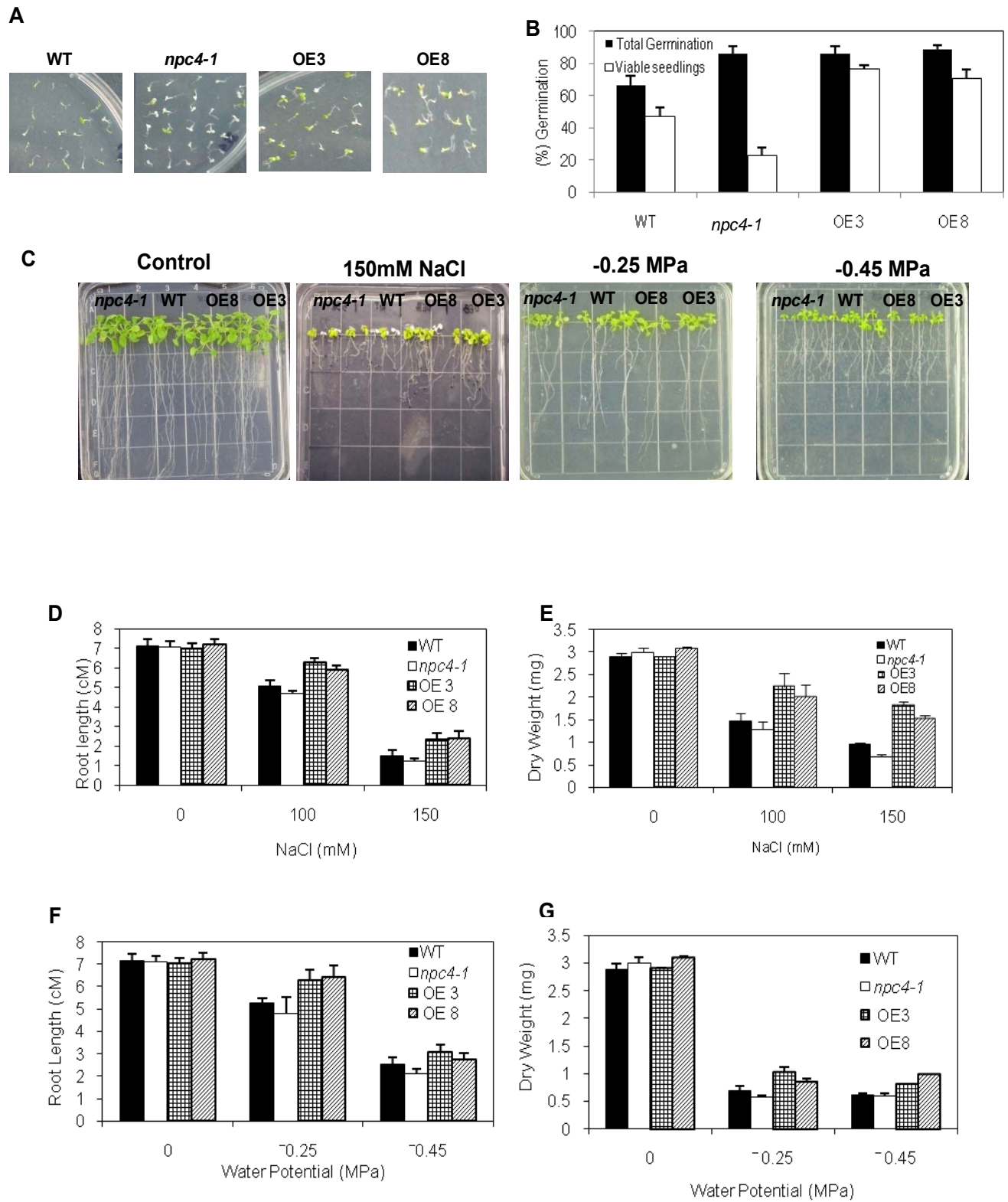


Figure 8

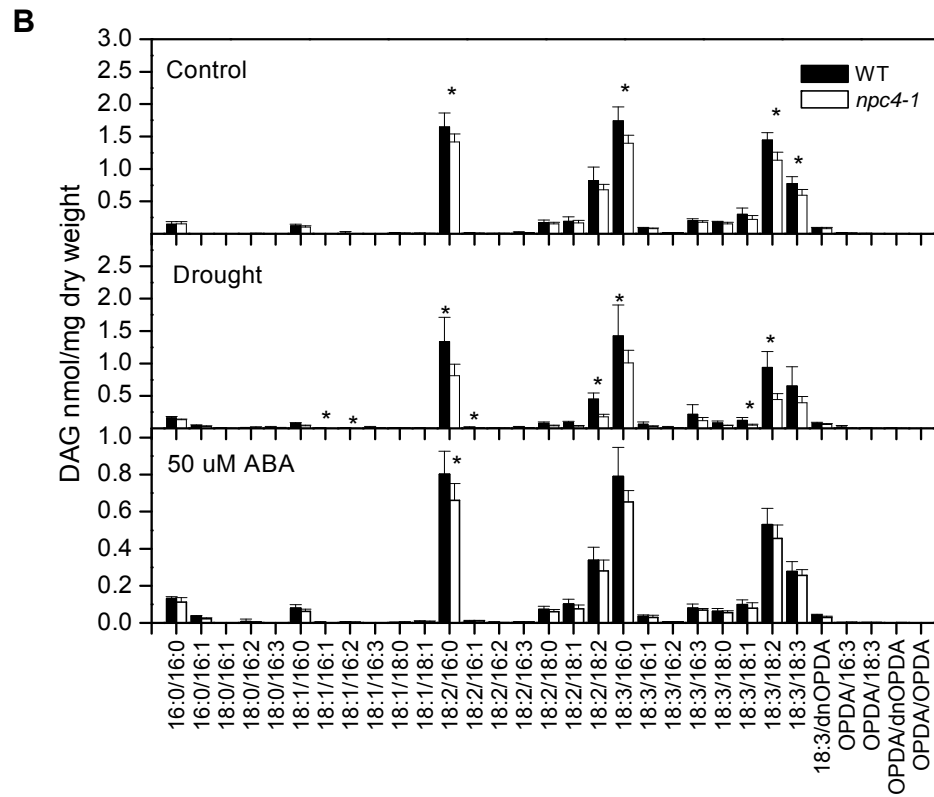
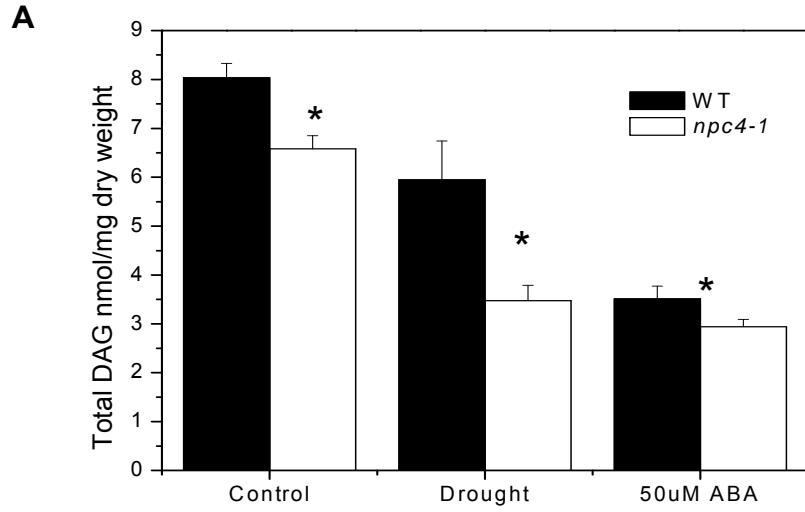
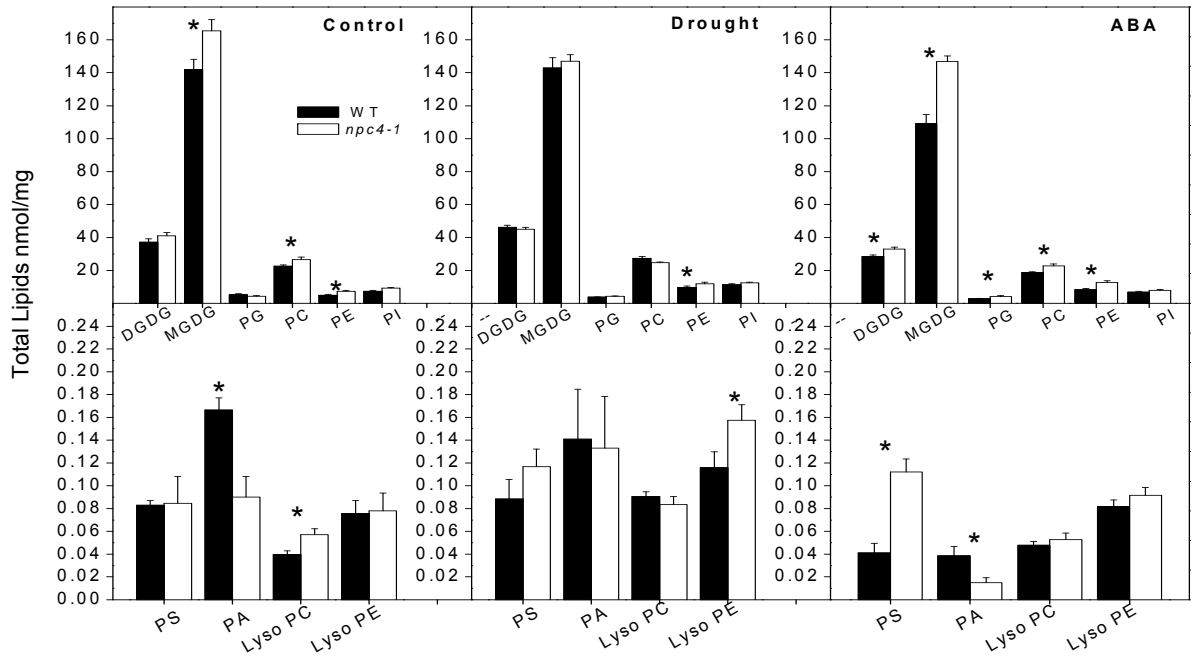
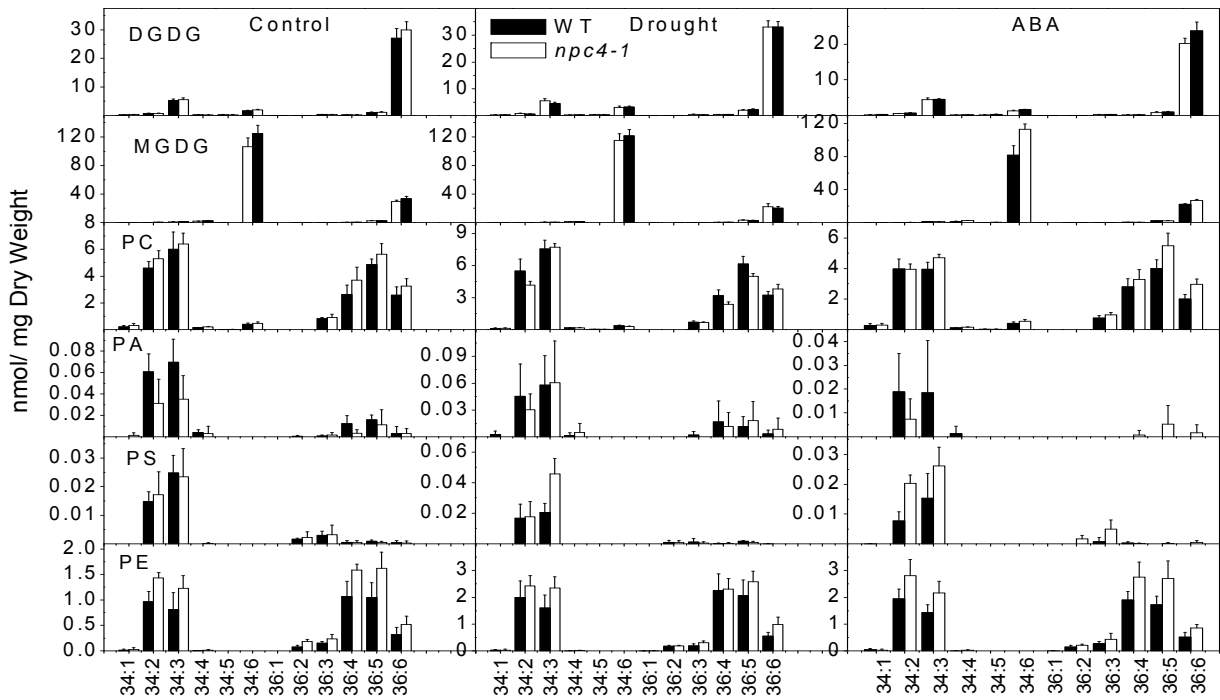


Figure 9

A**B****Figure 10**

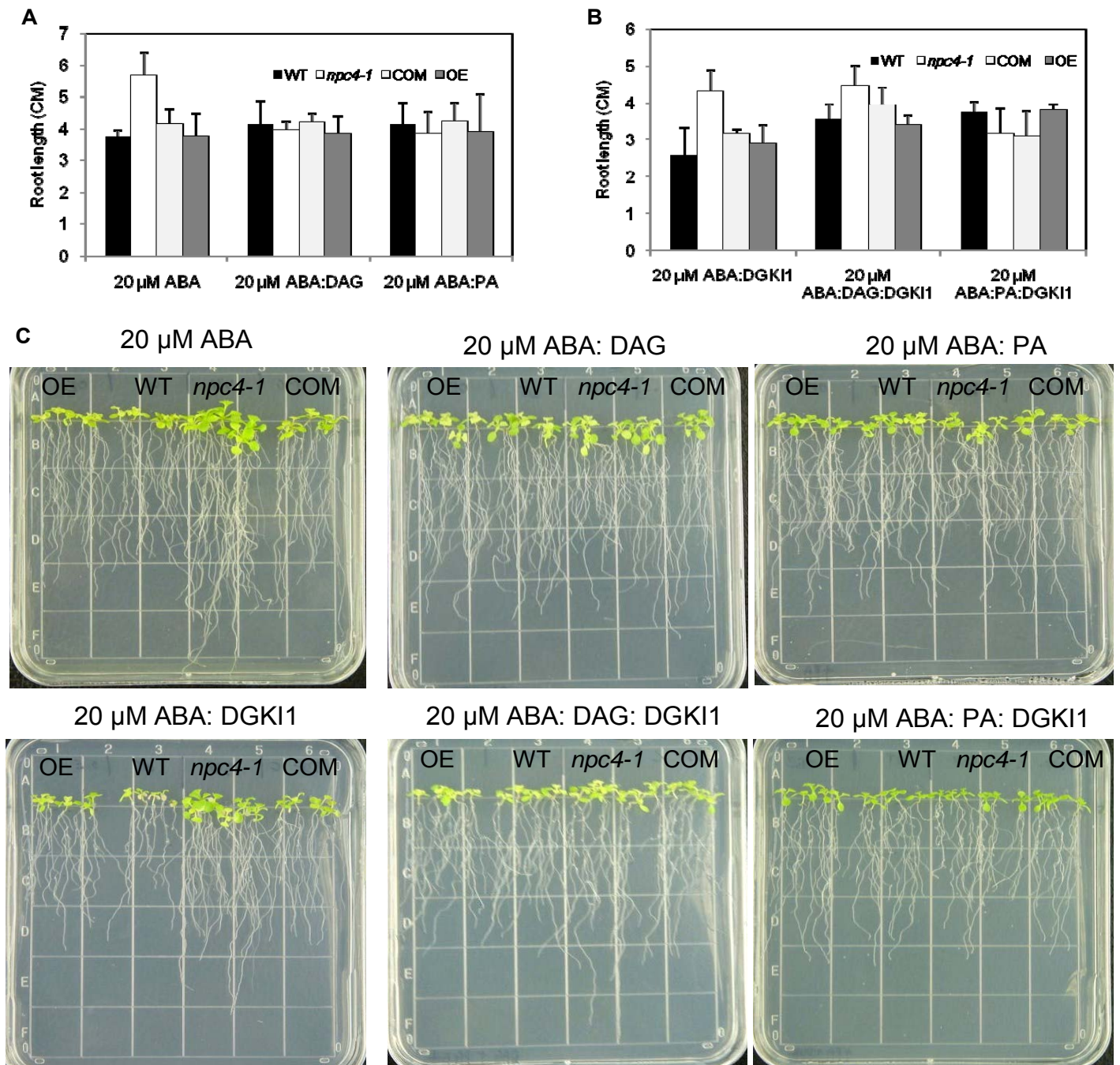


Figure 11

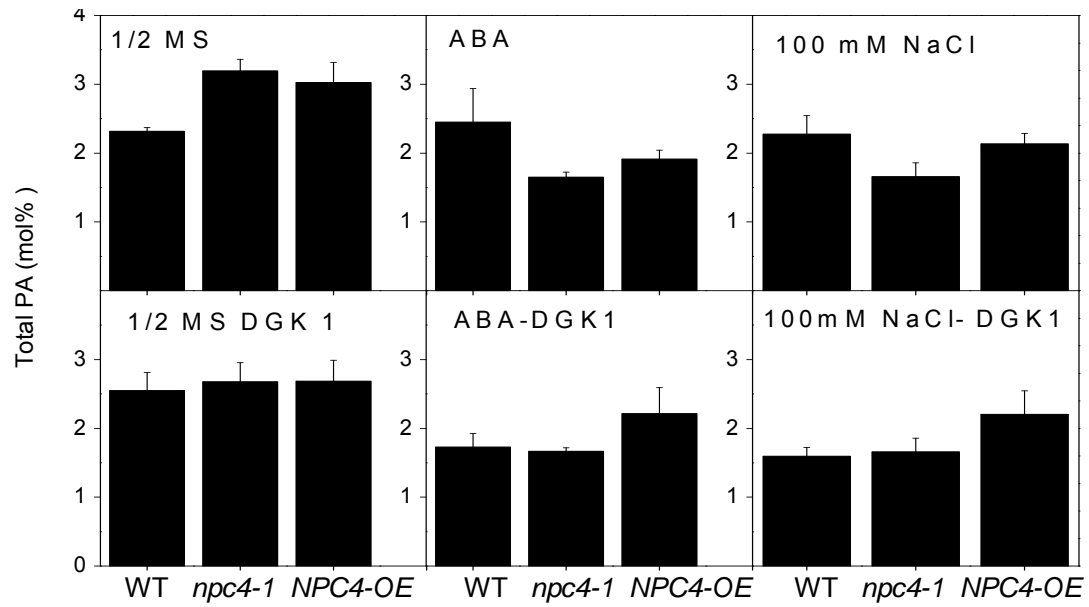
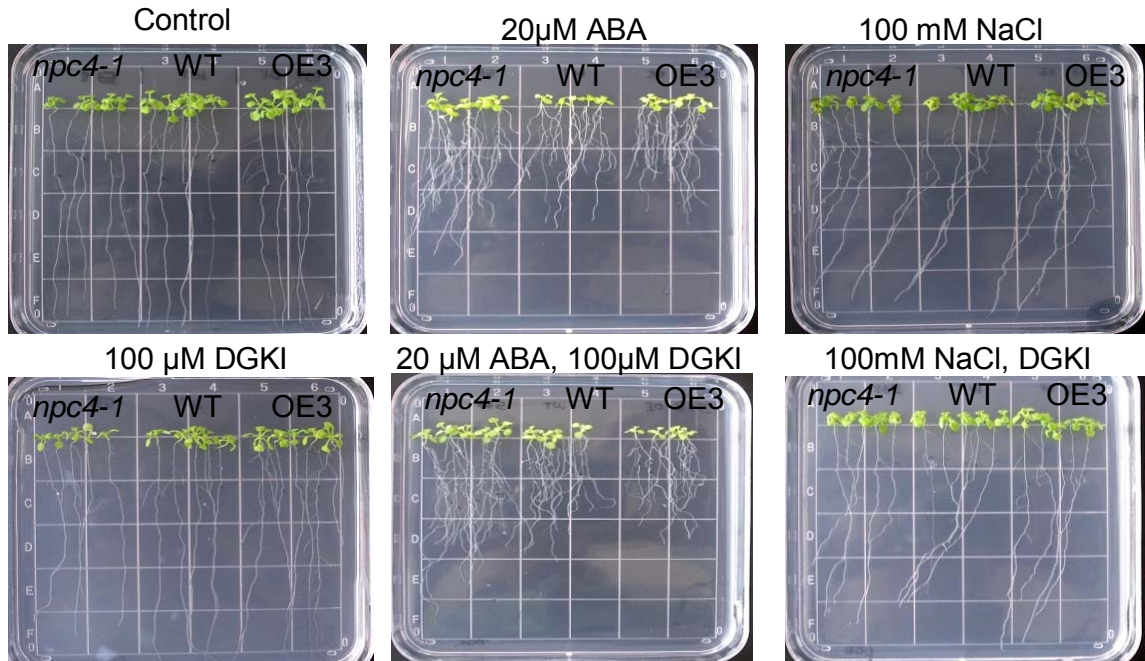
A**B****Figure 12**

Table 1. List of Primers

	Gene	Primer Sequence
Real time PCR- ABA responsive genes	<i>ABI1</i>	Forward 5'-TGTGGTGGTGGTTGATTTGAAGCC-3' Reverse 5'-GCCTCAGTTCAAGGGTTTGCTCTT-3'
	<i>ABI2</i>	Forward 5'-AAGTGTGCGATTTGGCTCGGAAAC-3' Reverse 5'-TCCGGCCATCGCGTTCTTCTTAT-3'
	<i>KAT1</i>	Forward 5'-TGCAAGTGAGAAGTTTGGAGGCTG-3' Reverse 5'-TCAATCTCAGCGTTGTCCGCATTG-3'
	<i>KAT2</i>	Forward 5'-AGTTACCATCCACTTGAAGTCCCG-3' Reverse 5'-GGAAGCAGGAAGGATTATCAGCTTCG-3'
	<i>RAB18</i>	Forward 5'-GCAGTCGCATTCGGTCGTTGTATT-3' Reverse 5'-ACAACACACATCGCAGGACGTACA-3'
	<i>RD29B</i>	Forward 5'-ACAATCACTTGGCACCACCGTT-3' Reverse 5'-AACTCACTTCCACCGGAATCCGAA-3'
	<i>RCN1</i>	Forward 5'-GCGAAGCTGCAGCAAACAACCTAA-3' Reverse 5'-CTGCATTGCCATTTCAGGACCAAAA-3'
	<i>OST1</i>	Forward 5'-TGGAGGAAGACTTAGAGAGCGACCTT-3' Reverse 5'-TGCGTACACAATCTCTCCGCTACT-3'
	<i>ABH1</i>	Forward 5'-AGTTGCGAAGTCGGTGAGAGAGAA-3' Reverse 5'-TGCCGTGAGATAGCCAAGTGTGA-3'
	<i>ERA1</i>	Forward 5'-TGTGGCTCAGCACGCTTGGTTAAA-3' Reverse 5'-ACCCATAATGTCGCGAGTCAAAGG-3'
<i>NPC4</i>	Forward 5'-AGCATCAAATGCTGCTGCTCAACC-3' Reverse 5'-TCCACCCACACACAAGAGAAGTGA-3'	

Chapter 4. Double-knockouts of *NPC3* and *NPC6* are involved in DAG production and accumulation of DGDG under phosphate deprived conditions.

Abstract

It is known that under phosphate-limiting conditions phospholipids are decreased and replaced with non-phosphate containing galactolipids, particularly digalactosidyl-diacylglycerol (DGDG). DGDG accumulates in extraplastidic membranes of both roots and shoots. The Arabidopsis genome contains six non-specific phospholipase Cs (NPCs), which could be involved in hydrolyzing phospholipids to releasing phosphate and diacylglycerol (DAG) for DGDG formation. Of these, *NPC4* was highly induced by phosphate deprivation, but genetic ablation of *NPC4* did not alter DGDG content, and the loss of *NPC5* only affected DGDG accumulation in shoots but not roots in Arabidopsis. Here we show *NPC3* and *NPC6* affect DAG and DGDG accumulation under phosphate deprived conditions. *NPC3* and *NPC6* are active phospholipases, hydrolyzing phosphatidylcholine (PC) and phosphatidylethanolamine (PE) in a calcium-independent manner. *NPC3* is associated with the plasma membrane and *NPC6* with the cytosol. Knockout (KO) of *NPC3* reduces root length under phosphate starvation while KO of *NPC6* increases root length. Double KO of *NPC3* and *NPC6* reduces root elongation under phosphate starvation. KO of *NPC3* results in reduced DAG accumulation by 35%, while *NPC6* accounts for more than 50% of the DAG formed under phosphate deprivation in roots. Double KO of *NPC3* and *NPC6* accumulates 36% less DGDG and 50% less DAG than wild-type roots. These results indicate that *NPC3* and *NPC6* play a role in DAG production for DGDG synthesis under phosphate limiting conditions in Arabidopsis roots.

Introduction

Phosphorous is an essential macronutrient required for plant growth and development. Phosphorous is incorporated in organic compounds such as ATP, phospholipids, nucleic

acids, and proteins (Porier et al., 1991). In times of low phosphate availability, the most profound phenotypic change occurs as the root to shoot ratio of plants increase in attempt to sequester phosphate. Molecular changes also occur, changing transcript levels of RNases and phosphatases to release inorganic phosphate (Clarkson, 1985; Liu et al., 1998). The effects of phosphate deprivation have been extensively characterized on the metabolic and morphological level. It was first observed in nonphotosynthetic bacteria that under phosphate deprived conditions the membrane phospholipids were replaced by nonphosphorous containing lipids (Minnikin et al., 1974). This phenomenon was later observed in plants. At the sub-cellular level phospholipids are replaced with non-phosphate containing membrane lipids such as digalactosyldiacylglycerol (DGDG) sterolglycosides, glycosylceramides and sulfoquinovosyldiacylglycerol (SQDG) (Andersson et al., 2005). The substitution of phospholipids with non-phosphorous lipid is widespread among plant species such as oats (Andersson et al., 2005), soybean (Gaude et al., 2004), and Arabidopsis roots and shoots (Li et al., 2006; Guade et al.; 2008). In plants, the lipid that predominantly replaces phospholipids is DGDG. Lipid replacement has been shown to occur in the plasma membrane (Nakamura et al. 2005), and membranes of plastids (Hartel et al., 2000), mitochondria (Jouhet et al., 2004), and tonoplasts (Andersson et al., 2005).

Phosphate limitation greatly hinders plant growth and productivity. Genetic and biochemical approaches have been used in order to find mechanisms to improve plants performance under phosphate limitation. Genetic approaches seek to identify genes that are upregulated under phosphate deprivation. Several genes involved in phosphate starvation have been identified to date but phosphate signaling pathways in higher plants is still poorly understood. Phosphate response 1 (*PHR1*), a MYB like transcription factor contributes to downstream signaling and regulates a few phosphate starvation inducible genes (Rubio et al., 2001; Bari et al., 2006). *PHO2* and *microRNA399* are downstream of *PHR1*. *PHO2* is a unique ubiquitin like E2 conjugate that is regulated by *microRNA399*. *PHO2* mutants show increased amounts of phosphate in shoots but not in roots. *PHR1* regulates the transcription of *microRNA399* but does not affect all phosphate responses in plants (Bari et al., 2006). Upon phosphate starvation, hundreds of genes are induced

(Mission et al., 2005), but only a small subset of these genes show reversal within 3 hours after phosphate is resupplied (Bari et al., 2006). This small subset of genes is likely to be involved in the primary response. Other genes involved in phosphate starvation are *PHO1* and phosphate under-producer (*PUPI*). *PHO1* is a transporter involved in transporting phosphate from the root cortical and epidermal cells to the xylem (Hamburger et al., 2002). *PHO1*-deficient mutants show reduced phosphate in leaves but not in roots. *PUPI* encodes an acid phosphatase that hydrolyzes phosphate in soil (Trull and Deikman, 1998, Tomscha et al., 2004). *WRKY75*, a transcription factor involved in phosphate starvation response, modulates root growth and affect the expression of phosphatases and high affinity phosphate transporters (Devaiah et al., 2007). More recently, members of the AMP/SnRK1/SNF1 family were shown to play a signaling role in phosphate starvation (Fragoso et al., 2009).

One of the main biochemical approaches looks at the changes in glycerolipid metabolism and content. The most common glycerolipids in plants include phosphatidylcholine (PC), phosphatidylethanolamine (PE), phosphatidylinositol (PI), phosphatidylglycerol (PG), phosphatidylserine (PS), phosphatidic acid (PA), monogalactosyldiacylglycerol (MGDG), and digalactosyldiacylglycerol (DGDG). PC is the most abundant phospholipid in extraplastidic membranes. PC is also the transient acyl carrier in the synthesis of DGDG under phosphate starvation in oats (Tjellstrom et al., 2008). DGDG is synthesized through the addition of galactose from UDP-galactose to MGDG and this reaction is catalyzed by *DGDI* and *DGD2* synthases (Hartel et al., 2000; Kelly and Dormann 2002). In Arabidopsis, *MGDI*, *MGD2*, and *MGD3* encode MGDG synthases that produce MGDG by transferring a galactose from UDP-galactose to diacylglycerol (DAG) forming MGDG (Awai et al., 2001).

Under phosphate-starved conditions, there is a concomitant decrease in phospholipids and an increase in DAG and DGDG (Johet et al., 2003). Changes in lipid metabolism involve lipid-metabolizing and lipid-signaling enzymes. Phospholipase D (PLD) cleaves phospholipids to produce PA and a free head group. Double knockouts of *PLD ζ 1* and *PLD ζ 2* show a decrease in PA content and DGDG accumulation (Li et al., 2006; Cruz-

Ramirez et al., 2006). Recent reports show that a novel group of enzymes, non-specific phospholipase Cs (NPCs) is also involved in phospholipid degradation under phosphate deprivation. There are six NPCs in Arabidopsis. *NPC4* is greatly induced by phosphate deprivation but does not significantly affect DGDG accumulation in roots (Nakamura et al., 2005). *NPC5* affects DGDG accumulation in Arabidopsis shoots but not roots (Gaude et al., 2008). In this report we characterized two NPCs from Arabidopsis, *NPC3* and *NPC6*. These two enzymes play a role in Arabidopsis response to phosphate deprivation. Double knockouts of *NPC3* and *NPC6* had an additive effect on DAG production and DGDG accumulation under phosphate deprived conditions.

RESULTS

Expression Levels and Sub-cellular Localization of *NPC3* and *NPC6*

To determine the steady state expression of *NPC3* and *NPC6* transcripts, quantitative real time PCR was performed on various organs of 6-week old soil grown Arabidopsis plants. Transcripts of both *NPC3* and *NPC6* were detected in roots and siliques (Figure 1A). The highest level of expression of *NPC3* was found in roots followed by stems and old leaves. Transcripts of *NPC3* were barely detectable in young leaves, inflorescences, siliques and flowers. The highest level of expression of *NPC6* was observed in siliques followed by roots, flowers, and inflorescences (Figure 1A). To test whether *NPC3* and *NPC6* are upregulated by phosphate deprivation, quantitative real time PCR was performed. The transcript level of *NPC3* and *NPC6* in shoots under normal growth conditions was comparable but higher than that of *NPC4* (Figure 1B). In roots, the transcript level of *NPC3* is two-fold greater than *NPC6*. Under phosphate-deprivation, *NPC3* expression increased by two fold in shoots and an increase also occurred in roots. *NPC6* expression is not significantly affected by phosphate deprivation. In agreement with these findings are previous reports that showed by northern analysis, *NPC4* is the most induced of the NPCs under phosphate deprivation followed by *NPC5*. Transcripts of *NPC3* and *NPC6* were low and barely detectable (Nakamura et al., 2005).

To determine the subcellular localization of *NPC3* and *NPC6*, the cDNA were C-terminally fused to GFP and transiently expressed in tobacco leaves. The vector was used

as a negative control and NPC4-GFP as a positive control. The sub-cellular localization of NPC3-GFP, NPC4-GFP and NPC6-GFP was analyzed by confocal microscopy. The negative control displayed a diffuse fluorescence pattern. NPC4 is associated with the plasma membrane (Nakamura et al., 2005; Gaude et al., 2008). NPC3 is largely localized to the plasma membrane but a small portion could be detected in the cytosol (Figure 1C). NPC6, on the other hand, had a diffuse intracellular fluorescence pattern and several GFP points were observed, indicating that NPC6 is mostly cytosolic but may also be associated with organelles (Figure 1C).

Double KO of *NPC3* and *NPC6* Reduces Primary Root elongation under Phosphate Starvation

To determine the physiological function of *NPC3* and *NPC6* in Arabidopsis, we isolated T-DNA insertional mutants in Columbia ecotype. Mutants were obtained from ABRC (Ohio State University). *NPC3* has five exons and bears a T-DNA insert in the fourth exon (Figure 2A). *NPC6* has three exons and carries the T-DNA insertion in the second exon (Figure 2B). Double mutants were generated by crossing single homozygous *npc3-1* and *npc6-1* mutants. Homozygous double knockout (KO) mutants were identified and isolated in the F3 generation (Figure 2C). We also produced *NPC3*-overexpression (OE) and *NPC6*-OE, in which the C-termini of the NPCs were fused with a STREP-tag under the control of the cauliflower mosaic virus 35S promoter. The KO plants were confirmed by PCR and the OE plants were confirmed by immunoblotting with anti-STREP antibody. The KO and OE lines were used to investigate the potential effects of NPCs on plant response to phosphate starved conditions.

Seeds were germinated on ½ Muskashige and Skoog (MS) agar media, and 5 day old seedlings were transferred to plates containing 500 μ M or 0 μ M phosphate. On 500 μ M phosphate, there was no difference in root growth among *npc3-1*, *npc6-1*, *npc3-1npc6-1*, *NPC3-OE*, *NPC6-OE* and wild-type plants (Figures 2D and 2E). On 0 μ M phosphate, *npc3-1* roots were ~10% shorter than wild-type roots while *npc6-1* roots were ~12% longer than wild-type roots. *NPC3-OE* roots were 8% longer than wild-type roots while *NPC6-OE* were 10% shorter than wild-type roots (Figures 2D and 2E). The opposite

phenotypes observed on the single KO and OE indicate that both *NPC3* and *NPC6* affect plant response to phosphate deprivation, but their functions are different. When both were abrogated, the primary root growth of *npc3-1npc6-1* was reduced; the primary root length was reduced by 41% compared to wild-type roots (Figures 2D and 2E).

NPC3 and NPC6 are Involved in DGDG Accumulation and PC Degradation During Phosphate Deprivation

To investigate the effect of *NPC3* and *NPC6* on lipid metabolism under phosphate starvation, glycerophospholipids and galactolipids were analyzed by ESI-MS/MS. In wild-type leaves, the amount of DGDG increased 15% from 16 mol% to 19 mol% during phosphate starvation (Figure 3). A similar increase was observed in DGDG in *npc3-1* leaves. In *npc6-1* leaves, the DGDG increased to 18 mol% and the increase was 6% less than that in wild-type leaves. Even though the difference was small, it is significantly lower than wild-type leaves. The DGDG content in *npc3-1npc6-1* leaves was similar to wild-type under phosphate deprivation. The result suggests that NPC3 does not affect DGDG accumulation in leaves and NPC6 contributes to some extent to DGDG accumulation in leaves.

In roots, upon phosphate starvation the DGDG content in wild-type increased by four fold from 2.5 mol% to 10 mol%. A similar increase was observed in *npc3-1* and *npc6-1* plants. The accumulation of DGDG was impaired in *npc3-1npc6-1* roots, which only increased from 2 mol% to 6.5 mol%. The molecular species that were significantly affected in *npc3-1npc6-1* were 36:5 and 36:6 DGDG (Figure 4). The DGDG content in *npc3-1npc6-1* was 36% lower than wild-type levels, suggesting that NPC3 and NPC6 are responsible for one third of the DGDG accumulation in roots under phosphate deprivation. The MGDG content in *npc3-1* was 60% of wild-type levels, suggesting that NPC3 may be involved in MGDG accumulation under normal conditions. The MGDG content was also affected under phosphate starvation in *npc6-1* roots compared to wild-type, while *npc3-1* and *npc3-1npc6-1* were similar to wild-type. Wild-type increased from 9 mol% to 13 mol% while *npc6-1* increased from 9 mol% to 16 mol% (Figure 4). *npc6-1* had 23% more MGDG than wild-type roots under phosphate deprivation.

The increase in galactolipids was accompanied by a decrease in phospholipids. In leaves, the decrease in major phospholipids content was not affected in *npc3-1*, *npc6-1* and *npc3-1npc6-1*. In roots, under normal growth conditions, the PC level in *npc3-1* and *npc6-1* was 12% and 10%, respectively, higher than wild-type, whereas *npc3-1npc6-1* was 5% higher than wild-type. This data indicates that NPC3 and NPC6 are involved in phospholipid turnover under normal conditions. Under phosphate sufficient conditions, PA levels were significantly higher in *npc3-1* and *npc3-1npc6-1* roots (Figures 3 and 4). PA levels in *npc6-1* were comparable to wild-type. During phosphate starvation, PC levels were reduced similarly in wild-type, *npc3-1* and *npc6-1* roots. However, *npc3-1npc6-1* had 23 % more PC compared to wild-type roots. PE levels were 12 % higher in *npc3-1* roots than wild-type roots. Additionally, PE levels were slightly elevated in *npc6-1* and *npc3-1npc6-1*. These results indicate that NPC3 and NPC6 have overlapping functions in the degradation of phospholipids under phosphate limited conditions, as the single KOs were similar to wild type and the double knockout had higher levels than wild-type .

Disruption of NPC3 and NPC6 affect Lysophospholipids Content

Lysophospholipids are signaling molecules, and it was recently determined that lysolipids are reduced under phosphate starved conditions (Li et al., 2006). Under normal growth conditions, the level of lysoPG (LPG), lysoPC (LPC) and lysoPE (LPE) was elevated in the leaves of *npc3-1npc6-1* as opposed to wild-type (Figure 5). The molecular species elevated in *npc3-1npc6-1* were 16:0, 18:0, 18:2 and 18:3 LPC (Figure 6). The LPC content was also higher in *npc3-1* leaves than wild-type. No differences were observed for *npc6-1*. Upon phosphate deprivation, LPC in *npc3-1npc6-1* was higher than wild-type leaves. The molecular species elevated in *npc3-1npc6-1* under phosphate starvation was 16:0 (Figure 6). LPE was higher in *npc3-1* than wild-type leaves (Figure 6). No differences were seen in *npc6-1* compared to wild-type leaves. In Arabidopsis roots, under phosphate sufficient conditions, *npc3-1* and *npc3-1npc6-1* contained higher levels of LPC than wild-type. *npc3-1* contained higher levels of 16:0, 18:2 and 18:3 LPC compared to wild-type. *npc3-1npc6-1* contained higher levels of 16:0 LPC (Figure 6). A

higher level of LPE was also observed in *npc3-1*, with molecular species 16:0 being elevated. No differences were seen in *npc6-1* compared to wild type. Induction of phosphate starvation did not result in any significant changes among the genotypes, even though LPC and LPE remained higher than wild type in *npc3-1* plants. These data suggest that under normal and phosphate limited conditions, NPC3 plays a more pivotal role in degradation of lysophospholipids than NPC6.

NPC3 and NPC6 are Involved in DAG Production under Phosphate Limitation

To investigate the metabolic consequences of ablating *NPC3* and *NPC6* on DAG content, the direct lipid product of NPC, we quantitatively profiled the DAG content of *npc3-1*, *npc6-1*, *npc3-1npc6-1* and wild-type plants under phosphate sufficient and deficient conditions. Under standard phosphate conditions, *npc3-1* and *npc3-1npc6-1* leaves DAG content was ~55% of wild-type leaves. DAG content in *npc6-1* was 75% that of wild type leaves (Figure 7A). These differences in DAG content were due primarily to molecular species 18:2/16:0, 18:3/16:0 and 18:3/18:2 (Figure 7B). Under phosphate starved conditions DAG levels were reduced in wild-type leaves but no significant differences were observed among the genotypes.

In roots no differences in total DAG content was seen among the genotypes under phosphate-sufficient conditions (Figures 6A and 6B). Upon phosphate starvation a two fold increase in DAG was seen in wild-type plants. This increase in DAG was not observed in *npc3-1*, *npc6-1* and *npc3-1npc6-1*. Moreover, the DAG content in these genotypes were lower than wild-type levels. *npc6-1* and *npc3-1npc6-1* contained 46% the DAG of wild type roots. *npc3-1* contained ~65% the DAG of wild-type roots. These results indicate that NPC6 is responsible for more than 50% of DAG accumulation in roots under phosphate starvation. Therefore NPC6 contributes more to the DAG pool than NPC3 under phosphate starvation in roots.

NPC3 and NPC6 Encode Active Phospholipases that Use PE and PC as Substrates

To test whether *NPC3* and *NPC6* encode active PLCs, the cDNA was N-terminally fused with Histidine (His) and expressed in *E. coli*. The expression of NPC3 and NPC6 was

detected by immunoblotting with anti-His antibody conjugated with alkaline phosphatase (AP) (Figure 8A). Activity assay was performed as previously described by Nakamura et al., (2005). An empty vector control was used to discern background PLC activity. NPC3 and NPC6 hydrolyzed PC and PE in the absence of calcium. The activity of NPC3 towards PE was four fold higher than PC (Figure 8B). NPC6 activity toward PC was two fold higher than PE. NPC3 was 5 fold more active toward PC than NPC6, and 40 fold more active toward PE than NPC6 (Figure 8B). These results indicate that *NPC3* encodes a more active phospholipase than *NPC6*.

Discussion

Phosphorous is an essential macronutrient that is important for plant growth and development (Raghothama, 2000). As a result, when plants are grown on phosphate limiting conditions distinct morphological and metabolic changes occur. The most prominent morphological change is that the root system becomes enlarged to increase the root surface area to obtain phosphate (Lynch, 1995). In this report, we show that *NPC3* and *NPC6* are involved in primary root growth modification and these two PLC gene products have both overlapping and unique functions. The loss of both *NPC6* and *NPC3* reduces primary root growth (Figures 2D and 2E), and the loss of either *NPC3* or *NPC6* results in lower DAG content in roots but not shoots under low phosphate conditions (Figure 7) . The loss of *NPC3* reduces primary root growth, but the loss of *NPC6* increases primary root growth under phosphate deprivation while overexpression of each gene has the opposite effect.

Under phosphate-limiting conditions, prominent metabolic changes include increases in the activity of DGDG-synthesizing enzymes such as DGD1 and DGD2, (Hartel et al., 2000; Gaude et al., 2008) and of enzymes that degrade phospholipids. Of the six NPCs in Arabidopsis, *NPC4* and *NPC5* were previously cloned and characterized. NPC4 does not affect DGDG accumulation in roots and leaves while NPC5 accounts for 50% of the DGDG pool in leaves under phosphate starvation (Nakamura et al. 2005; Gaude et al., 2008). NPC3 bears 64% amino acid identity to NPC4. The basal level of *NPC4* is lower than both *NPC3* and *NPC6* in root and shoots under normal conditions. Under control

conditions, NPC4 does not impact the phospholipid composition, whereas NPC3 and NPC6 hydrolyze PC, the major membrane phospholipid (Figures 3 and 4). The reason for the low level of expression of NPCs could be due to their potential toxicity especially in photosynthetic tissues (Nakamura et al., 2005). *NPC3* and *NPC6* are not greatly induced by phosphate deprivation compared to *NPC4* (Figure 1B). However, ablation of both *NPC3* and *NPC6* decreases the accumulation of DGDG and MDGD in response to phosphate starvation. PC degradation was impaired in *npc3-1npc6-1* and other lipids, such as PI, PS, and PG were increased. These results show that NPC3 and NPC6 are involved in bulk phospholipid degradation under normal and phosphate starved conditions.

These data show that *NPC3* and *NPC6* are differentially expressed in Arabidopsis tissues (Figure 1A). *NPC3* is highly expressed in roots, whereas *NPC6* is highly expressed in aerial tissues. Consistent with their expression pattern, NPC3 does not affect lipid composition in aerial tissue, whereas NPC6 modestly affects DGDG accumulation in leaves. The subcellular localization of NPC3 and NPC6 also varies; NPC3 is mostly associated with the plasma membrane and NPC6 is in the cytosol. The fact that NPC3 largely localizes to the plasma membrane suggests that it is involved in the local degradation of plasma membrane phospholipids. Thus, DAG accumulation in *npc3-1* roots under phosphate starvation is not severely impaired as in *npc6-1*, which is cytosolic and can associate with various organelles. In addition a small portion of NPC3 is cytosolic while NPC6 is localized in the cytosol. Their cytosolic localization may provide a means by which NPC3 and NPC6 target different cellular membranes, since the association of these enzymes with the membrane is required for phospholipid degradation. The cytosolic localization of NPC6 causes greater impact on the DAG composition under phosphate starvation in roots than NPC3. No additive effect was observed on DAG content when both genes were ablated. Translocation of phospholipases to the membrane is not uncommon and is widespread among species. Activation of PLD in castor bean by wounding led to translocation from the cytosol to the membrane (Ryu and Wang, 1996).

The DGDG composition was lower in *npc3-1npc6-1* but not in *npc3-1* and *npc6-1*, indicating the overlapping functions of these genes. The molecular species of DGDG accounting for this difference is due mainly to 36:5 and 36:6. In Arabidopsis DGDG can be made from the plastidic pool, the ER extraplastidic pool or the ER plastidic pool (Li et al., 2006; Somerville 2000). 36 carbon DGDGs are derived from the eukaryotic pathway, whereas 34 carbons come from the prokaryotic pathway (Hartel et al., 2000). Differences in DAG in *npc6-1* and *npc3-1npc6-1* phosphate starved roots stemmed mainly from differences in 18:2/16:0, 18:3/16:0 and 18:3/18:2. Taken together, these results suggest that NPC6 affects both the prokaryotic and eukaryotic pathways involving DAG production and DGDG synthesis.

Materials and Methods

Mutant Isolation

Arabidopsis (Columbia-0) was used in this study. Mutants were obtained from ABRC (Ohio State University). PCR was used to confirm the presence of T-DNA in the F2 generation. Homozygous mutants were identified using gene specific primers NPC3 5'-CGTGGACAGTTGGACACATGC-3'(forward); NPC3 5'-TTCGGGATCTAAACCG GGAAA-3'(reverse); NPC6 5'-GAATCCAAGGCGAAACCATAATGGT-3' (forward), NPC6 5'-CAGTAAACCCGACAATAAACGGT-3' (reverse) and LBA1 5'TGGTTCAC GTAGTGGGCCATC3'.

To generate *npc3-1npc6-1* double mutants, homozygous *npc3-1* was crossed to homozygous *npc6-1* plants. F1 plants were self-pollinated and F2 plants were screened for homozygous double mutants. Homozygous plants were self-fertilized and further verified to be homozygous in F3 generation.

Plant Growth conditions

For phosphate treatments, seeds were surface sterilized and sown on ½ MS medium under a 12-h-day/12-h-night at 22°C. Seedlings were transferred to a modified medium

(Li et al., 2006). The medium contained 60 mM MES 1.25 mM KNO₃, 1.5mM Ca(NO₃)₂, 0.75 mM MgSO₄, 0.5 mM KH₂PO₄, 75 μM FeEDTA, 50 μM H₃BO₃, 10 μM MnCl₂, 2 μM ZnSO₄, 1.5 μM CuSO₄ and 0.075 μM (NH₄)₆Mo₇O₂₄. For phosphate starved media, no KH₂PO₄ was added. For phenotypic analysis, plants were grown on a modified ¹/₁₀ MS medium under a 12-h-day/ 12-h-night at 22°C as described by Lopez-Bucio et al. (2002). Briefly, the basic medium contained 2.0 mM NH₄NO₃, 1.9 mM KNO₃, 0.3 mM CaCl₂.2H₂O, 0.15 mM MgSO₄.7H₂O, 5 μM KI, 25 μM H₃BO₃, 0.1 mM MnSO₄.H₂O, 0.3 mM ZnSO₄.7H₂O, 1 μM Na₂MoO₄.2H₂O, 0.1 μM CuSO₄.5H₂O, 0.1 μM CoCl₂.6H₂O, 0.1 mM FeSO₄.7H₂O, 0.1 mM Na₂EDTA.2H₂O, inositol (10 mg L⁻¹), and Gly (0.2 mg L⁻¹). Low P (0 μM NaH₂PO₄) or high P (0.5 mM NaH₂PO₄), pH 5.7, 0.5% (w/v) Suc, and 1% (w/v) agar.

Lipid Extraction and Profiling:

The process of lipid extraction, lipid analysis and quantification was performed as described by Welti et al. (2002). Rosettes and roots were excised from 2-week old Arabidopsis plants and immersed immediately in 3 mL hot isopropanol containing 0.01% butylated hydroxytoluene at 75°C. Samples were kept at 75°C for 15 min and 1.5 mL of chloroform and 0.6 mL water of were added. Samples were place on a shaker for 1 h, and the solvent was transferred to a new tube. The samples were reextracted using chloroform:methanol (2:1) for at least 4 times for 30 min each on a shaker. The lipid extracts were combined and washed with 1 M KCl followed by washing with 1 mL water. The solvent was dried under a stream of nitrogen gas and the remaining tissue was oven dried at 100°C and weighed. Lipids composition was analyzed by an electrospray ionization triple quadrupole mass spectrometer (API4000). Data was analyzed using Q-test to remove aberrant data points followed by student's t-test to determine significance.

Enzyme Activity Assay of NPC3 and NPC6 expressed in *E.coli*

NPC3 and *NPC6* cDNA were amplified from 5'RACE pollen cDNA library using Phusion high fidelity Taq polymerase. The PCR product was cloned into pCR® 2.1-

TOPO® (Invitrogen) vector to screen for a positive clone. A positive clone was selected, purified and cloned into pET28a(+) expression vector under the T7 promoter and transformed into *E. coli* Rosetta (DE3). To induce the expression of NPC3 and NPC6, 0.1mM of isopropyl β -D-thiogalactopyranoside was added when the culture had an A_{600} of \sim 0.4. Culture was incubated for 36h at 12 °C. Cells were harvested by centrifugation (12,000 rpm, 2 min) and resuspended in extraction buffer containing 50mM Tris-HCl (pH 7.3), 50mM NaCl, 5% glycerol, 1mM DTT, 0.5mM PMSF. Cells were lysed by sonication and centrifuged (1,500 rpm, 10min) to remove cell debris. The supernatant was used for the enzyme activity as described below.

Protein concentration in the supernatant was quantified using Bradford reagent (BIO-Rad, CA) with BSA as a standard. The activity assay was carried out using previously defined conditions (Nakamura et al., 2005). Briefly, the reaction mixture contained 100 μ L of enzyme, 100 μ L of substrate and 300 μ L of assay buffer (50mM Tris-HCl (pH 7.3), 50mM NaCl, and 5% glycerol). The substrate was prepared as follows: 0.5% of 18:1 PC (Avanti Polar lipids), 0.5% egg transphosphatidylated PE(Avanti Polar lipids) were dried under a stream of nitrogen gas and resuspended in 250mM Tris-HCl (pH 7.3) and 0.25% deoxycholate. The samples were incubated for 1 hour at 37°C. The reaction was stopped by the addition of 0.75ml ethyl acetate followed by vigorous vortex and the addition 0.75ml of NaCl. The upper phase was dried under a stream of nitrogen gas and dissolved in 20 μ L of chloroform methanol (2:1, v/v) and separated on a TLC plate. The solvents used to separate the product are petroleum ether/ethyl ether/acetic acid (50:50:1, v/v/v). The product DAG was scraped from TLC plates and transmethylated using methanol, 1% H₂SO₄, and 0.05% butylated hydroxytoluene (BHT). 2.5 μ L of 5.4 μ M/mL 17:0 TAG was added as an internal standard. The samples were heated for 1h at 90°C. The fatty acid methyl esters were separated on a SHIMADZU GC-17A supplied with a hydrogen flame ionization detector and a capillary column DB-5MS (30 m; 0.25mm i.d.) with helium carrier at 11 ml/min. The oven temperature was maintained at 170°C for 3 min and then increased linearly to 210°C (5°C min⁻¹). Fatty acid methyl esters (FAMES) were identified by comparison of their retention times with known

standards (37-component FAME mix, Supelco 47885-U).

Subcellular Localization of GFP Fusion Proteins by Fluorescence Microscopy

The cDNAs of *NPC3* and *NPC6* were amplified from a 5' RACE pollen cDNA library and ligated into pMDC83 (Curtis & Grossniklaus, 2003) using the *PacI* and *AscI* enzyme sites. Both *NPC3* and *NPC6* expression were under the control of the 35S promoter. The primers used to amplify *NPC3* are: 5'-GGGTAAATTAATGGTGGAGGAAACGAGCTCTG3' (forward), 5'-CCCGGCGCGCCCATTATCACAAATCAAACACGAGAATAACTTCTG-3' (reverse). The primers used to amplify *NPC6* are: 5'-GGGTAAATTAATGAAACCATCATCAGCTTCAAGATTTT-3' (forward) and 5'-AAAGGCGCGCCCGTTGTGTGGCCGTGTAGTGAG-3' (reverse). C-terminally fused *NPC3*-GFP and *NPC6*-GFP were generated from the pMDC83 construct. Constructs were transformed into *Agrobacterium* C58 and grown at 30°C in LB broth supplemented with 50 µg ml⁻¹ kanamycin. The cells were harvested by centrifugation at 5000 g for 10 min at room temperature and resuspended in 10 mM MgCl₂ and 150 µg ml⁻¹ acetosyringone. Cells were left for 3 h at room temperature and then infiltrated into 3-week old tobacco leaves. After 48 h the samples were analyzed using a Zeiss LSM 510 confocal/multi-photon microscope (<http://www.zeiss.com/>).

Quantitative Real Time PCR

Total RNA was isolated from 6-week old *Arabidopsis* tissues or 2-week old tissues grown on agar plates using a rapid CTAB method (Stewart and Via, 1993; Li et al., 2006), and RNA was precipitated using 2M LiCl at 4°C. RNA integrity was checked on 1% (w/v) agarose gel. Eight µg of total RNA was digested with DNaseI according to manufacturer's instructions (Ambion, Inc.) to remove DNA contamination. The RNA was reverse transcribed using iScript cDNA Synthesis Kit (BIO-Rad, CA). The efficiency of cDNA synthesis was analyzed by real time PCR amplification of *UBQ10* (At4g05320). The level of gene expression was normalized to that of *UBQ10*. PCR was performed with MyiQ Sequence Detection System (Bio-Rad, CA) using SYBR Green to monitor dsDNA synthesis. Reaction mix contained 7.5 µl 2xSYBR Green Master Mix reagent Kit (BIO-Rad, CA), 1.0 ng cDNA, and 200 nM

of each gene specific primer in a final volume of 15 μ l. The qRT-PCR cycling conditions comprised 90 sec denaturation at 95°C and 50 cycles at 95°C for 30 sec, 55°C for 30 sec, and 72°C for 30 sec, with the final cycle being terminated at 72°C for an additional 10 min. The primers used are *NPC4*, *NPC3* and *NPC6* (Chapter2, Table 2).

Immunoblotting and Detection of NPC3-His and NPC6-His

Bacterial cells were harvested by centrifugation (10,000 rpm, 2 min) and resuspended in an extraction buffer (50 mM Tris-HCl (pH 7.3), 50 mM NaCl, 5% glycerol, 1 mM DTT, and 0.5 mM PMSF). Cells were lysed by sonication and centrifuged at 1,500 rpm for 5 min. The supernatant proteins were separated by 10% SDS-PAGE. After electrophoresis, proteins were transferred to a polyvinylidene difluoride membrane. The membrane was blotted with anti-His antibody (1:10000) conjugated with alkaline phosphatase for two hours. The protein bands were visualized by alkaline phosphatase reaction.

References

1. **Andersson MX, Larsson KE, Tjellstrom H, Liljenberg, Sandelius AS** (2005) the plasma membrane and the tonoplast as major targets for phospholipid to glycolipid replacement and stimulation of phospholipases in the plasma membrane. *JBC* **280**: 27578- 27586
2. **Awai, K., Marechal, E., Block, A.M., Brun, D., Masuda, T., Shimada, H., Takamiya, K., Ohta, H., and Joyard, J.** (2001) Two types of MGDG synthase genes, found widely in both 16:3 and 18:3 plants, differentially mediate galactolipids syntheses in photosynthetic and nonphotosynthetic tissues in *Arabidopsis thaliana*. *PNAS*. **98**, 10960-10965.

3. **Bari R, Pant BD, Stitt M, Scheible W-R** (2006) PHO2, MicroRNA399, and PHR1 define a phosphate-signaling pathway in plants. *Plant physiol.* **141**: 988-999
4. **Chiou T-J, Aung K, Lin S-I, Wu C-C, Chiang S-F, Su C-L** (2006) Regulation of phosphate homeostasis by microRNA in Arabidopsis. *Plant Cell* 18:412–421
5. **Clarkson DT** (1985) Factors affecting mineral nutrient acquisition by plants. *Annu. Rev. Plant Physiol.* 36: 77-115
6. **Clough SJ, Bent AF** (1998) Floral dip: a simplified method for Agrobacterium-mediated transformation of Arabidopsis thaliana. *Plant J* 16:735–743
7. **Devaiah BN, Karthikeyan SA, and Raghothama KG** (2007) WRKY75 Transcription factor is a modulator of phosphate acquisition and root development in Arabidopsis. *Plant Physiol.* **143**, 1789-1801
8. **Dong J, Chen C, Chen Z** (2003) Expression profiles of the Arabidopsis WRKY gene superfamily during plant defense response. *Plant Mol Biol* 51: 21–37
9. **Dong B, Rengel Z, Delhaize E** (1998) Uptake and translocation of phosphate by pho2 mutant and wild-type seedlings of Arabidopsis thaliana. *Plant Physiol* **205**: 251–256
10. **Fragoso S, Espindola L, Paez-Valencia Julio, Gamboa A, Camacha Y, Martinez-Barajas E, and Coello P** (2009) SnRK1 Isoforms AKIN10 and AKIN11 are differentially regulated in Arabidopsis Plants under phosphate starvation. *Plant Physiol.* **149**, 1906-1916.
11. **Gaude N, Nakamura Y, Scheible WR, Ohta H, Dormann P** (2008) Phospholipase C5 (NPC5) is involved in galactolipid accumulation during phosphate limitation in leaves of Arabidopsis. *Plant Journal* **56**: 28-39
12. **Karthikeyan AS, Varadarajan DK, Jain A, Held MA, Carpita NC, Raghothama KG** (2007) Phosphate starvation responses are mediated by sugar signaling in Arabidopsis. *Planta* 225: 907–918
13. **Karthikeyan AS, Varadarajan DK, Mukatira UT, D’Urzo MP, Damz B, Raghothama KG** (2002) Regulated expression of Arabidopsis phosphate transporters. *Plant Physiol* 130: 221–233

14. **Kelly AA, Dormann P** (2002) DGD2, an Arabidopsis gene encoding a UDP-Galactose-dependent digalactosyldiacylglycerol synthase is expressed during growth under phosphate-limiting conditions. *JBC*. **277**, 1166-1173
15. **Li M, Qin C, Welti R, Wang X** (2006) Double knockouts of phospholipases D ζ 1 and D ζ 2 in Arabidopsis affect root elongation during phosphate-limited growth but do not affect root hair patterning. *Plant Physiol*. **140** 761-770
16. **Li M, Welti R, and Wang X** (2006) Quantitative Profiling Of Arabidopsis Polar Glycerolipids in Response to Phosphorous Starvation. Roles of Phospholipase D ζ 1 and D ζ 2 in Phosphatidylcholine Hydrolysis and Digalactosyldiacylglycerol Accumulation in Phosphate-Starved Plants. *Plant Physiol*. **142**, 750-761
17. **Liu CM, Muchhal US, Mukatira U, Kononowicz AK, Raghothama KG** (1998) Tomato phosphate transporter genes are differentially regulated in plant tissues by phosphorous. *Plant Physiol*. **116**: 91-99
18. **Lopez-Bucio J, Hernandez-Abreu E, Sanchez-Calderon L, Nieto-Jacobo MF, Simpson J, Herrera-Estrella L.** (2002) Phosphate availability alters architecture and causes changes in hormone sensitivity in the Arabidopsis root system. *Plant Physiol*. **129**, 244-256
19. **Lopez-Bucio J, Hernandez-Abreu E, Sanchez-Calderon L, Perez-Torres A, Rampey RA, Bartel B, Herrera-Estrella L.** (2005) An Auxin Transport Independent Pathway Is Involved in Phosphate Stress-Induced Root Architectural Alterations in Arabidopsis. Identification of *BIG* as a Mediator of Auxin in Pericycle Cell Activation . *Plant Physiol*. **135**, 681-691.
20. **Hamburger D, Rezzonico E, MacDonald-Comber Pete'tot J, Somerville C, Poirier Y** (2002) Identification and characterization of the Arabidopsis PHO1 gene involved in phosphate loading to the xylem. *Plant Cell* **14**:889–902
21. **Hartel H, Dormann P, Benning C** (2000) DGD1-independent biosynthesis of extraplastidic galactolipids after phosphate deprivation in Arabidopsis. *Proc Natl Acad Sci USA* **97**, 10649–10654.
22. **Minnikin DE, Abdolrahimzadeh H, Baddiley J** (1974) Replacement of acidic phospholipids by acidic glycolipids in *Pseudomonas diminuta*. *Nature* **249**: 268-269

23. **Misson J, Raghothama K, Jain A, Jouhet J, Block M, Bligny R, Ortet P, Creff A, Somerville S, Rolland N, et al** (2005) A genome-wide transcriptional analysis using *Arabidopsis thaliana* affymetrix gene chips determined plant responses to phosphate deprivation. *Proc Natl Acad Sci USA* **102**, 11934–11939
24. **Nakamura Y, Awai K, Masuda T, Yoshioka Y, Takamiya K, and Ohta H** (2005) A Novel Phosphatidylcholine-hydrolyzing Phospholipase C Induced by Phosphate Starvation in *Arabidopsis*. *J. Biol. Chem.* **280**, 7469-7476.
25. **Poirier Y, Thoma S, Somerville C, Schiefelbein J** (1991) Mutant of *Arabidopsis* deficient in xylem loading of phosphate. *Plant Physiol* **97**:1087–1093
26. **Raghothama, K.G** 2000. Phosphate transport and signaling. *Current opinion plant biology* **3**: 182-187
27. **Raghothama KG** (1999) Phosphate acquisition. *Annu Rev Plant Physiol Plant Mol Biol* **50**: 665–693
28. **Rubio V, Linhares F, Solano R, Martin AC, Iglesias J, Leyva A, Paz-Ares J** (2001) A conserved MYB transcription factor involved in phosphate starvation signaling both in vascular plants and in unicellular algae. *Genes Dev* **15**: 2122–2133
29. **Stewart CN Jr, Via LE** (1993) A rapid CTAB DNA isolation technique useful for RAPD fingerprinting and other PCR applications. *Biotechniques* **14**: 748-758
30. **Tomscha JL, Trull MC, Deikman J, Lynch JP, Guiltinan MJ** (2004) Phosphatase Under-Producer mutants have altered phosphate relations. *Plant Physiol* **135**(1): 334-345
31. **Trull MC, Deikman J** (1998) An *Arabidopsis* mutant missing one acid phosphatase isoform. *Planta* **206**: 544–550
32. **Tjellstrom H, Andersson MX, Larsson KE, Sandelius AS** (2008) Membrane phospholipids as a phosphate reserve: the dynamic nature of phospholipid to digalactosyl diacylglycerol exchange in higher plants. *Plant Cell and Envir.* **31**: 1388-1398
33. **Welti R, Li W, Li M, Sang Y, Biesiada H, Zhou H-E, Rajashekar CB, Williams TD, Wang X** (2002) Profiling membrane lipids in plant stress

responses. Role of phospholipase D α in freezing-induced lipid changes in Arabidopsis. JBC 277: 31994-32002

- 34. Wu P, Ma L, Hoi X, Wang M, Wu Y, Liu F, Deng XW (2003)** Phosphate starvation triggers distinct alterations of genome expression in Arabidopsis roots and leaves. Plant Physiol. 132: 1260-1271

Figure Legends

Figure 1. Expression pattern and sub-cellular localization of NPC3 and NPC6

(A) Expression of *NPC3* and *NPC6* in Arabidopsis tissues, as quantified by qRT-PCR normalized to *UBQ10*. Values are means \pm SD (n=3).

(B) Gene expression of *NPC3*, *NPC4*, and *NPC6* in response to phosphate limitation. Four-day old seedlings were transferred to plates containing 500 μ M or 0 μ M phosphate and tissues were harvested ten days later. Expression level was quantified by qRT-PCR and normalized to *UBQ10*. Values are means \pm SD (n=3).

(C) Subcellular localization of NPC3 and NPC6. The NPC4-GFP, NPC3-GFP and NPC5-GFP fusion proteins were transiently expressed in tobacco leaves. The vector harboring only GFP was used as a negative control. Red fluorescence indicates chlorophyll.

Figure 2. The T-DNA insertion mutant of *NPC3* and *NPC6* and the effects of *npc3-1*, *npc6-1* and *npc3-1npc6-1* alteration on phosphate limitation

(A) and (B) Location of the T-DNA insertion in *NPC3* and *NPC6*. T-DNA inserts are indicated by an inverted triangle. Arrows indicate the direction of *NPC3* and *NPC6* gene specific primers.

(C) Confirmation of T-DNA insertion in *NPC3* and *NPC6*. Genomic DNA isolated from *npc3-1*, *npc6-1* and *npc3-1npc6-1* plants were used as template for PCR. i, products obtained using *NPC3* specific primers. The mutation is homozygous both in *npc3-1* plants and *npc3-1npc6-1* plants. The presence of the T-DNA insert in *npc3-1* and *npc3-*

Inpc6-1 is confirmed by using the left border primer with *NPC3* gene specific primer as shown in ii and iii. The presence of T-DNA for *npc6-1* is confirmed as shown in iv. The mutation is homozygous as shown in iii.

(D) Root length on phosphate sufficient and phosphate starved media. Five-day old seedlings were transferred to $1/10$ MS medium containing 0.5 mM or 0 mM phosphate. Pictures were taken 12 days after transfer.

(E) Quantification of root length under phosphate sufficient and phosphate starved conditions. Values are means \pm SE (n=15).

Figure 3. Lipid Changes in Response to Phosphate starvation.

(A) Total lipid levels in rosettes of *npc3-1*, *npc6-1*, *npc3-1npc6-1* and wild type plants under phosphate sufficient and phosphate deprived conditions. Five-day old seedlings were transferred to $1/2$ MS containing 0 (-Pi) or 0.5 mM (+ Pi) phosphate and tissues were harvested for lipid extraction ten days after transfer. Values are means \pm SE (n=5). * Denotes that the mutant and wild-type values are significantly different ($p < 0.05$) based on student's t-test.

(B) Total lipid levels in roots of *npc3-1*, *npc6-1*, *npc3-1npc6-1* and wild-type plants under phosphate sufficient and phosphate deprived conditions. Values are means \pm SE (n=5). * Denotes that the mutant and wild-type values are significantly different ($p < 0.05$) based on student's t-test.

Figure 4. Changes in lipid molecular species of DGDG, MGDG, PC, PE, PI, PG, PS, and PA in roots of *npc3-1*, *npc6-1*, *npc3-1npc6-1* and wild-type under 500 μ M and 0 μ M phosphate conditions. Five-day old seedlings were transferred to plates containing 500 μ M or 0 μ M phosphate. After ten days, the roots and rosettes were harvested for lipid analysis by ESI-MS/MS. Values are means \pm SE (n=5). * Denotes that the mutant and wild-type values are significantly different ($p < 0.05$) based on student's t-test.

Figure 5. Concentration of lysoPC, lysoPG and lysoPE in rosettes and roots of *npc3-1*, *npc6-1*, *npc3-1npc6-1* and wild-type under 500 μ M and 0 μ M phosphate conditions.

Five-day old seedlings were transferred to plates containing 500 μM or 0 μM phosphate. After ten days, the roots and rosettes were harvested for lipid analysis by ESI-MS/MS. Values are means \pm SE (n=5). * Denotes that the mutant and wild-type values are significantly different ($p < 0.05$) based on student's t-test

Figure 6. Concentration of individual molecular species of lysoPC, lysoPG and lysoPE in rosettes and roots of *npc3-1*, *npc6-1*, *npc3-1npc6-1* and wild-type under 500 μM and 0 μM phosphate conditions.

(A) Lysophospholipid content in rosettes. Values are means \pm SE (n=5).

(B) Lysophospholipid content in roots. Values are means \pm SE (n=5). * Significant at $P < 0.05$ compared to wild-type based on Student's t-test.

Figure 7. Concentration of DAG in rosettes and roots of *npc3-1*, *npc6-1*, *npc3-1npc6-1* and wild-type under 500 μM and 0 μM phosphate conditions. Five-day old seedlings were transferred to plates containing 500 μM or 0 μM phosphate. After ten days, the roots and rosettes were harvested for lipid analysis by ESI-MS/MS.

(A) Total DAG in rosette and root. Values are means \pm SE (n=5).

(B) DAG molecular species in rosettes. Values are means \pm SE (n=5).

(C) DAG molecular species in roots. Values are means \pm SE (n=5). * Significant at $P < 0.05$ compared to wild-type based on Student's t-test.

Figure 8. NPC3 and NPC6 expression and hydrolytic activity

(A) Expression of NPC3-His and NPC6-His recombinant proteins in *E. coli*. Protein was extracted from NPC3 or NPC6 expressing cells and separated on a 10 % polyacrylamide gel. Empty vector-transformed *E. coli* cells were used as a negative control. Proteins were transferred to a polyvinylidene difluoride membrane and NPC3-His and NPC6-His were

visualized by alkaline phosphatase (AP) after blotting with His antibody conjugated with AP. T indicates total cell lysate (insoluble fraction), S indicates supernatant (soluble fraction), and C indicates empty vector control. Arrows indicate NPC3 and NPC6 proteins.

(B) Phospholipase C activity of protein extracts from *E. coli* expressing NPC3 or NPC6, measured using PC and PE. Lipid spots on thin layer chromatography plates corresponding to DAG were scraped, and the lipids were extracted and transmethylated. The resulting product was quantified by GC analysis.

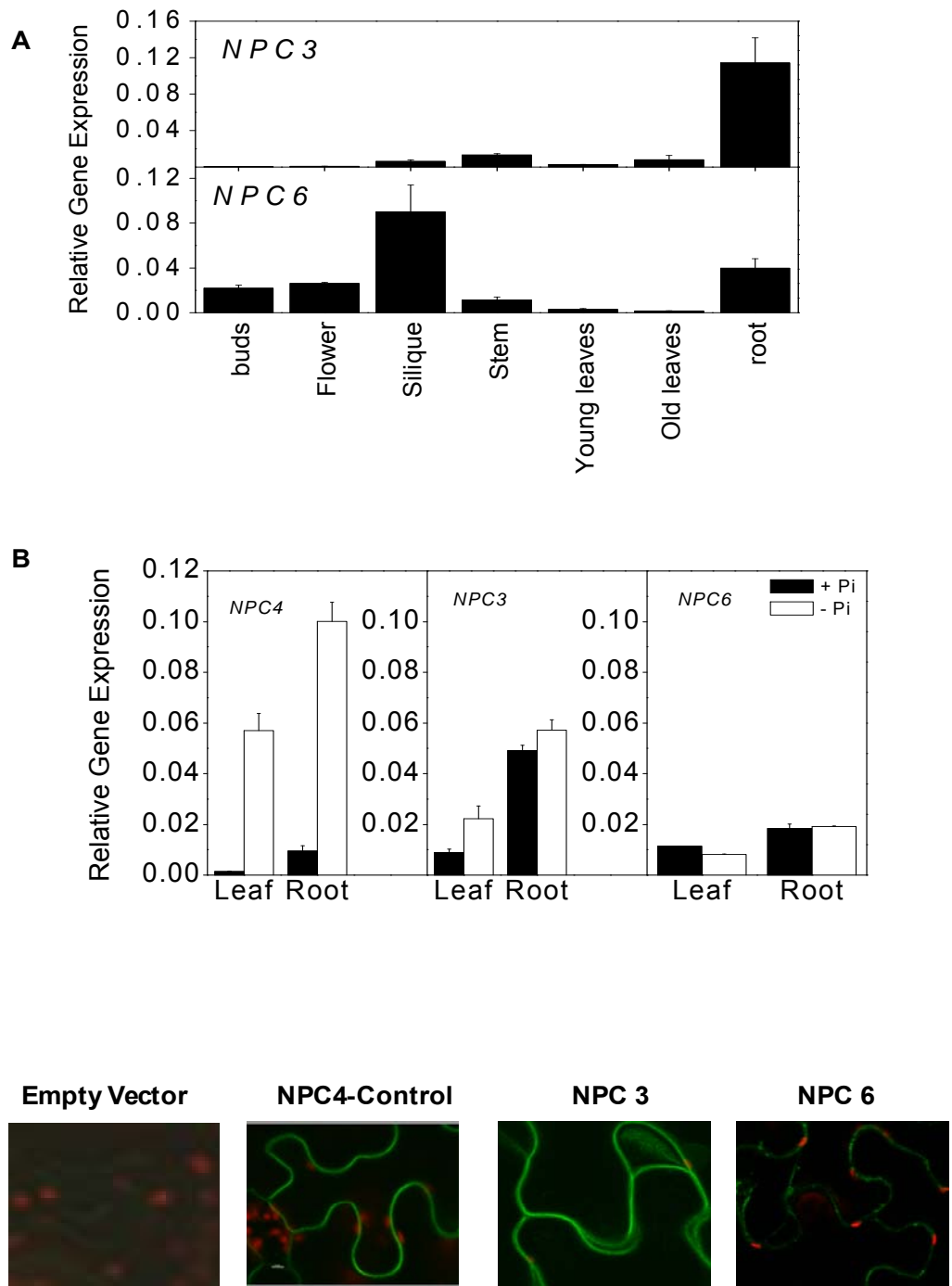


Figure 1

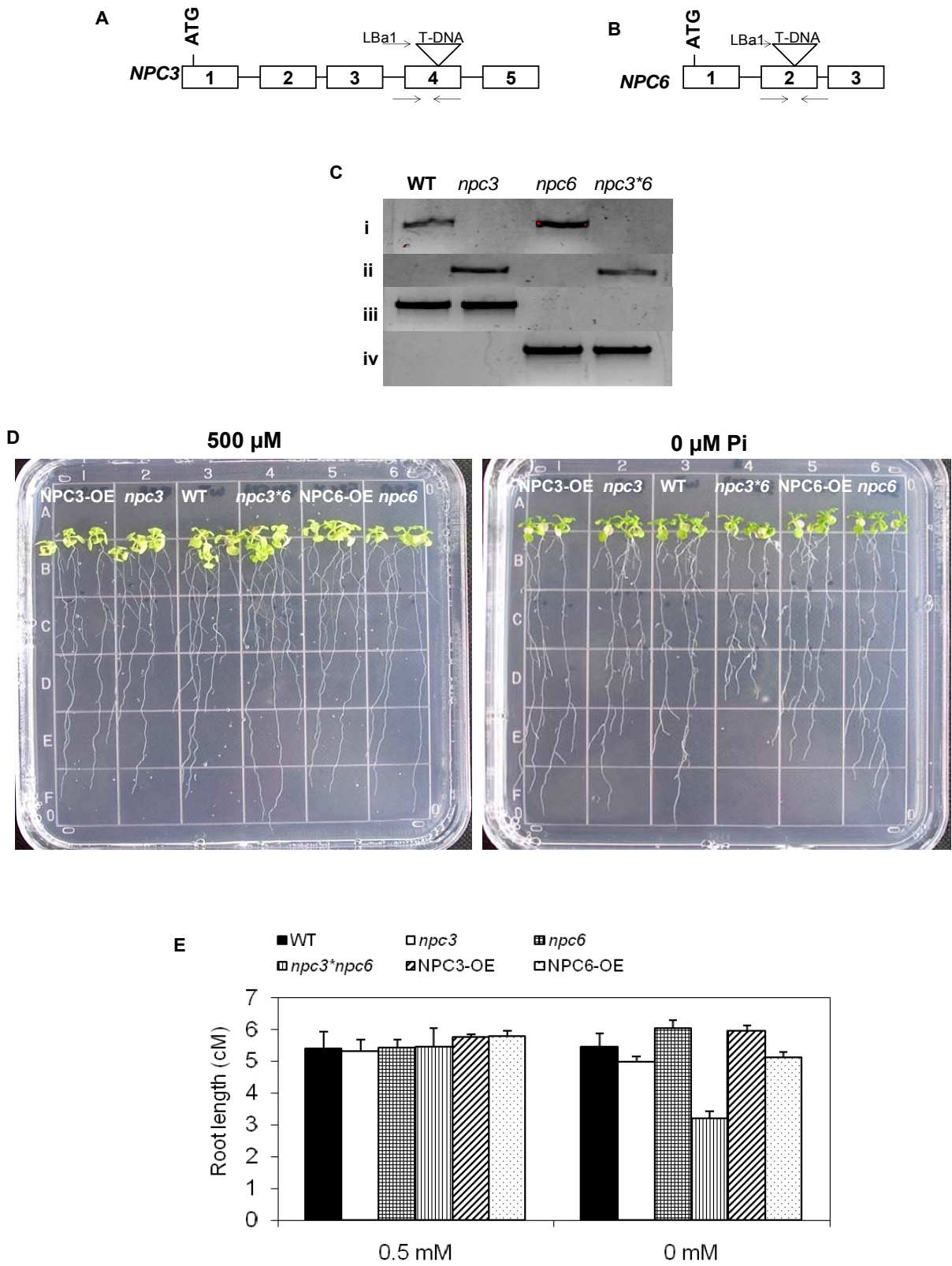


Figure 2

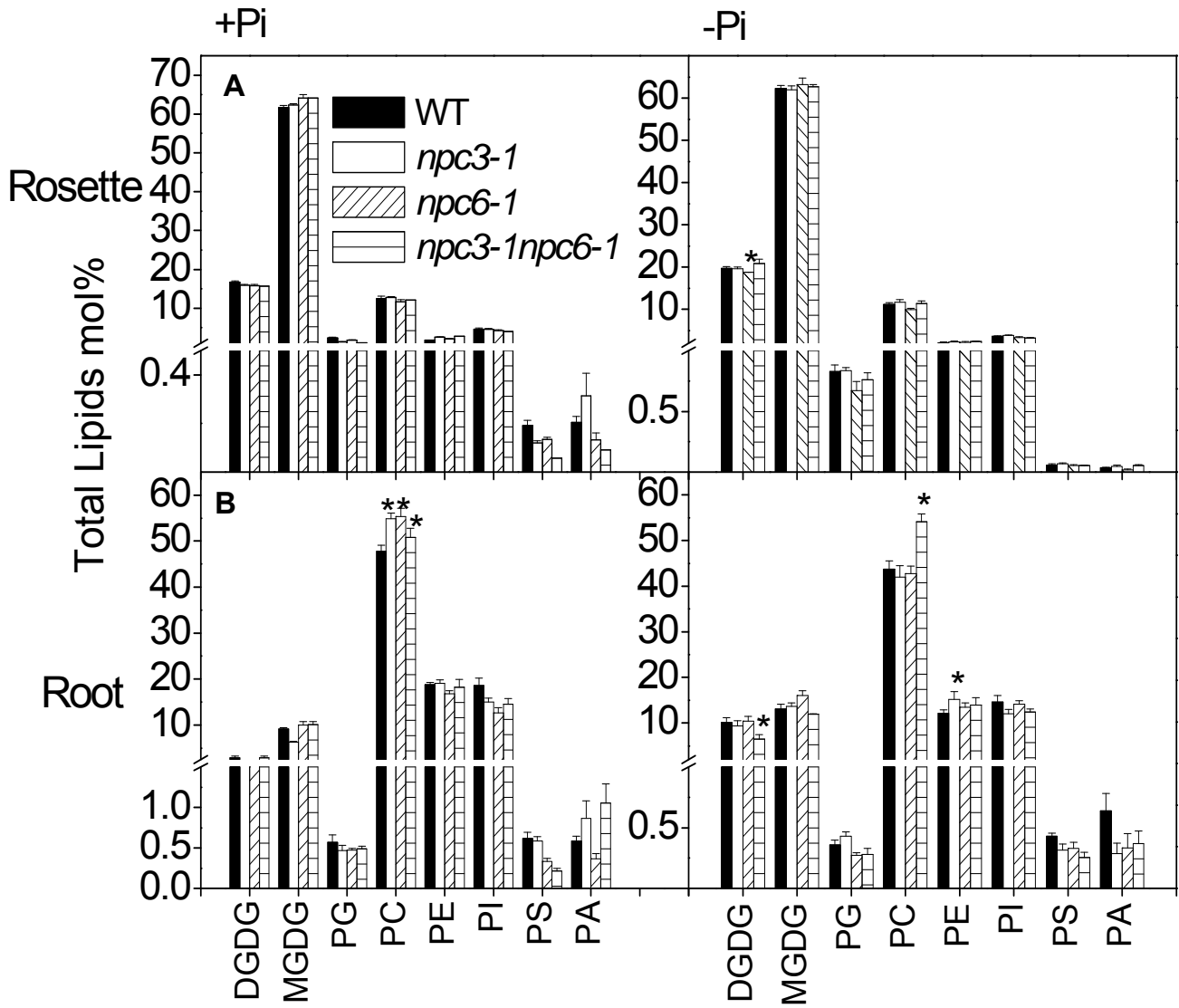


Figure 3

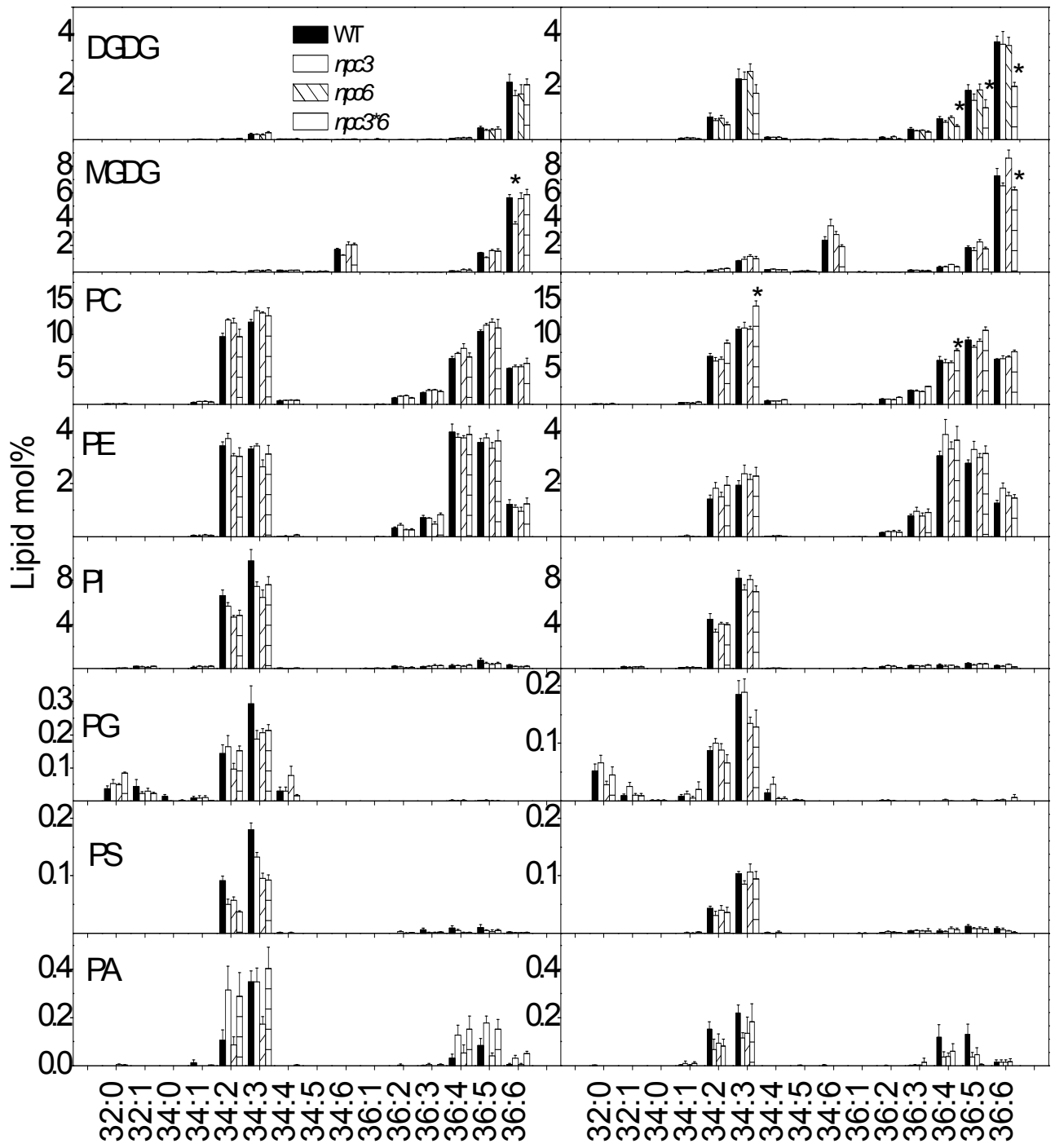


Figure 4

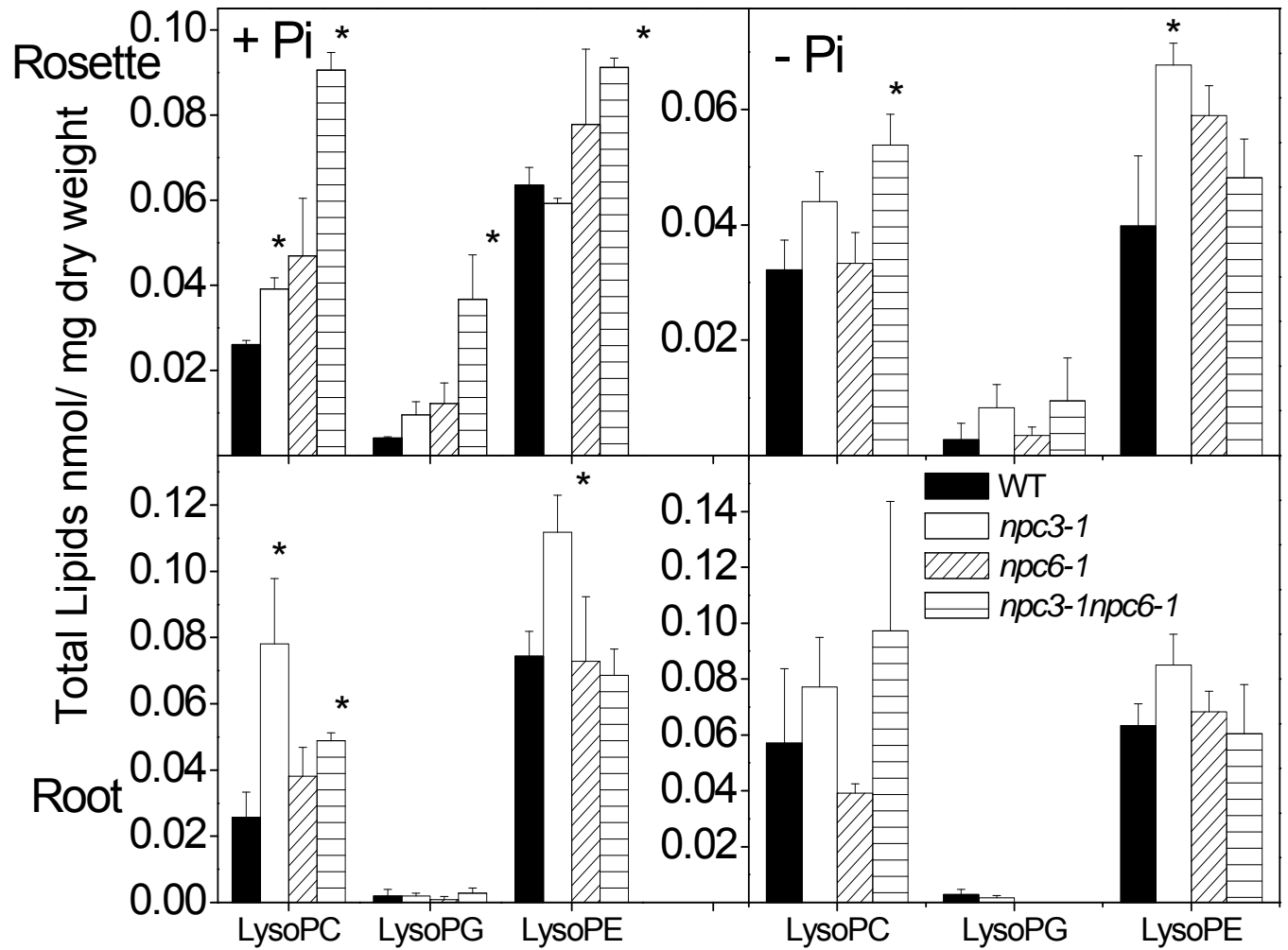


Figure 5

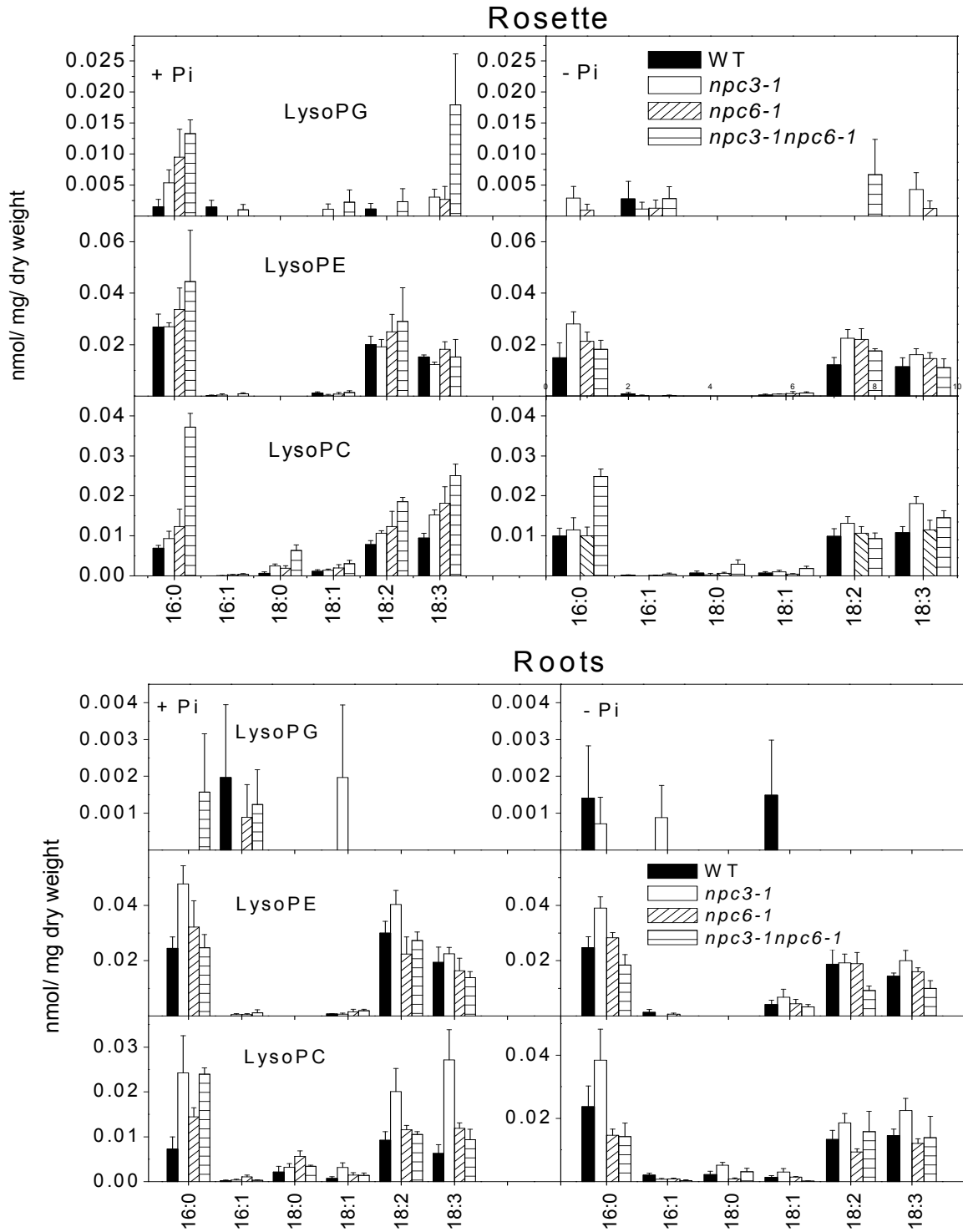


Figure 6

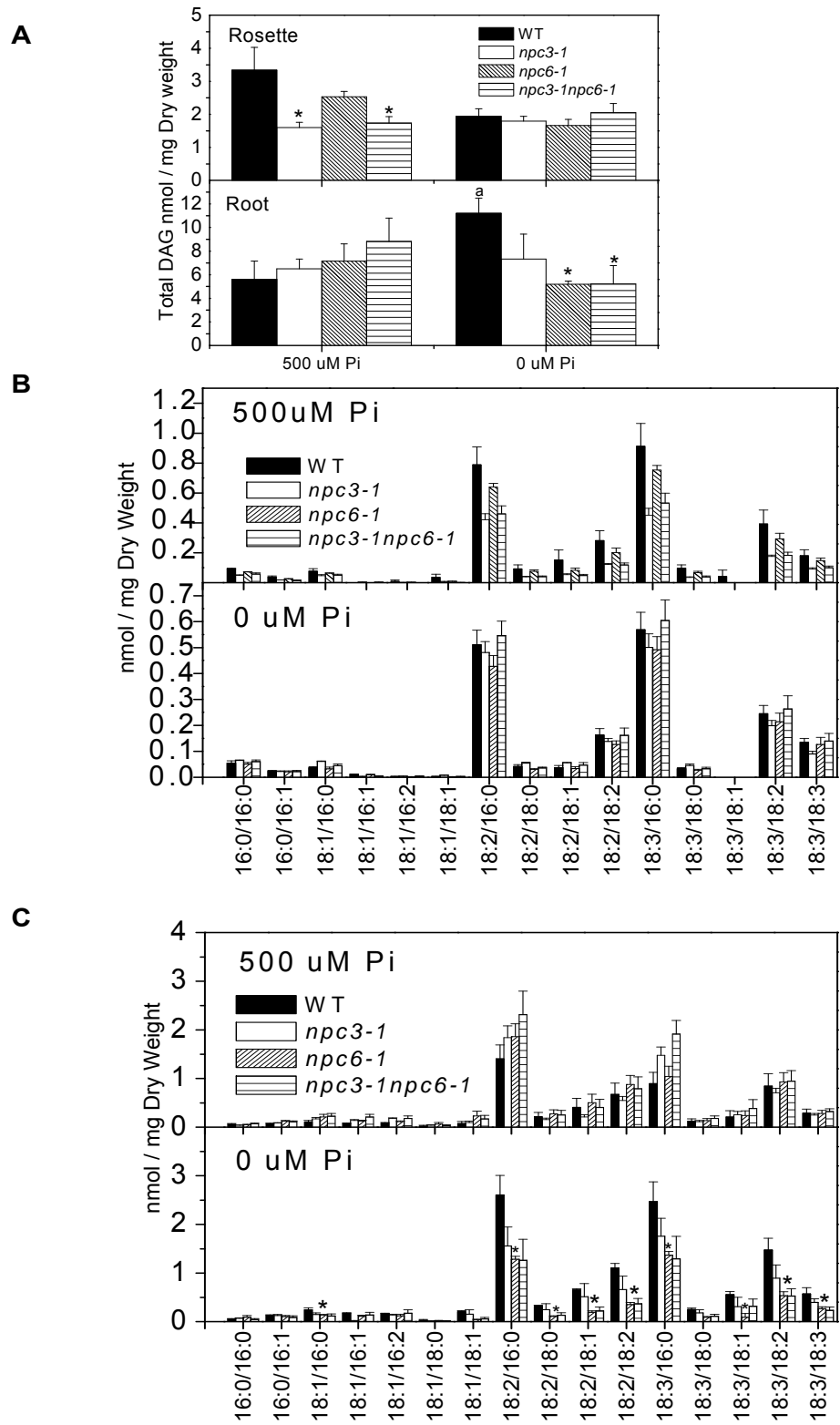


Figure 7

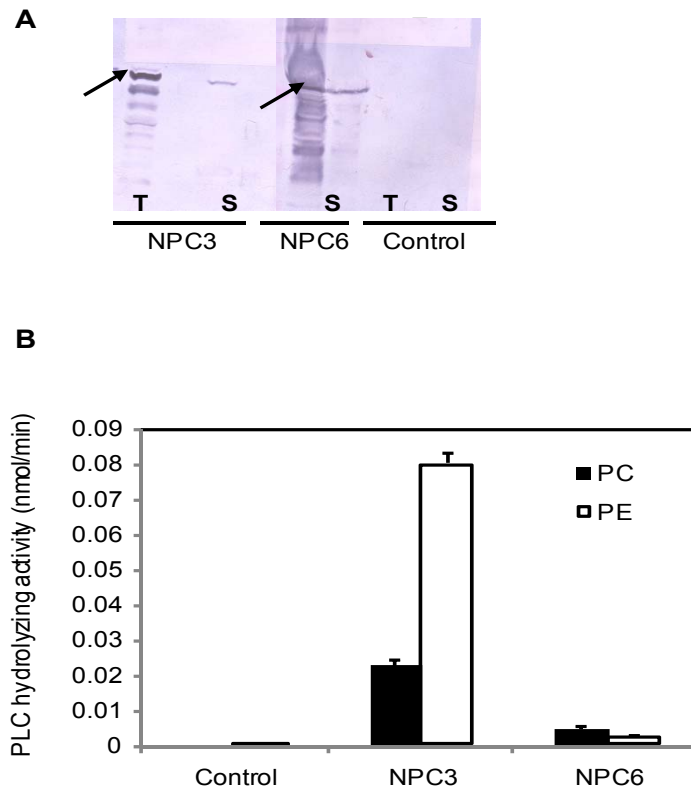


Figure 8

Chapter 5. NPC5 and its Lipid Product DAG Modulate Lateral Root Development Under Mild Salt Stress.

Abstract

Lateral root development in *Arabidopsis* is post-embryonic and varies in response to environmental and developmental signals. We found that one *Arabidopsis thaliana* non-specific phospholipase C (NPC), *NPC5*, is involved in lateral root development during mild salt stress. The *npc5-1* mutant produces few to no lateral roots when treated with 75mM NaCl. Under non-stress conditions, *npc5-1* is indistinguishable from wild-type plants. The over-expression of *NPC5* promotes lateral root formation. Lipid profiling reveals that the roots of *npc5-1* have lower levels of PC and DAG than wild-type plants. The formation of lateral roots in the presence of 75 mM NaCl in *npc5-1* can be rescued with the application of exogenous DAG and DAG kinase inhibitor I. The addition of PA is less potent than DAG, requiring ten fold more to restore lateral root growth in *npc5-1*. These results indicate that *NPC5* and its lipid product DAG play a role in modulating lateral root development in response to mild salt stress.

Introduction

Plants are sessile organisms that possess the ability to acclimate to various environmental conditions. As a result, the root architecture of plants is influenced by many environmental and biotic factors. The root system in higher plants is divided into three classes; the main root (commonly referred to as the tap or primary root), lateral roots and adventitious roots (Smet, et al., 2003). The primary root meristem is formed during embryogenesis, while the lateral and adventitious root meristems are initiated post-embryogenically during a plant's lifecycle. Consequently, the number and location of these organs is not predetermined, and rather they are determined by the age of the plant and environmental conditions (Malamy and Ryan, 2001).

The *Arabidopsis* root system is ideal for organ development studies, since the arrangement of cells in both the primary and lateral roots is simple and predictable (Malamy and Benfey, 1997). There are four distinct cell types: the epidermis, the outermost layer, is followed by the cortex, endodermis and the pericycle. Each of these cell types are one cell layer thick. The pericycle envelopes the stele, which contains the xylem, phloem and the parenchyma cells. The root cells are formed from specialized cells in the meristematic region called initials (Schiefelbein, et al., 1997). There are four types of initial cells in the root apical meristem: one that forms the root cap; one that forms the epidermis and the lateral root cap; one that forms the cortex and endodermis; and one that forms the stele. After cell division, the initials are regenerated and are responsible for cellular organization. The initials for the primary root are formed embryogenically, while in lateral roots the initials are post embryogenically.

Lateral root development in *Arabidopsis* has been dissected to reveal the pattern in which lateral roots form. Lateral roots are formed from a single layer of pericycle cells within the primary root (Laskowski, et al., 1995; Malamy and Benfey, 1997). Lateral root development is defined by two distinct stages: the formation of a lateral root primordium (LRP) followed by the formation of a meristem that produces a mature lateral root (Laskowski, et al., 1995). The first stage of lateral root initiation is triggered by pericycle cells called founder cells. Pericycle founder cells are cells that are programmed for a different developmental fate than the parent cells from which they originate (Laskowski, et al., 1995). Two founder cells adjacent to the xylem poles undergo simultaneous asymmetric division, producing two short cells followed by two long cells (Casimiro et al., 2003). The daughter cells continue to divide, giving rise to groups of 8–10 cells that are similar in length (Casimiro et al., 2003). These cells expand in a radial direction followed by periclinal division (division in a longitudinal orientation) of the central daughter cells (Malamy and Benfey, 1997, Casimiro et al., 2003). An inner and outer lateral root primordium is formed. The peripheral layer of daughter cells does not participate in cell division; hence the radial expansion of the newly formed primordial layers takes on a dome shape (Malamy and Benfey, 1997). Both the outer and inner layer of primordial cells undergo a subsequent periclinal division producing four layers of

cells. At this stage, the LRP is able to penetrate the endodermal layer of the parent root. Subsequent anticlinal (transverse orientation) and periclinal division of the LRP aids full emergence through the epidermal cells of the parent root. At this point the LRP begins to resemble the cell files of the mature root tip of the parent. The emergence of the LRP is followed by an increase in cell number near the lateral root apex (Malamy and Benfey, 1997; Casimiro et al., 2003). This is due to a functional lateral root apical meristem and the LRP is referred to as a lateral root at this stage of development.

It has been known for over 50 years that auxin promotes lateral root growth (Torrey, 1950). Auxin is involved in various developmental processes in plants including gravitropic responses, cell division/elongation, and root, shoot and vascular development. To date, compelling evidence indicates that auxin is involved in the initiation, establishment of LRP and the activation of lateral root meristem. Pretreatment of *Arabidopsis* and radish root with auxin resulted in increased lateral root initiation. After several days, a large number of closely spaced lateral roots were formed (Laskowski et al., 1995). Further evidence was provided for the requirement of auxin in LRP establishment. Excised root segments at any developmental stage developed into lateral roots in the presence of auxin. Only excised segments containing 3-5 cell layers were able to develop into lateral roots while, segments containing less than three cell layers, were arrested in the absence of auxin (Laskowski et al., 1995). Thus, it appears that development beyond the 3-5 cell layer stage may be auxin independent or auxin sufficient. Nevertheless, the mutant phenotype of aberrant lateral root formation 3 (*alf3-1*) suggests that auxin is required for lateral root development beyond the 3-5 layers stage. Lateral root growth is prematurely arrested in *alf3-1* mutants and can be rescued by the addition of exogenous auxin or endogenous auxin from *alf1-1* that overproduces auxin (Celenza et al., 1995).

The isolation of several other mutants in *Arabidopsis* with auxin-related defects further supports the pivotal role that auxin plays in lateral root development. *aux1* mutants produce less lateral roots than wild-type due to impaired auxin transport between IAA source and sink tissues (Marchant et al., 2002). *iaa3* and *iaa28-1* form fewer lateral roots

due to reduced auxin sensitivity (Malmay, 2005; Rogg and Bartel, 2001). *iaa14*, an AUX/IAA transcriptional repressor, also exhibits reduced auxin sensitivity. This mutant produces normal primary roots but is specifically defective in lateral root initiation (Fukaki et al., 2002).

Auxin is not the only hormone modulating lateral root formation. Experimental evidence supports a role for ABA in lateral root development. Low concentrations of ABA, ranging from 0.1 μ M -10 μ M arrest lateral root development in Arabidopsis. Lateral root arrest occurs at a specific developmental stage, right before the activation of the lateral root meristem (Smet et al., 2003). Further examination of the mechanism underlying the arrest of LRP in response to ABA revealed that ABA downregulates the auxin effect in the LRPs (Smet et al., 2003, Deak and Malamy, 2005). Nevertheless, ABA inhibition of lateral roots appears to be independent of auxin response, since LRPs were capable of responding to exogenous auxin in the presence of ABA but were still unable to overcome lateral root arrest. In addition, elevated levels of endogenous auxin failed to rescue the ABA mediated lateral root arrest.

Lateral root development is also influenced by environmental cues. The availability of nitrogen is one such factor that affects lateral formation. Low nitrate stimulates the formation of lateral roots; high nitrogen supply inhibits lateral roots (Zhang and Forde, 2000); and a high sucrose to nitrogen ratio dramatically represses lateral root development (Malamy and Ryan, 2001). The regulatory mechanism underlying nitrogen related lateral root inhibition occurs at different developmental stages. High nitrate inhibits lateral root development soon after emergence before the meristem becomes activated. On the other hand, high sucrose to nitrogen conditions occur at initiation due to the inability of auxin to move from the shoot to initiation sites in the root. The isolation of a mutant termed *lateral root initiation 1 (lin1)* gave further insight on the mechanism underlying nitrogen related lateral root regulation (Malamy and Ryan, 2001; Little et al., 2005). *lin1* produces highly branched roots under repressive conditions of high sucrose to nitrogen ratio. Under normal conditions, lateral root formation in *lin1* is comparable to wild type. Since lateral root formation in *lin1* only differs from wild type under high

sucrose to nitrogen conditions, it is apparent that LIN1 is a component of a signaling pathway that connects nutritional cues with lateral root development. Mutants of this nature have rarely been reported, because the formation of lateral roots is intact but the signal that stimulates its formation is defective under a specific set of conditions (Malamy and Ryan, 2001). Sucrose is also involved in stimulating lateral root formation in *Arabidopsis* grown in culture (MacGregor et al., 2008; Karthikeyan et al., 2007).

Another such mutant that links nutritional status to lateral root development is the low phosphate resistant root (*lpr*) (Lopez –Bucio, et al., 2005). *LPR* is required for normal auxin transport in *Arabidopsis*. Under phosphate deprived conditions more carbon is relocated to the roots resulting in an increase in the root to shoot ratio (Li et al, 2006). The primary root growth is inhibited, and lateral root formation is promoted, resulting in a shallower and wider root system. However, under low phosphate conditions, the *lpr* mutant exhibits reduced lateral root formation. *LPR* is required for activation of pericycle cells that form LRP. This process is not altered by phosphate availability, but mutations in *LPR* affect this process leading to reduced emergence of LRP in low phosphate conditions (Lopez –Bucio, et al., 2005).

In addition to nutrient availability, osmotic stress also alters root architecture. Osmotica represses the elongation of lateral roots in wild-type *Arabidopsis* seedlings, but does not affect lateral root initiation. This phenotype is attributed to optimization of the root system by repressing root growth in zones where water is not readily available (Deak and Malamy, 2005; Malamy 2008). Conversely, salt stress is more complex and induces osmotic stress in combination with ionic stress. As a result, various metabolic processes are disrupted in response to decreased water potential and cellular ion leakage. The root system also responds differently to salt and osmotic stress. Salt stress promotes lateral root formation and inhibits primary root growth in wild-type *Arabidopsis* (He et al., 2005). Additionally, the cell cycle is arrested and cyclin-dependent kinase (CDK) activity is transiently reduced. Overall the primary roots are shortened due to a decrease in cell production and smaller mature cells (West et al., 2004). However, none of the genes involved in lateral root production under salt stress have been identified to date. The most

promising candidates to date are members of the *NAC* family, a group of plant specific transcription factors that regulate many aspects of plant growth and development (Olsen et al., 2005). *AtNAC2* is induced by salt stress that requires both ethylene and auxin signaling. Overexpression of *AtNAC2* promotes lateral root formation under non stressed and salt stress growth conditions. However, *AtNAC2* null mutant produced lateral roots comparable to wild-type both in normal and salt stress conditions (He et al., 2005). Members of the NAC family are known for being redundant in their function, therefore other members of this family or other unidentified genes involved in root formation may be responsible for *nac2-1* lack of phenotype (Montiel et al., 2004; He et al., 2005).

In this report, we characterized a non-specific phospholipase C (*NPC5*) from Arabidopsis whose phenotype shows reduced lateral root formation when grown in mild salt stress conditions. *NPC5* belongs to a gene family that hydrolyzes phosphatidylcholine (PC) and other common membrane lipids, and are therefore referred to as non-specific phospholipase C. In Arabidopsis, there are six putative NPC genes bearing homology to bacterial PC-PLC and designated *NPC1-NPC6* (Nakamura et al., 2005). The NPC family does not contain any of the X, Y domains or EF-hand motif found in PI-PLC. Furthermore, none of the domains present in the PLD family, such as a calcium binding or lipid binding motif, are present in the NPC family. *NPC5* has been shown to be involved in digalactosyldiacylglycerol (DGDG) accumulation in Arabidopsis leaves under phosphate starvation (Gaude et al., 2008). Profiling of membrane lipids in response to salt stress revealed reduced levels of DAG in *npc5-1* T-DNA mutants. Further analysis of this mutant showed that *NPC5* and its lipid product DAG play a role in lateral root formation under mild salt stress.

Results

Expression and Subcellular localization of *NPC5* in Arabidopsis Tissues

To determine the spatial expression of *NPC5*, real time PCR was performed using various organs from 6-week-old soil grown Arabidopsis plants. The transcript of *NPC5* was

detected in the buds (Figure 1A). The expression level of *NPC5* was very low in the other organs tested. Therefore, discernable differences among tissues could not be determined. To further investigate the expression levels of *NPC5* in Arabidopsis tissues, a promoter GUS fusion of *NPC5* was constructed. This method showed expression in the vascular tissues of young seedlings and older leaves. Some expression could be seen in the tip of the buds but no expression was detected in primary and lateral roots of 7 day old seedlings (Figure 1B).

To determine the subcellular localization of *NPC5*, the cDNA was C-terminally and N-terminally fused to green fluorescence protein (GFP) and transiently expressed in tobacco leaves. *NPC4* is plasma membrane localized and served as a positive control. *NPC5*-GFP protein was analyzed by confocal microscopy. A diffuse subcellular pattern was observed, and a portion could be seen in the nucleus. Therefore, *NPC5* is cytosolic in localization (Figure 1C) (Gaude et al., 2008).

T-DNA Insertion and Expression of *NPC5* under Abiotic Stress

To determine the physiological function of *NPC5* in Arabidopsis, we isolated a T-DNA insertional mutant in the Columbia ecotype. A single T-DNA insert is present in the third exon, 801 nucleotides downstream of the start codon (Figure 2A). Homozygous lines were identified by PCR, and the single T-DNA insert in *npc5-1* was verified by the 3:1 segregation for kanamycin resistance in the F2 generation (Figure 2B). The loss of expression of *NPC5* was confirmed by quantitative real time PCR (Fig. 2C). *npc5-1* deficient plants grew and developed normally under non stressed growth conditions. These mutants were subjected to nutrient, ionic and osmotic stress (mannitol and sorbitol). Also, responses in the presence of ABA, IAA or ACC were tested. No apparent differences in root length or architecture were observed for nutrient deprivation or osmotic stress when compared to wild-type. However, *npc5-1* exhibited reduced sensitivity to IAA mediated primary root elongation (Figure 3A). Lateral roots were also reduced when *npc5-1* seedlings were treated with IAA (Figure 3B). The IAA content of wild-type and *npc5-1* seedlings was measured under control and 75 mM NaCl. Under control and treatment conditions the IAA content in wild-type and *npc5-1* seedlings was

similar (Figures 3C and 3D). Reduced lateral root formation was observed under salt stress compared to wild-type.

Loss of *NPC5* Reduces Lateral Root Formation Under Salt Stress

In order to determine the function of *NPC5*, gene expression data in response to abiotic and hormone stress were obtained from genevestigator (www.genevestigator.ethz.ch/at) (Figure 4A). The data obtained from this database showed that *NPC5* was greatly induced by nitrogen deprivation (20 fold). There was a two fold induction of *NPC5* in response to ABA and salt stress, and a three fold induction by osmotic stress. Real time PCR data using 10 day old wild-type seedlings treated with 200 mM NaCl show a three fold induction of *NPC5* (Figure 4B). To investigate the potential effect of *npc5-1* mutation under these conditions, wild-type and *npc5-1* seeds were germinated on ½ concentration Murashige and Skoog agar media (MS), and four day old seedlings were transferred to plates containing 0.5 mM nitrogen, 25 mM- 150 mM NaCl, 10-25 µM ABA or 100 and 200 mM mannitol and sorbitol. The *npc5-1* plants responded similarly to wild-type under nitrogen deprivation, ABA, sorbitol and mannitol treatments. However, under salt stress the primary roots of *npc5-1* elongated at a faster rate than wild type on 75 mM -125 mM NaCl (data not shown). Additionally, *npc5-1* plants had fewer lateral roots than wild-type (Figures 4C-4I). The reduction in lateral roots was most prominent when the mutants were treated with 75 mM NaCl; with some of the mutants completely lacking lateral roots (Figures 4C and 4G). On 75 mM NaCl, the number of lateral roots in *npc5-1* was ~5% of wild-type seedlings. At 100 mM NaCl, *npc5-1* had ~30% the lateral roots of wild-type plants. On 125 and 150 mM NaCl, the number of lateral roots in *npc5-1* increased to 65% of wild type levels (Figures 4I and 4J). This phenotype was not observed under osmotic stress induced by sorbitol and mannitol, indicating that the reduction in lateral roots is specific to salt stress in *npc5-1*.

To further corroborate this phenotype, the full length genomic *NPC5* sequence, including the promoter and 3'UTR, was cloned from Arabidopsis and introduced into *npc5-1* via Agrobacterium mediated transformation. Transformed plants were selected based on hygromycin resistance and further verified by PCR. These complemented (*npc5-1-C*)

plants were transferred to vertical plates containing 25-150 mM NaCl. The number of lateral roots were restored to wild-type levels under the concentrations of NaCl tested (Figures 4D-4I). This validates that *NPC5* is responsible for the reduced number of lateral roots seen under salt stress.

To investigate whether *npc5-1* is affected in the lateral root elongation or the formation of lateral root primordia, wild-type and *npc5-1* seedlings were examined under the microscope. Under control conditions both wild-type and *npc5-1* seedlings produced lateral root primordia that elongated into mature lateral roots (Figure 5). However, under mild salt stress, lateral root primordia were absent in *npc5-1* roots compared to wild-type that had fully developed lateral roots (Figure 5).

Overexpression of NPC5 Stimulates Lateral Root Growth

NPC5 was ectopically overexpressed to further study its physiological function. The coding region of *NPC5* was cloned into the modified p35S-FAST binary vector under the control of the cauliflower mosaic virus 35S promoter. The resulting cassette was introduced into wild-type *Arabidopsis* via *Agrobacterium* transformation. A total of 21 independent transformants were obtained. The expression level of *NPC5* was monitored by immunoblotting. On $\frac{1}{2}$ MS media, *NPC5-OE* produced more than twice as many lateral roots compared to wild-type plants (Figures 6A and 6B). Under salt stress number of lateral roots in *NPC5-OE* plants was more than that of wild-type plants, but there was no further increase in the number of lateral roots when compared with *NPC5-OE* plants under normal growth conditions (Figures 6A and 6C). Therefore, overexpression of *NPC5* stimulates lateral root formation constitutively.

***NPC5* is Involved in DAG Production under Salt Stress**

DAG is the direct product of *NPC5* (Gaude et al., 2008). Therefore, we wanted to determine the effect of salt stress and *npc5-1* defect on lipid composition. We quantified the lipid composition of wild-type and *npc5-1* seedlings grown on either $\frac{1}{2}$ MS media or $\frac{1}{2}$ MS media supplemented with 75mM NaCl. In wild-type plants subjected to mild salt stress, there were subtle changes in the lipid composition. There was a 2 mol% increase

of MGDG, a non phosphorous containing lipid, and a 1mol% increase of PI in wild-type roots under salt stress (Figures 7A and 7B). In contrast a 5mol% and a 2mol% decrease were seen for PE and PS respectively. In *npc5-1* roots subjected to mild salt stress a 1mol% increase of MGDG and a 2mol% increase of PI was seen. However, no changes in PE and PS were seen. A 3mol% decrease in PC was seen in *npc5-1*, but this was not seen in wild type roots. Under normal growth conditions, significantly higher levels of PC (43.9mol %) was observed in *npc5-1* as compared to wild-type roots (38.6mol %). Also, higher levels of PS were seen in wild-type roots under these growth conditions compared to *npc5-1* (Figure 7A).

We compared the DAG molecular composition in wild-type and *npc5-1* seedlings in the absence and presence of NaCl. Under normal growth conditions, 18:2/16:0 DAG was the most abundant molecular species in both wild-type and *npc5-1* roots. However, after treatment with 75mM NaCl, 18:3/18:1 DAG became the most abundant species in both wild-type and *npc5-1* roots (Figures 8C and 8D). On ½ MS media the total DAG in *npc5-1* was 58% of wild-type level (Figure 8A). The molecular species of DAG that were significantly lower in *npc5-1* than wild-type were 16:0/16:1, 16:0/16:0, 18:2/16:3, 18:3/16:1, 18:3/16:0, 18:2/16:0, 18:1/16:0, 18:0/16:1, 18:2/18:2 and 18:1/18:1 (Figure 8C). On ½ MS media supplemented with 75mM NaCl the total DAG in *npc5-1* was 76% of wild-type level (Figure 8B). The total DAG content in *npc5-1* remained unchanged after treatment with 75mM NaCl, whereas the DAG content in wild-type roots was reduced by 22.8% compared to DAG levels on ½ MS. Taken together these results suggest that the reduction of DAG in *npc5-1* is not critical for lateral root development under normal growth conditions. However, under mild salt stress conditions the reduction of DAG in *npc5-1* may adversely affect lateral root formation.

Exogenous DAG Restores Lateral Root Formation in *npc5-1* Under Salt Stress

We next tested whether exogenous DAG could restore lateral root formation in *npc5-1* seedlings on 75mM NaCl. In plants, DAG can be derived from various pathways, including de novo synthesis in ER or the plastid; the action of PA phosphatase on PA; hydrolysis of membrane lipids by phospholipase C or phospholipase D/PA phosphatase

reaction. On the other hand, diacylglycerol kinase (DGK) can convert DAG to PA (Gomez-Merino et al., 2005). Therefore, we hypothesized that either DAG, the direct product of NPC5, or PA may be responsible for lateral root formation under salt stress. In order to test this hypothesis, 100 μM of DAG, PA, or a DAG kinase inhibitor 1 (DGK1) was prepared, and a volume of 100 μl was spread evenly on solidified 75mM NaCl plates. In wild-type plants treated with 75mM NaCl, there was a slight increase in lateral root number compared to plants on $\frac{1}{2}$ MS media. On media containing 75mM NaCl and DAG, wild-type produced slightly more lateral roots compared to $\frac{1}{2}$ MS and 75mM NaCl media (Figure 8A). The addition of DGKI1 also mimicked the effect of added DAG and a modest increase of lateral root formation was observed in wild-type seedlings (Figure 9A). *npc5-1* seedlings regained the ability to produce lateral roots at wild-type levels following treatment with DAG and DAGKI1 in the presence of 75mM NaCl (Figures 9A, 9G, and 9H). Treatment with PA did not affect lateral root formation in wild-type seedlings and was unable to restore lateral root formation to wild-type levels in *npc5-1* seedlings treated with NaCl (Figures 9A and 9I).

We then tested the effect of DAG and PA on the formation of lateral roots over a range of DAG and PA concentrations, as this might reveal a more complex relationship between the DAG/PA balance and lateral root formation. Wild-type and mutant seedlings were grown on $\frac{1}{2}$ MS media containing 75mM NaCl and DAG or PA, with concentrations ranging from 10 μM -100 μM . The appropriate amount of DAG and PA was added to the media before solidification. When plants were treated with 10 μM DAG, lateral root formation in *npc5-1* was restored to 50% of wild-type level. 25 μM -100 μM DAG restored lateral root formation in *npc5-1* to wild-type level (Figure 10A). On the other hand, PA treatment had a less potent effect on the restoration of lateral roots in *npc5-1*. Treatment with 10 μM -75 μM PA had little effect on mutant plants, while 100 μM PA was able to restore lateral root growth in *npc5-1* to roughly 33% of wild-type level (Figure 10B). Therefore, it appears that DAG is ten times more potent than PA in lateral root restoration in *npc5-1*.

Discussion

Salt stress is one of the most growth-limiting stresses affecting plant growth and productivity worldwide (Qiu et al, 2002). Salt stress signal transduction includes a combination of ionic and osmotic homeostasis signaling pathways, detoxification pathways, and growth regulation pathways (Zhu, 2002). Due to the complexity of salt stress signaling, a considerable percentage of the genome is induced by salt stress (Zhu, 2002). Over recent years, considerable progress has been made in identifying some of the important players involved in mediating salt tolerance. The Salt Overly Sensitive (*SOS1*, *SOS2* and *SOS3*) genes are responsible for sensing salt stress and maintaining ion homeostasis (Qiu et al, 2002). Interestingly, *SOS2*, a serine threonine protein kinase, has been identified as a negative regulator of *AtPLC1* (Zhu et al, 1998). Additionally, numerous downstream genes that are involved in dehydration stress are also involved in salt stress. These genes include members of the dehydration response element binding factor 2 (*DREB2*), members of the ethylene response factor (*ERF*)/*APETALA2* (*AP2*) and members of the NAC homeodomain-ZIP transcription factors (Gosti et al., 1995; Yamaguchi-Shinozaki and Shinozaki, 2006; He et al, 2005). In addition to the signaling components involved in salt stress, distinct morphological alterations are evident. Salt stress promotes lateral root formation and greatly inhibits primary root growth; this can be viewed as an adaptive response in which the lateral roots compensate for the primary roots in obtaining water and minerals (He et al, 2005). *AtNAC2* has been identified as one of the players involved in promoting lateral root growth in Arabidopsis (He et al., 2005). Nevertheless, very little is known about the genes involved in promoting lateral roots under salt stress. We show here that *NPC5* is induced by salt stress and is involved in promoting lateral root growth under salt stress.

Indeed the molecular regulation of root system architecture is quite complex. Despite the identification of several genes involved in this process, our understanding of how root architecture is regulated in response to environmental stimulus is rudimentary. *Lateral Root Development* (*LRD2*) in conjunction with ABA is responsible for repressing lateral root development under osmotic growth conditions (Deak and Malamy, 2005). *lrd2* disrupts *Long Chain Acyl-CoA Synthetase2*, a gene that is involved in cutin biosynthesis

(MacGregor et al., 2008). *LINI*, a putative high affinity nitrogen transporter, coordinates lateral root initiation in response to carbon: nitrogen ratios (Malamy and Ryan, 2001; Little et al., 2005). *ANRI*, a MADS-box transcription factor is required for coordinating lateral root development with exogenous nitrate (Zhang and Forde, 1998). *NIT3*, a nitrilase that converts indole-3-acetonitrile to IAA, is highly upregulated by sulfur starvation and accounts for the highly branched root system under sulfate deprivation (Kutz et al., 2002). *PDR2* and *LPRI* coordinate root system architecture with phosphate levels to maximize Pi acquisition (Ticconi et al., 2004; Lopez-Bucio et al., 2005). Overexpression of *NAC-2* promotes lateral root growth under normal growth conditions and mild salt stress (He et al., 2005).

The data presented here show that the loss of *NPC5* decreases lateral root formation under mild salt stress, while overexpression of *NPC5* promotes lateral root formation constitutively (Figures 4C and 6). Under normal growth conditions *npc5-1* mutants grow and develop similarly to wild-type plants. *npc5-1* falls under a category of mutants described by Malamy and Ryan (2001) in which the program for lateral root growth is functional but the signal transduction that stimulates the program is defective. Indeed mutants of this nature are rare. Defects in genes involved in the signaling pathway that promote or inhibit lateral roots in response to environmental cues do not cause dramatic alterations under normal conditions. However, under environmental changes the plant's ability to adapt morphologically becomes affected (Malamy and Ryan, 2001). Under the growth conditions defined in our experiments, the *npc5-1* phenotype is most dramatic at 75 mM NaCl. When treated with 150 mM NaCl, lateral root formation increased but was still lower than wild-type (Figure 4J). Also of interest, *npc5-1* mutants display defects in morphological fine tuning of the primary roots that elongate at a faster rate than wild-type on 75 mM-125 mM NaCl. These results indicate that *NPC5* functions under mild salt stress and other signaling components may become involved at higher levels of salt stress attenuating the *npc5-1* phenotype. Direct evidence exists for the differential regulation of genes depending upon the severity of osmotic stress. In alfalfa cells, the MAP kinase SIMK was activated under moderate osmotic stress. However, at severe hyperosmotic stress SIMK is no longer activated, instead a smaller kinase becomes activated (Munnik

et al, 1999). Likewise, in yeast, the EHA1 pathway is only induced by extreme hyperosmotic stress (Serrano et al., 1997), and the HOG1 MAP kinase pathway is activated by mild to moderate hyperosmotic stress (Brewster et al., 1993; Ferrigno et al., 1998).

Root morphology in Arabidopsis is governed by many factors. Aside from hormonal signaling, lipid based signaling is now being recognized as an important player in root morphology under stress conditions. Recent studies indicate that PA, which can be derived directly from the action of PLD or indirectly by the phosphorylation of DAG produced via the PLC/DGK pathway, is involved in root apical growth and initiation through its interaction with an Arabidopsis phosphoinositide dependent protein kinase 1 (AtPDK1) (Anthony, et al, 2004). Additionally, PA produced by PLD ζ s modulates root architecture under phosphate deprived conditions in Arabidopsis (Li et al., 2006). Other studies showed that levels of PA increased rapidly in response to hyperosmotic stress (Munnik et al., 2000). Another novel lipid second messenger, diacylglycerol pyrophosphate (DGPP), is unique to plants. DGPP is formed through the action of PA kinase and attenuates the PA effect (Zalejski et al., 2005). On the other hand, DGPP is proposed to be involved in signaling itself, increasing rapidly in plants subjected to ABA, hyperosmotic stress and pathogens (Zalejski et al., 2005; Munnik et al., 2000; van der Luit et al., 2000). In contrast, DAG has been identified as a known activator of protein kinase C (PKC) in animals. However, whether DAG transduces a direct signal in plants is unknown, since no PKCs have been found in Arabidopsis. Additionally, DAG failed to accumulate in various plant organs upon activation of the PI-PLC pathway. Therefore, it was speculated that DAG produced by the action of PI-PLC on phosphatidylinositol 4,5-bisphosphate is immediately phosphorylated to PA (Meijer and Munnik, 2003; Munnik, 2001). This implies that DAG does not transduce a direct signal. However, two independent studies provide evidence that suggest that DAG function in plants is more profound than it merely being converted to PA. The first study shows that the majority of DAG produced via the action of PC-PLC (NPC4) under phosphate starved conditions is not converted to PA (Nakamura et al, 2005). Secondly, DAG accumulation was observed in Arabidopsis pollen tubes and is believed to act as a signaling molecule (Helling et al., 2006). Our present results show that DAG, but not PA, can fully rescue *npc5-1*

phenotype (Figure 10). The lipid profiling analysis revealed that the level of PA of *npc5-1* was comparable to wild-type, but the level of DAG levels was significantly lower than wild-type in normal and salt-stressed conditions (Figures 7 and 8). Further evidence that DAG is responsible for *npc5-1* phenotype stems from the results obtained when *npc5-1* seedlings were treated with DAGKI1. Blocking the pathway that converts DAG to PA fully restores lateral root formation in *npc5-1* seedlings treated with 75mM NaCl. This indicates that the conversion of DAG to PA is not required for lateral root formation in *npc5-1* under salt stress, whereas, increasing the intrinsic pool of DAG with DAGKI1 or the exogenous application of DAG to *npc5-1* promotes lateral root formation under mild salt stress.

The genetic and physiological experiments presented here indicate that *NPC5* is required for coordinating lateral root development in response to mild salt stress conditions. We propose that *NPC5* mediates plant response to mild salt stress through its lipid product DAG. Our studies define a novel regulatory role for *NPC5* and its lipid product DAG in salt stress signaling. Identification of the possible downstream targets of *NPC5* and DAG will elucidate the mechanism by which this phospholipase regulates lateral root development in response to abiotic cues. This would represent a significant step in understanding the plastic nature of root development and possibly establish DAG as a signaling molecule in plants.

Materials and Methods

Plant Growth Conditions

Arabidopsis thaliana ecotype Columbia-0 seeds were sterilized in 70% ethanol for 5 min followed by 20% bleach for 3 min and then rinsed three times with sterile distilled water. The seeds were stratified at 4°C for 48 h. Seeds were sown on ½ Murashige and Skoog (MS) media containing 1.5% sucrose and grown at 23 °C under 12-h light, 12-h dark light cycle.

Phenotypic Analysis of *npc5-1* and Transgenic Plants

Seeds were sterilized as described above and germinated on ½ MS media containing 1.5% sucrose. After four days the seedlings were transferred to vertical ½ MS plates with different concentrations of NaCl (25-150 mM) or 1 µM IAA for nine days, and primary root was measured and the lateral roots were counted. For rescue experiments using 8:0 DAG and PA obtained from Avanti Polar Lipids, the lipids were prepared by drying the chloroform under a stream of nitrogen gas and resuspending the dried lipid in water followed by sonication. The DGK11 (Calbiochem) was dissolved in DMSO. These solutions were either added to the surface of solidified agar plates (100 µl of 100 µM) or directly to the media before solidification (10-100 µM). Lateral root number was scored after nine days.

Identification of *npc5-1* Knockout Mutant

A putative knockout mutant of *NPC5*, SALK_045037, was identified in the Salk Institute T-DNA insertion library database (<http://signal.salk.edu/cgi-bin/tdnaexpress>; Alonso et al., 2003) and seeds were ordered from the ABRC (Ohio State University). The seeds were sown on soil and the seedlings were analyzed individually by PCR to confirm the presence of the T-DNA insertion using LBA1 primer that amplifies the left border of the T-DNA and gene-specific primer P2 (5'-TTGTGGTTGAACAACGTTGGTATG-3'). Plants bearing the T-DNA insert were self fertilized and probed with gene-specific primers P1 (5'-TCACCTCCCCTTTCTCTTGCC-3') and P2. The plants that were homozygous for the T-DNA insertion were checked for the lack of *NPC5* transcript using primers P3 (5'-GGAGACTACAAAAACGAAGAATTGCTAT-3') and P4 (3'-GTGATGGTGGTGGTTTCACAACATTAT-5') by qRT-PCR as described below.

Quantitative Real Time PCR

Total RNA was isolated using a rapid CTAB method (Stewart and Via, 1993; Li et al., 2006), and RNA was precipitated using 2M LiCl at 4°C. RNA integrity was checked on 1% (w/v) agarose gel. Eight µg of total RNA was digested with DNaseI according to manufacturer's instructions (Ambion, Inc.) to remove DNA

contamination. The RNA was reverse transcribed using iScript cDNA Synthesis Kit (BIO-Rad, CA). The efficiency of cDNA synthesis was analyzed by real time PCR amplification of *UBQ10* (At4g05320). The level of gene expression was normalized to that of *UBQ10*. PCR was performed with MyiQ Sequence Detection System (Bio-Rad, CA) using SYBR Green to monitor dsDNA synthesis. Reaction mix contained 7.5 μ l 2xSYBR Green Master Mix reagent Kit (BIO-Rad, CA), 1.0 ng cDNA, and 200 nM of each gene specific primer in a final volume of 15 μ l. The qRT-PCR cycling conditions comprised 90 sec denaturation at 95°C and 50 cycles at 95°C for 30 sec, 55°C for 30 sec, and 72°C for 30 sec, with the final cycle being terminated at 72°C for an additional 10 min.

Overexpression of *NPC5* and Complementation of *npc5-1*

The *NPC5* cDNA was amplified from 5'RACE pollen cDNA library and cloned into modified p35S-FAST in the sense orientation. The resulting construct was used to overexpress NPC5 in wild-type *Arabidopsis*. For genetic complementation of *npc5-1* genomic DNA was amplified from wild-type *Arabidopsis* plants, 1403 bp from the start codon and 263 bp after the stop codon. The *AscI* restriction site was incorporated using primers 5'-ATGGCGCGCCGTTTATGTTGGCATGTCCAGTC-3' and 3'-ATGGCGCGCGCCTGCTAATATCCAAGGCTAGAGCAC-5'. The resulting product was subcloned into pCR[®]2.1-TOPO[®] vector. The fragment was subsequently cloned into pEC291 vector. Genetic transformation was performed by transforming the constructs into *Agrobacterium* C58. The presence of the construct in *agrobacterium* was confirmed by PCR and used to transform *npc5-1* and wild-type *Arabidopsis*. Transformants were selected based on hygromycin resistance for *npc5-1-C* plants and were further confirmed by PCR. Plants overexpressing *NPC5* were selected based on kanamycin resistance and western blotting. Confirmed transformants were transplanted to soil for self-pollination, and T2 seeds from individual T1 plants were germinated to screen for homozygous T2 lines.

Histochemical Localization of GUS Activity

The promoter region of *NPC5* was amplified, 1601 bp upstream of the start codon and cloned into pCAMBIA1301 using *SacI* and *NcoI* restriction sites. The primers used are: 5'- CGCCCATGGTCTATTTGTTTTCCAATTGAATTATTGATGAAAGTTTG-3' and 5'- GCGGAGCTCATTGCATGGGATCCAGGGCC-3'. The resulting construct was transformed into wild-type Arabidopsis and T2 plants were used for GUS activity. 7 day old seedlings and organs from 4 week old were used for histochemical localization. The GUS substrate solution contained 1 mg of 5-bromo-4-chloro-3-indolyl β -D-Glucuronide (X-Gluc) in 0.1 mL methanol, 1 mL 0.1 M sodium citrate buffer, 20 μ L 0.1 M potassium ferrocyanide, 20 μ L 0.1 M ferricyanide, 10 μ L 10% (w/v) triton X-100, and 0.85 mL water. Samples were incubated at 37°C for 24 h. Green tissues were incubated in 70% ethanol to remove chlorophyll. Specimens were placed in 50% glycerol and examined a dissecting microscope.

Subcellular Localization of GFP Fusion Proteins

For generation of NPC5-GFP, cDNA was cloned into pMDC43 and pMDC83 vectors (Curtis & Grossniklaus, 2003). The primers used to clone *NPC5* into pMDC43 are: 5'- TTTGGCGCGCCTATGGCCGAGACGAAAAAAGGCT'3' and 5'-CCCTTAATTAAT TAATTTGACCAAGGAGTAGCATGTGATGG-3'. The primers used to clone *NPC5* into pMDC83 are: 5'-GGGTTAATTAATGGCCGAGACGAAAAAAGGCTC3' and 5'- TTTGGCGGCCCATTTGACCAAGGAGTAGCATGTGATGG-3'.

C-terminally fused NPC5-GFP was generated from pMDC83 construct and N-terminally fused NPC5-GFP was generated from pMDC43. Constructs were transformed into *Agrobacterium* C58 and grown at 30°C in LB broth supplemented with 50 μ g ml⁻¹ kanamycin. The cells were harvested by centrifugation at 5000 g for 10 min at room temperature and resuspended in 10 mM MgCl₂ and 150 μ g ml⁻¹ acetosyringone. Cells were left for 3 h at room temperature and then infiltrated into 3-week old tobacco leaves. After 48 h the specimens were analyzed using a Zeiss LSM 510 confocal/multi-photon microscope (<http://www.zeiss.com/>).

Lipid Profiling

The process of lipid extraction, lipid analysis and quantification was performed as

described by Welti et al. (2002). Leaves were collected from 4 week old *Arabidopsis* plants and immersed immediately in 3 ml hot isopropanol containing 0.01% butylated hydroxytoluene at 75°C. Lipids were extracted from the tissue using chloroform/methanol. The remaining tissue was oven dried at 100°C and weighed. Lipids composition was analyzed by an electrospray ionization triple quadrupole mass spectrometer (API4000). Total lipids were quantified based on the dry weight of the samples.

IAA Content

100 mg of root or leaf tissues were ground in liquid nitrogen and 0.5 ml of 1-propanol:H₂O: Concentrated HCL (2:1:0.002 v/v) was added to the homogenate and vortexed well. 1 ml of dichloromethane and IAA internal standard (d₅ IAA) was added. The samples were vortexed and centrifuged at 11300g for 1 min. The lower phase was transferred and IAA was quantified by mass spectrometry.

References

1. **Alonso, J.M., et al.** (2003). Genome-wide insertional mutagenesis of *Arabidopsis thaliana*. *Science*. **301**, 653–657.
2. **Anthony, R.G., Henriques, R., Helfer, A., Meszaros, T., Rios, G., Testerink, C., Munnik, T., Deak, M., Koncz, C., and Bogre, L.** (2004) A protein kinase target of a PDK1 signaling pathway is involved in root hair growth in *Arabidopsis*. *EMBO J.* **23**, 572-581.
3. **Brewster, J.L., deValoir, T., Dwyer, N.D., Winter, E. and Gustin, M.C.** (1993) An osmosensing signal transduction pathway in yeast. *Science*. **259**, 1760-1763.

4. **Cao, W., Liu, J., He, X., Mu, R., Zhou, H., Chen, S., and Zhang, J.** (2007) Modulation of Ethylene Responses Affects Plant Salt-Stress Responses. *Plant Physiol.* **143**, 707-719.
5. **Casimiro, I., Marchant, A., Bhalerao, R.P., Beeckman, T., Dhooge, S., Swarup, R., Graham, N., Sandberg, G., Casero, P.J., and Bennett, M.** (2001) Auxin Transport Promotes Arabidopsis Lateral Root Initiation. *Plant Cell.* **13**, 843-852.
6. **Casimiro, I., Beeckman, T., Graham, N., Bhalerao, R., Zhang, H., Casero, P., Sandberg, G., and Bennett, M.J.** (2003) Dissecting *Arabidopsis* lateral root development. *Trends in Plant Sci.* **8**(4), 1360-1385.
7. **Celenza, J.L., Grisafi, P.L., and Fink, G.R.** (1995) A pathway for lateral root formation in *Arabidopsis thaliana*. *Genes Dev.* **9**, 2131- 2142.
8. **Chen, J., Zhang, W., Song, F., and Zheng, Z.** (2007) Phospholipase C/diacylglycerol kinase-mediated signaling is required for benzothiadiazole-induced oxidative burst and hypersensitive cell death in rice suspension-cultured cells. *Protoplasma.* **230**, 13-21.
9. **Curtis M and Grossniklaus U.** (2003) A Gateway™ cloning vector set for high-throughput functional analysis of genes in plants. *Plant Physiology* **133**, 462-469
10. **Deak, K.I., and Malamay, J.** (2005) Osmotic regulation of root system architecture. *Plant J.* **43**, 17-28.
11. **Ferrigno, P., Posas, F., Koepf, D., Saito, H., and Silver, P.A.** (1998) Regulated nucleo/cytoplasmic exchange of HOG1 MAPK requires the importin^β homologs NMD5 and XPO1. *EMBO J.* **17**, 5606-5614.
12. **Fukaki, H., Tameda, S., Masuda, H., and Taska, M.** (2002) Lateral root formation is blocked by a gain-of-function mutation in the *SOLITARY-ROOT/IAA14* gene of *Arabidopsis*. *Plant J.* **29**(2), 153-168.
13. **Gaude N, Nakamura Y, Scheible WR, Ohta H, Dormann P.** (2008) Phospholipase C5 (NPC5) is involved in galactolipids accumulation during phosphate limitation in leaves of Arabidopsis. *Plant J* **56**: 28-39.

14. **Gomez-Merino, F.C., Arana-Ceballos, F.A., Trejo-Tellez, L.I., Skirycz, A., Brearley, C.A., Dormann, P., and Mueller-Roeber, B.** (2005) *Arabidopsis* AtDGK7, the Smallest Member of Plant Diacylglycerol Kinases (DGKs), Displays Unique Biochemical Features and Saturates at Low Substrate Concentration. The dgk inhibitor r59022 differentially affects atdgk2 and atdgk7 activity in vitro and alters plant growth and development. *J. of Biol. Chem.* **280** (41), 34888-34899.
15. **Gosti, F., Bertauche, N., Vartanian, N. and Giraudat, J.** (1995) Abscisic acid-dependent and -independent regulation of gene expression by progressive drought in *Arabidopsis thaliana*. *Mol. Gen. Genet.* **246**, 10–18.
16. **He, X., Mu, R., Cao, W., Zhang, Z., Zhang, J., and Chen, S.** (2005) AtNAC2, a transcription factor downstream of ethylene and auxin signaling pathways, is involved in salt stress response and lateral root development. *Plant J.* **44**, 903-916.
17. **Helling, D., Possart, A., Cottier, S., Klahre, U., and Kost, B.** (2006) Pollen Tube Tip Growth Depends on Plasma Membrane Polarization Mediated by Tobacco PLC3 Activity and Endocytic Membrane Recycling. *Plant Cell.* **18**, 3519-3534.
18. **Hibara, K., Takada, S., and Tasaka, M.** (2003) *CUC1* gene activates the expression of SAM-related genes to induce adventitious shoot formation. *Plant J.* **36**, 687-696.
19. **Himanen, K., Boucheron, E., Vanneste, S., Engler, J., Inze, D., and Beeckman, T.** (2002) Auxin-Mediated Cell Cycle Activation during Early Lateral Root Initiation. *Plant Cell.* **14**, 2339-2351.
20. **Igal, R.A., Cavigilia, J.M., Gomez Dumm, I.N.T., Coleman, R.A.** (2001) Diacylglycerol generated in CHO cell plasma membrane by phospholipase C is used for triacylglycerol synthesis. *J. of Lipid Research.* **42**, 88-95.
21. **Karthikeyan, A.S., Varadarajan, D.K., Jain, A., Held, M.A., Carpita, N.C., and Raghothama, K.G.** (2007) Phosphate starvation responses are mediated by sugar signaling in *Arabidopsis*. *Planta* **225**, 907–918.
22. **Koiwa, H., Li, F., McCully, M.G., Mendoza, I., Koizumi, N., Manabe, Y., Nakagawa, Y., Zhu, J., Rus, A., Padro, J.M., Bressan, R.A., and Hasegawa,**

- P.M.** (2003) The STT3a Subunit Isoform of the Arabidopsis Oligosaccharyltransferase Controls Adaptive Responses to Salt/Osmotic Stress. *Plant Cell*. **15**, 2273-2284.
- 23. Konishi, M., and Sugiyama, M.** (2006) A Novel Plant-Specific Family Gene, *ROOT PRIMORDIUM DEFECTIVE1*, Is Required for the Maintenance of Active Cell Proliferation. *Plant Physiol*. **140**, 591-602.
- 24. Kutz, A., Muller, A., Hennig, P., Kaiser, W., Piotrowski, M., and Weiler, E.** (2002) A role for nitrilase 3 in the regulation of root morphology in sulphur-starving *Arabidopsis thaliana*. *Plant J*. **30**, 95-106.
- 25. Laskowski, M.J., Williams, M.E., Nusbaum, H.C., and Sussex, I.M.** (1995) Formation of lateral root meristems is a two-stage process. *Development*. **121**, 3303-3310.
- 26. Laxalt, A.M., and Munnik, T.** (2002) Phospholipid signalling in plant defence. *Current Opinion in Plant Biol*. **5**, 1369.
- 27. Li, G., and Xue, H.** (2007) *Arabidopsis* *PLDζ2* Regulates Vesicle Trafficking and Is Required for Auxin Response. *Plant Cell*.
- 28. Li, M., Qin, C., Welti, R., Wang, X.** (2006) Double Knockouts of Phospholipases Dζ1 and Dζ2 in Arabidopsis Affect Root Elongation during Phosphate-Limited Growth But Do Not Affect Root Hair Patterning. *Plant Physiol*. **140**, 761-770.
- 29. Liu, J., Srivastava, R., Che, P., and Howell, S.H.** (2007) Salt stress responses in Arabidopsis utilize a signal transduction pathway related to endoplasmic reticulum stress signaling. *Plant J*. **51**, 897-909.
- 30. Little, D.Y., Rao, H., Oliva, S., Daniel-Vedele, F., Krapp, A., and Malamay, J.E.** (2005) The putative high-affinity nitrate transporter NRT2.1 represses lateral root initiation in response to nutritional cues. *PNAS*. **102**:38, 13693-13698
- 31. Lopez-Bucio, J., Hernandez-Abreu, E., Sanchez-Calderon, L., Perez-Torres, A., Rampey, R.A., Bartel, B., and Herrera-Estrella, L.** (2005) An Auxin Transport Independent Pathway Is Involved in Phosphate Stress-Induced Root Architectural Alterations in Arabidopsis. Identification of *BIG* as a Mediator of Auxin in Pericycle Cell Activation . *Plant Physiol*. **135**, 681-691.

32. **Macgregor, D.R., Deak, K.I., Ingram, P.A., Malamy, J.E.** (2008). Root system architecture in *Arabidopsis* grown in culture is regulated by sucrose uptake in the aerial tissues. *Plant Cell*. **20**, 2643-60
33. **Malamay, J.E., and Benfey, P.N.** (1997) Organization and cell differentiation in lateral roots of *Arabidopsis thaliana*. *Development*. **124**, 33-44.
34. **Malamay, J.E., and Ryan, K.S.** (2001) Environmental Regulation of Lateral Root Initiation in *Arabidopsis*. *Plant Physiol*. **127**, 899-909.
35. **Marchant, A., Bhalerao, R., Casimiro, I., Eklof, J., Casero, P.J., Bennett, M., and Sandberg, G.** (2002) AUX1 Promotes Lateral Root Formation by Facilitating Indole-3-Acetic Acid Distribution between Sink and Source Tissues in the *Arabidopsis* Seedling. *Plant Cell*. **14**, 589-597.
36. **Meijer, H.J.G. and Munnik, T.** (2003) Phospholipid-based signaling in plants. *Annu. Rev. Plant Biol.* **54**, 265–306.
37. **Munnik, T., Ligternik, W., Meskiene, I., Calderini, O., and Beyerly, J.** (1999). Distinct osmosensing protein kinase pathways are involved in signalling moderate and severe hyperosmotic stress. *Plant J.* **20**, 381-388.
38. **Montiel, G., Gantet, P., Jay-Allemand, C. and Breton, C.** (2004) Transcription factor networks. Pathways to the knowledge of root development. *Plant Physiol*. **136**, 3478–3485.
39. **Munnik, T., Meijer, H.J.G., Riet, B., Hirt, H., Frank, W., and Musgrave, A.** (2000) Hyperosmotic stress stimulates phospholipase D activity and elevates the levels of phosphatidic acid and diacylglycerol pyrophosphate. *Plant J.* **22(2)**, 147-154.
40. **Nakamura, Y., Awai, K., Masuda, T., Yoshioka, Y., Takamiya, K., and Ohta, H.** (2005) A Novel Phosphatidylcholine-hydrolyzing Phospholipase C Induced by Phosphate Starvation in *Arabidopsis*. *J. Biol. Chem.* **280**, 7469-7476.
41. **Olsen, A.N., Ernst, H.A., Leggio, L.L. and Skriver, K.** (2005) NAC transcription factors: structurally distinct, functionally diverse. *Trends Plant Sci.* **10**, 79–87.

42. **Qi, Z., and Spalding, E.P.** (2004) Protection of Plasma Membrane K⁺ Transport by the Salt Overly Sensitive1 Na⁺-H⁺ Antiporter during Salinity Stress. *Plant Physiol.* **136**, 2548-2555.
43. **Rogg L.E., Lasswell J. & Bartel B.** (2001) A gain of function mutation in IAA28 suppresses lateral root development. *Plant Cell* **13**, 465–480.
44. **Salman, M., and Pagano, R.E.** (1997) Use of a fluorescent analog of CDP-DAG in human skin fibroblasts: characterization of metabolism, distribution, and application to studies of phosphatidylinositol turnover. *J. of Lipid Research.* **38**, 482-490.
45. **Scherer, G.F.E., Paul, R.U., Holk, A., and Martinec, J.** (2002) Down-regulation by elicitors of phosphatidylcholine-hydrolyzing phospholipase C and up-regulation of phospholipase A in plants cells. *Biochem. and Biophysical Research Communications.* **293**, 766-770.
46. **Serrano, R., Marquez, J.A. and Rios, G.** (1997) Crucial factors in salt stress tolerance. In: *Yeast Stress Responses* (Hohmann,S. and Mager, W.h., eds). Austin, Texas: R.G. Landes Co., Heidelberg: Springer-Verlag, 147-164.
47. **Shinozaki, K. and Yamaguchi-Shinozaki, K.** (2007) Gene networksinvolved in drought stress response and tolerance. *J Exp Bot.* **58**, 221–227.
48. **Smet, I.D., Signora, L., Beeckman, T., Inze, D., Foyer, C.H., and Zhang, H.** (2003) An abscisic acid-sensitive checkpoint in lateral root development of Arabidopsis. *Plant J.* **33**, 543-555.
49. **Stewart CN Jr, Via LE** (1993) A rapid CTAB DNA isolation technique useful for RAPD fingerprinting and other PCR applications. *Biotechniques* **14**: 748-758
50. **Testerink, C., Dekker, H.L., Lim, Z., Johns, M.K., Holmes, A.B., de Koster, C.G., Ktistakis, N.T., and Munnik, T.** (2004) Isolation and identification of phosphatidic acid targets from plants. *Plant J.* **39**, 527-536.
51. **Ticconi, C.A., Delatorre, C.A., Lahner, B., Salt, D.E., Abel, S.** (2004) *Arabidopsis pdr2* reveals a phosphate sensitive checkpoint in root development. *Plant J.* **37**, 801-814.
52. **Torrey, J.G.,** (1950) Induction of lateral roots by indolacetic acid and decapitation. *Am J Bot.* **37**: 257-264.

53. Wang, X. (2004) Lipid Signaling. *Curr. Opin. in Plant Biol.* **7**,1–8.
54. Welti, R., Li, W., Li, M., Sang, Y., Biesiada, H., Zhou, H., Rajashekar, C.B., Williams, T.D., and Wang, X. (2002). Profiling membrane lipids in plant stress responses: role of phospholipase D α in freezing- induced lipid changes in Arabidopsis. *J. Biol. Chem.* **277**, 31994-32002.
55. West, G., Inze, D., and Beemster, G.T.S. (2004) Cell Cycle Modulation in the Response of the Primary Root of Arabidopsis to Salt Stress. *Plant Physiol.* **135**, 1050-1058.
56. Xie, Q., Frugis, G., Colgan, D., and Chua, N. (2000) Arabidopsis NAC1 transduces auxin signal downstream of TIR1 to promote lateral root development. *Genes Dev.* **14**, 3024-3036.
57. Zalejski, C., Paradis, S., Maldiney, R., Habricot, Y., Miginiac, E., Rona, J-P., and Jeanette, E. (2006) Induction of Abscisic Acid- Regulated Gene Expression by Diacylglycerol Pyrophosphate Involves Ca²⁺ and Anion Currents in Arabidopsis Suspension Cells. *Plant Physiol.* **141**, 1555-1562.
58. Zhang, H., and Forde B.G. (1998) An Arabidopsis MADS box gene that controls nutrient-induced changes in root architecture. *Science.* **279**, 407-408.
59. Zhang, H., and Forde B.G. (2000) Regulation of Arabidopsis root development by nitrate availability. *J Exp Bot* **51**: 51–59
60. Zhu, J-K. (2002) Salt and drought stress signal transduction in plants. *Annu. Rev. Plant boil.* **53**, 247-273.
61. Zhu, J-K., Liu, J., Xiong, L. (1998) Genetic analysis of salt tolerance in Arabidopsis. Evidence for a critical role of potassium nutrition. *Plant Cell* **10**:1181–1191

FIGURE LEGENDS

Figure 1. Expression levels of *NPC5* in Arabidopsis tissues.

(A) Expression patterns of *NPC5* as determined by qRT-PCR. Tissues were harvested from 6 week old soil grown plants. *UBQ10* was used to normalize mRNA in tissues. Values are means \pm SD (n=3) of three independent samples.

(B) Expression of *NPC5* detected by promoter GUS activity. Ten day old seedlings and four week old leaves and buds were used for GUS staining. The arrow indicates the region of GUS staining in the bud.

(C) Subcellular localization of *NPC5* in tobacco leaves. *NPC4* was used as a positive control. Two laser lines were used to detect chlorophyll fluorescence (red) and GFP fluorescence.

Figure 2. T-DNA insertion position in *NPC5*.

(A) Diagram showing the position of the T-DNA insert in *NPC5* genomic sequence and primers used to identify the *npc5-1* knockout mutant. A single T-DNA is inserted in the 3rd exon of *NPC5*.

(B) PCR confirmation of the T-DNA insertion in *npc5-1*. i, product obtained using primer P1 and P2; ii, product obtained using LBa1 primer and P2. The mutation in *npc5-1* is homozygous.

(C) Verification of the loss of *NPC5* transcript in *npc5-1* by qRT-PCR. *NPC5* gene specific primers (P3 and P4) were used to detect the mRNA of *NPC5*. The P3 and P4 primers failed to amplify the product in *npc5-1*, thereby confirming that *npc5-1* is a null mutant.

Figure 3. Root length and IAA content in wild-type and *npc5-1* in response to salt and IAA

(A) Root elongation of primary root on 1 μ M IAA. Five day old Arabidopsis were transferred to 1 μ M IAA and the root elongation was monitored over a 10 day period. Values are means \pm SD (n=15).

(B) Lateral root formation in response to 1 μ M IAA. Five day old Arabidopsis were transferred to 1 μ M IAA and lateral roots were scored after 10 days. Values are means \pm

SD (n=15). * indicates difference is significant with ($p < 0.05$) as determined by student's t-test.

(C) & (D) IAA content in wild type and *npc5-1* on $\frac{1}{2}$ MS and $\frac{1}{2}$ MS supplemented with 75 mM NaCl, respectively. The IAA content in 15 day old seedlings was determined by LC/MS/MS using d_5 IAA as an internal standard. Values are means \pm SD (n=3).

Figure 4. Effect of *npc5-1* mutation and complementation on root architecture under salt stress.

(A) Expression level of *NPC5* under abiotic stress as detected by Genevestigator (www.genevestigator.ethz.ch/at).

(B) Expression level of *NPC5* under salt stress. Ten day old Arabidopsis seedlings were treated with 200 mM NaCl for 3 hours and RNA was extracted and qRT-PCR was performed. *UBQ10* was used to normalize mRNA in tissues. Values are means \pm SD (n=3) of three independent samples.

(C) Lateral root number under salt stress. Four days old Arabidopsis seedlings were transferred to various concentrations of NaCl (0–150 mM). Lateral roots were quantified on day nine. *npc5-1* exhibited reduced lateral root formation under salt stress. The most dramatic reduction in lateral root was seen at 75 mM NaCl, hence all other experiments were performed using 75 mM NaCl unless otherwise specified.

(D) $\frac{1}{2}$ MS.

(E) $\frac{1}{2}$ MS-25mM NaCl.

(F) $\frac{1}{2}$ MS-50mM NaCl.

(G) $\frac{1}{2}$ MS- 75mM NaCl.

(H) $\frac{1}{2}$ MS-100mM NaCl.

(I) $\frac{1}{2}$ MS-125mM NaCl.

(J) $\frac{1}{2}$ MS-150mM NaCl.

Figure 5. Microscopic examination of wild-type and *npc5-1* roots under mild salt stress. Four day old seedlings were transferred from $\frac{1}{2}$ MS to plates containing 75 mM NaCl. Roots were examined under the microscope after seven days. The formation of the lateral

root primordia is indicated by the arrows.

Figure 6. Over expression of *NPC5* promotes lateral root formation.

(A) Lateral root formation of NPC5-OE. *NPC5* cDNA was amplified from pollen RACE cDNA library and cloned into p35S-FAST expression vector and expressed in wild-type *Arabidopsis*. Five day old seedlings were transferred from ½ MS plates to vertical plates 0 or 75 mM NaCl. Values are means ± SD (n=15).

(B) Phenotype of NPC5-OE on ½ MS. Pictures were taken ten days after seedlings were transferred.

(C) Phenotype of NPC5-OE on 75 mM NaCl. Pictures were taken ten days after seedlings were transferred.

Figure 7. Phospholipid composition of *npc5-1* and wild-type root in the presence and absence of NaCl .

(A) Phospholipid composition on ½ MS. Four day old *Arabidopsis* seedlings were transferred to ½ MS vertical plates for ten days. Rosettes and roots were separated and total lipids were extracted using chloroform-methanol and analyzed by MS/MS-ESI. a denotes that *npc5-1* and wild type values are significantly different (P<0.05).

(B) Phospholipid composition in wild type and *npc5-1* on 75 mM NaCl. Values are means ± SE (n=5).

Figure 8. Total DAG and DAG molecular species in wild type and *npc5-1*.

(A) & (B) Total DAG in wild type and *npc5-1* roots grown on ½ MS and 75 mM NaCl, respectively. The DAG content in *npc5-1* is significantly lower than wild type seedlings in the presence and absence of salt stress. a; denotes that *npc5-1* value is significantly lower than wild type (P<0.05).

(C) & (D) DAG molecular species in wild type and *npc5-1* roots grown on ½ MS and 100 mM NaCl, respectively. b; indicates that *npc5-1* value is significantly higher than wild type. Values are means ± SE (n=5).

Figure 9. DAG rescues *npc5-1* phenotype.

(A) Lateral root formation is rescued by DAG in *npc5-1* while PA effect is less dramatic. Four day old Arabidopsis seedlings were transferred to ½ MS media or ½ MS media supplemented with 75mM NaCl and 100 µL of 100 µM of DAG, PA or DGKI1. Lateral roots were quantified after 9 days.

(B) ½ MS.

(C) ½ MS-8:0 PA.

(D) ½ MS- DGKI1.

(E) ½ MS- 8:0 DAG.

(F) ½ MS-75mM NaCl.

(G) ½ MS-75mM NaCl-8:0 DAG.

(H) ½ MS-75mM NaCl-DGKI1.

(I) ½ MS-75mM NaCl- 8:0 PA.

Figure 10. The effect of various concentrations of DAG and PA on *npc5-1* phenotype.

(A) The effect of DAG on lateral root formation in *npc5-1*. Five day old seedlings were transferred to ½ MS-75 mM NaCl agar plates with 0-100 µM DAG. Lateral roots were scored 10 days after transfer. Values are means ± SD (n=15).

(B) The effect of PA application on lateral root formation in *npc5-1*. Five day old seedlings were transferred to ½ MS-75 mM NaCl agar plates with 0-100 µM PA. Lateral roots were scored 10 days after transfer. Values are means ± SD (n=15).

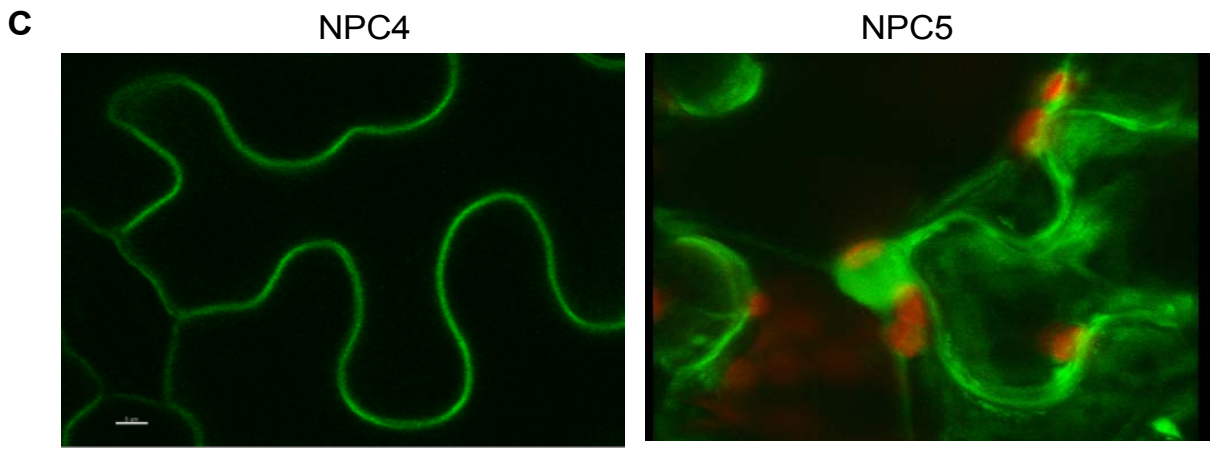
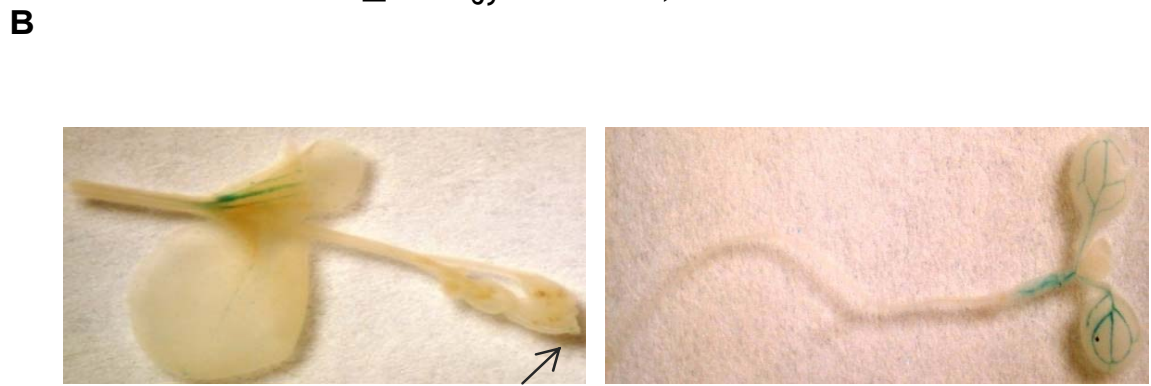
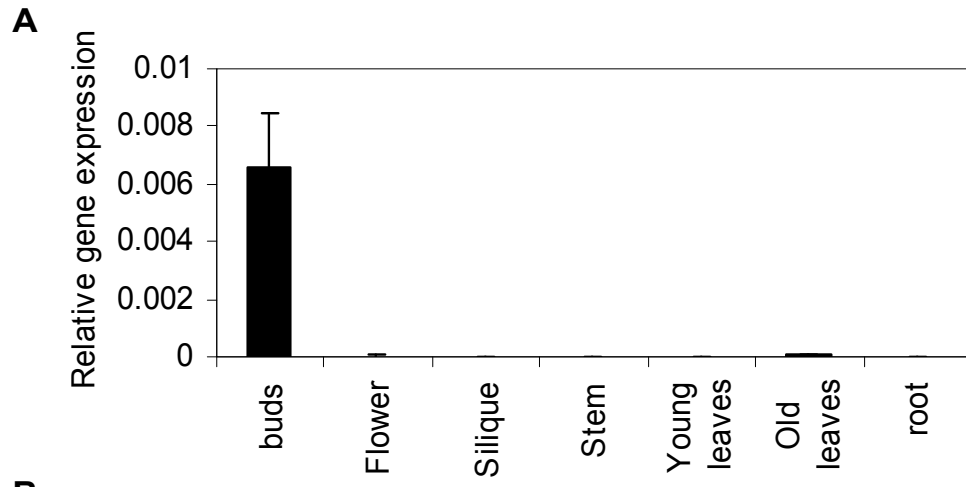


Figure 1

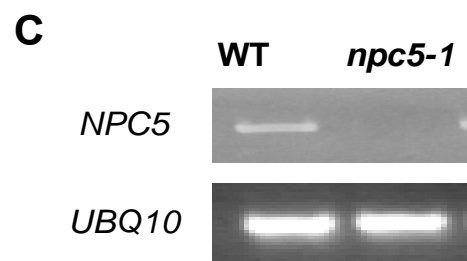
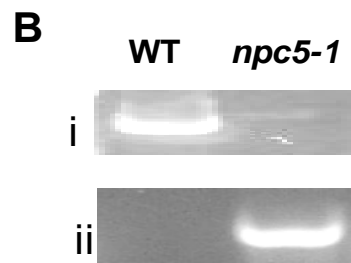
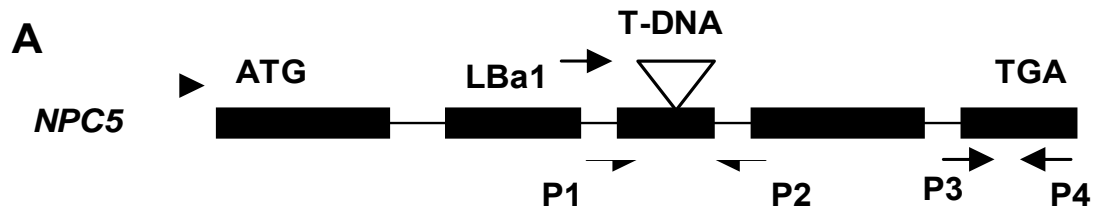


Figure 2

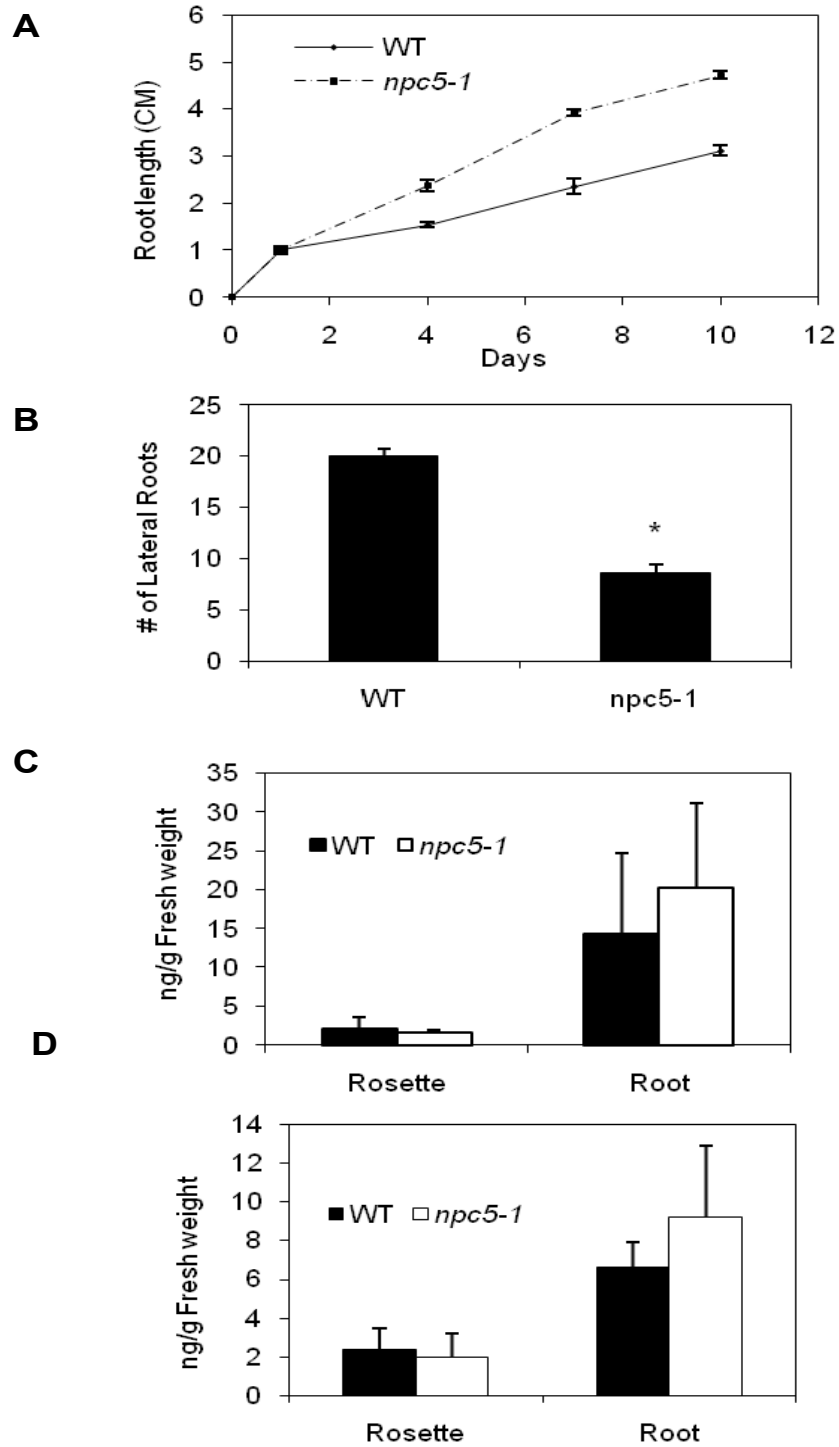


Figure 3

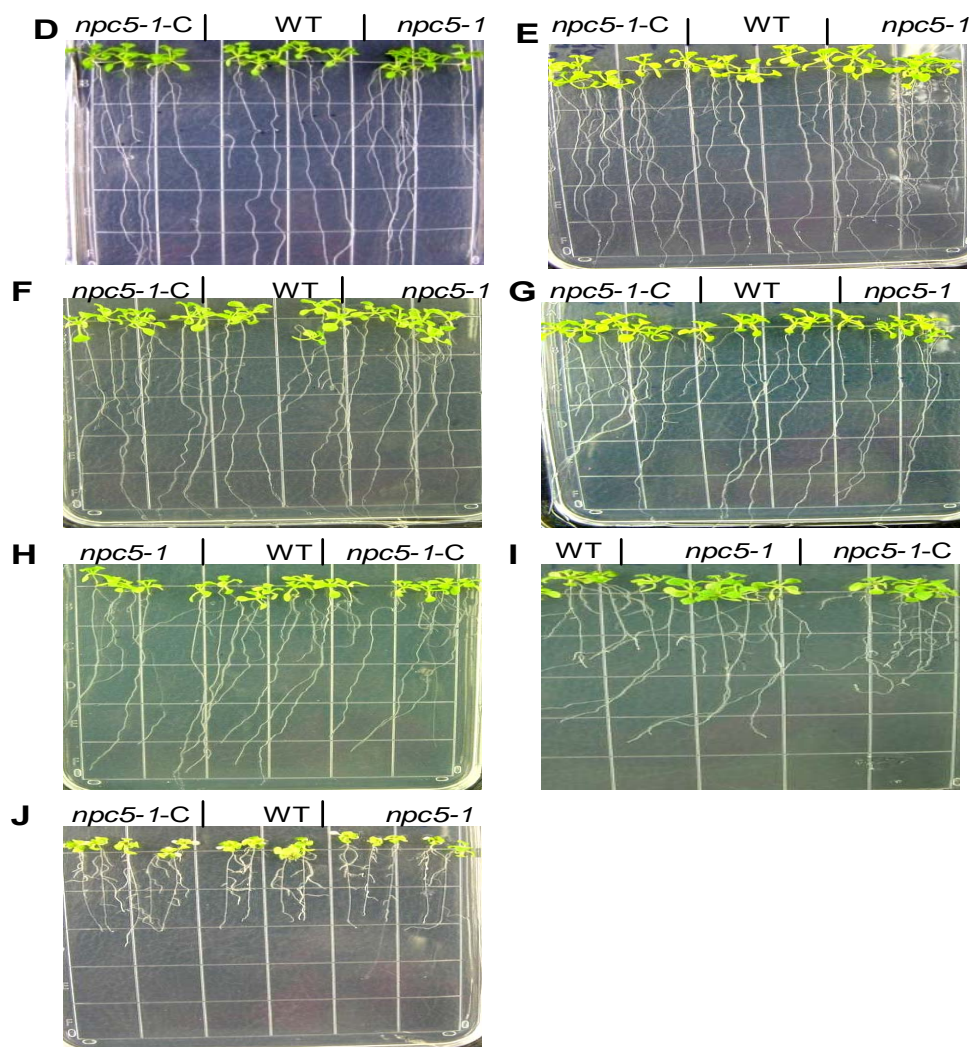
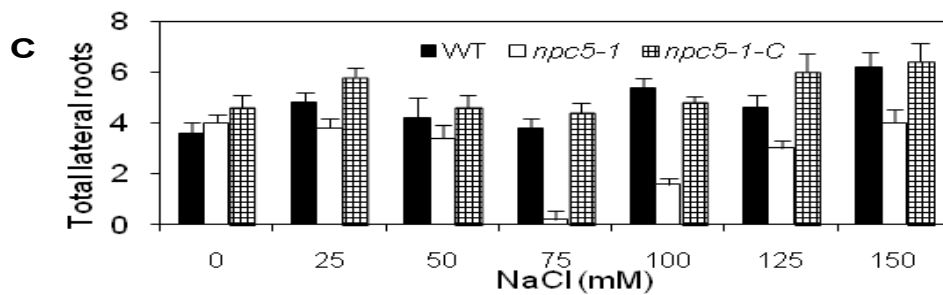
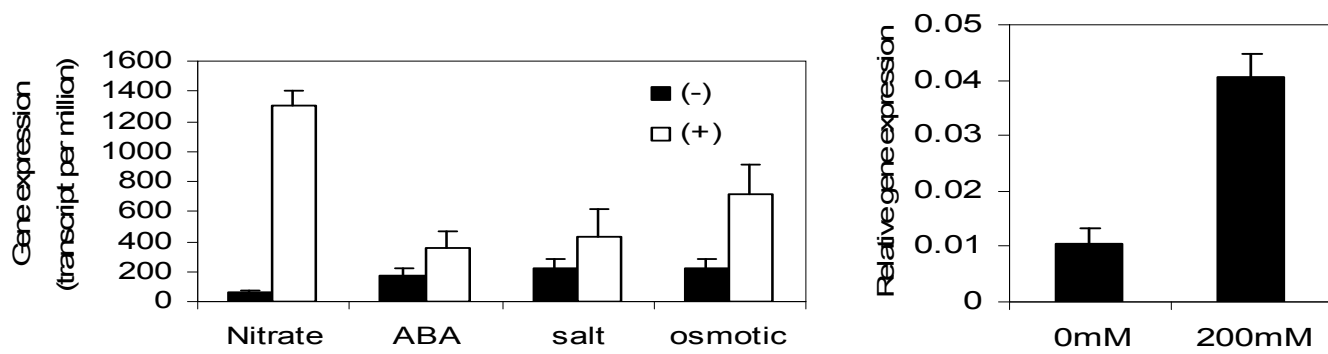


Figure 4

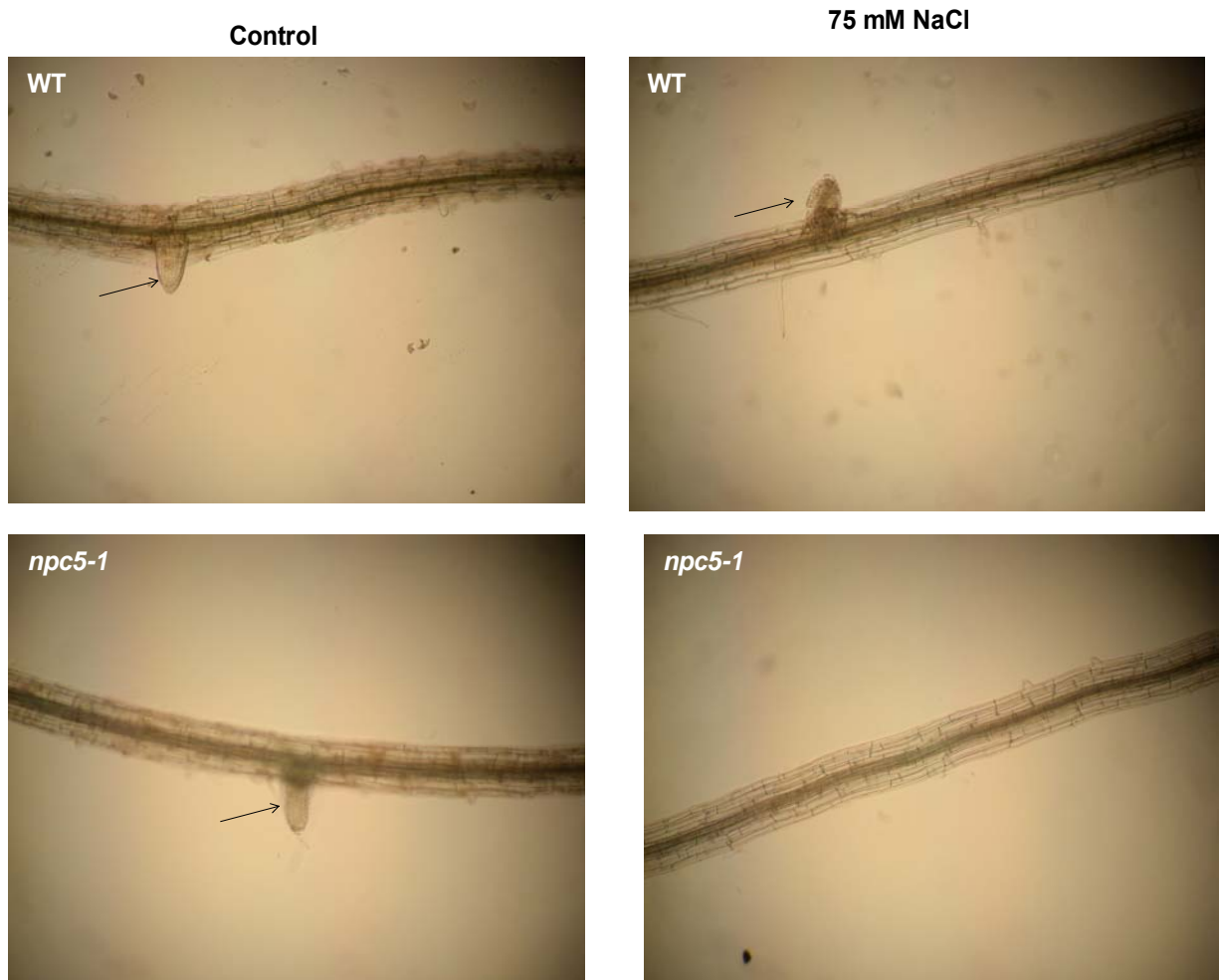


Figure 5

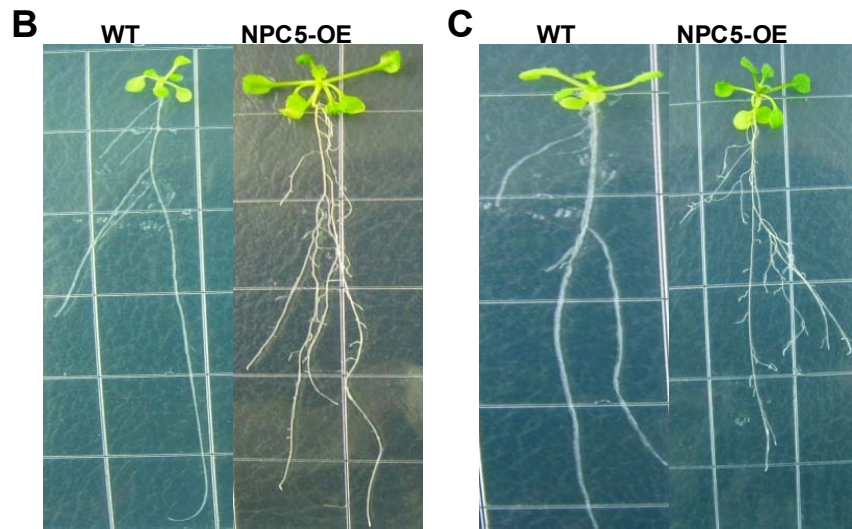
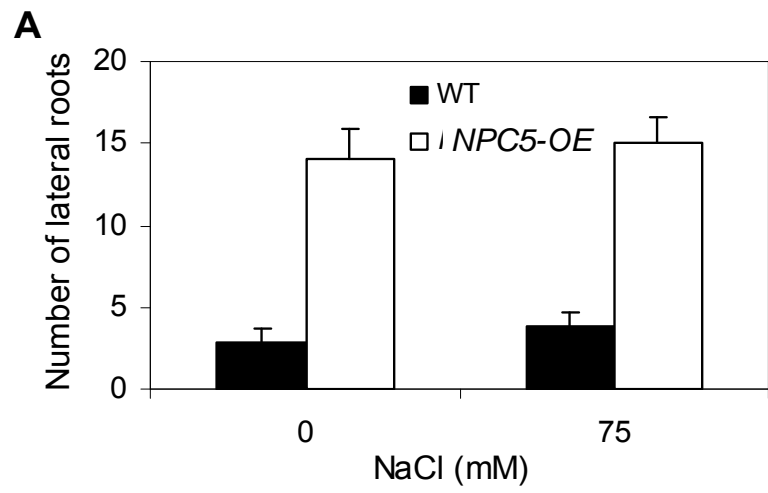


Figure 6

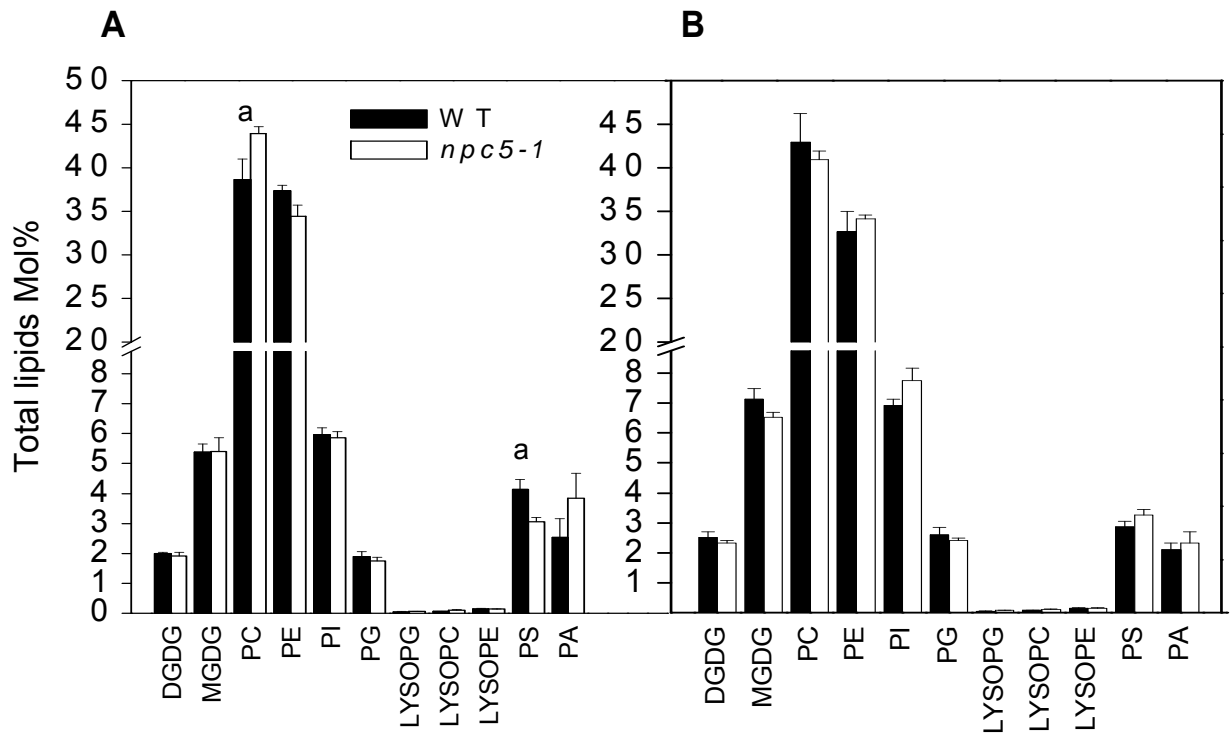


Figure 7

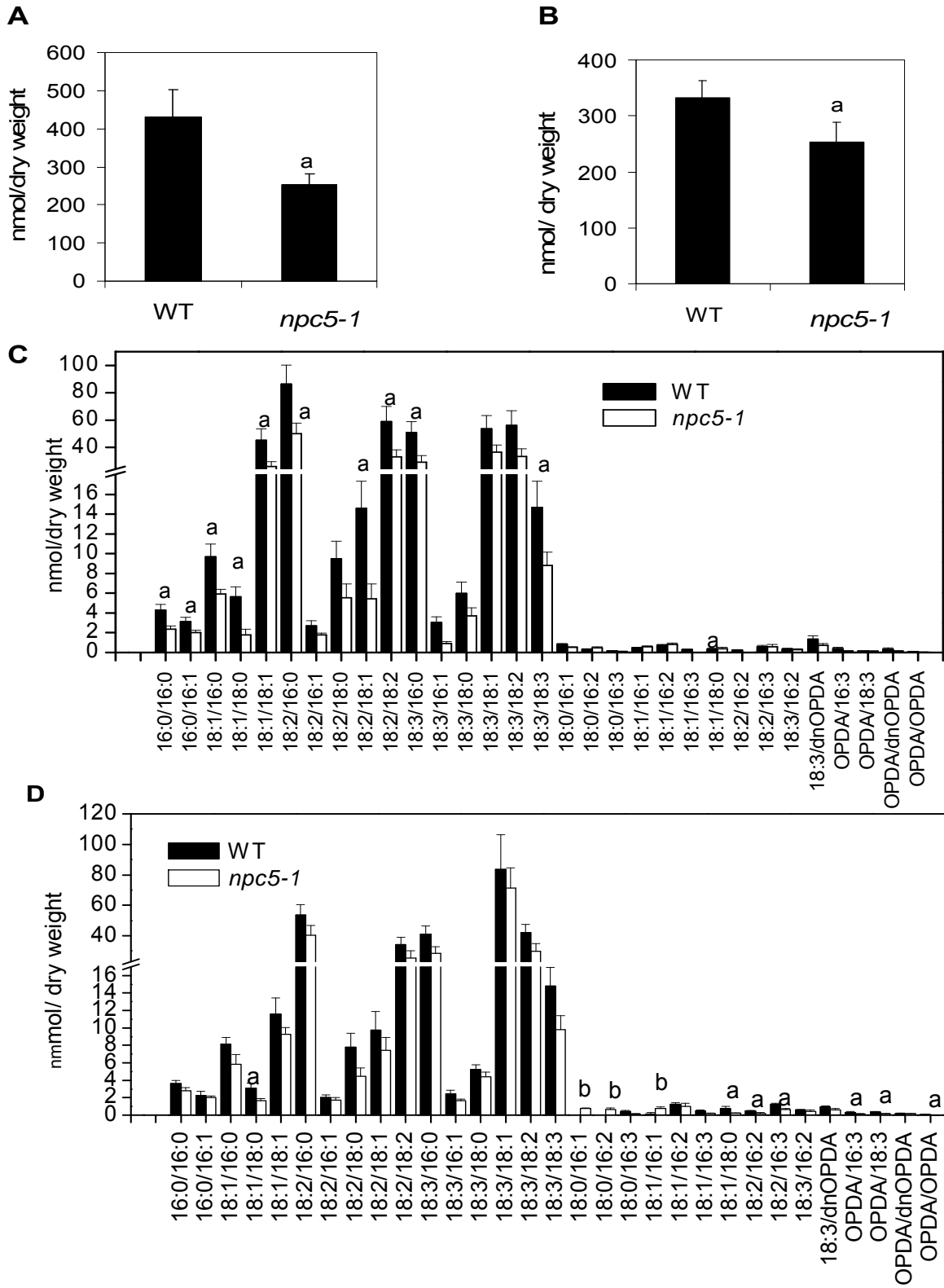


Figure 8

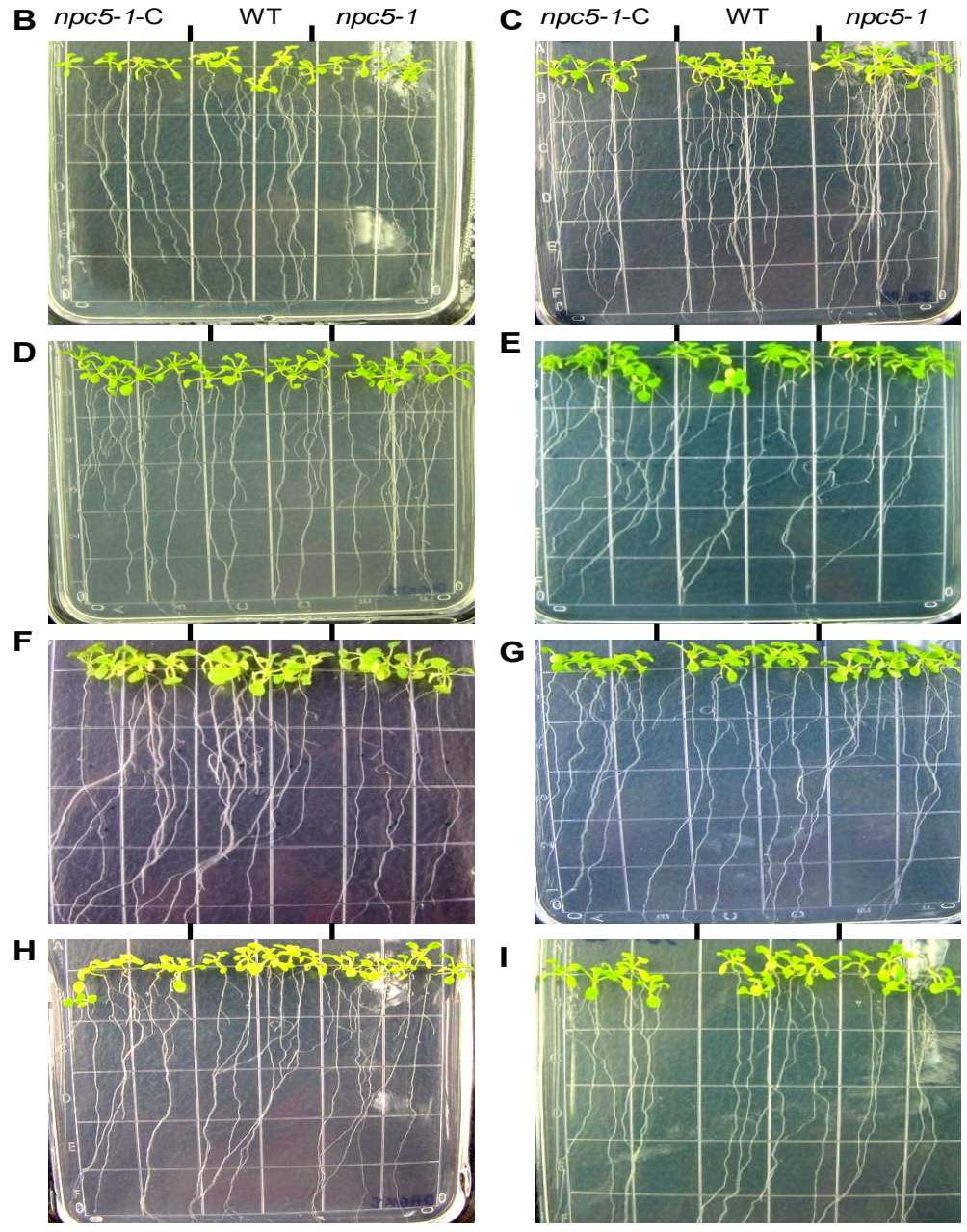
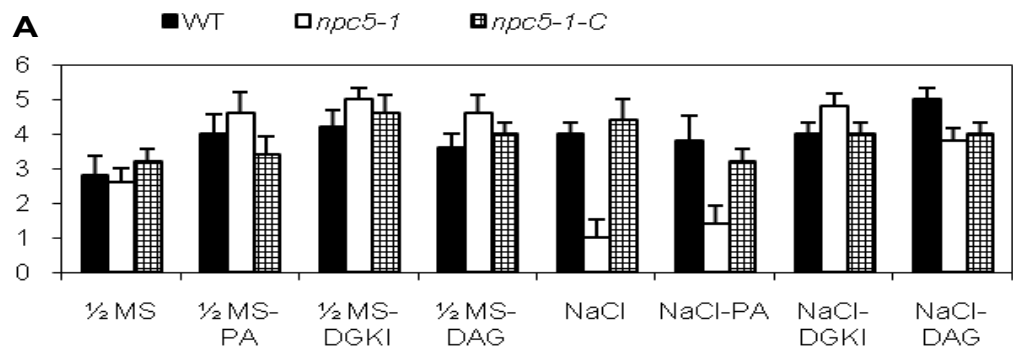


Figure 9

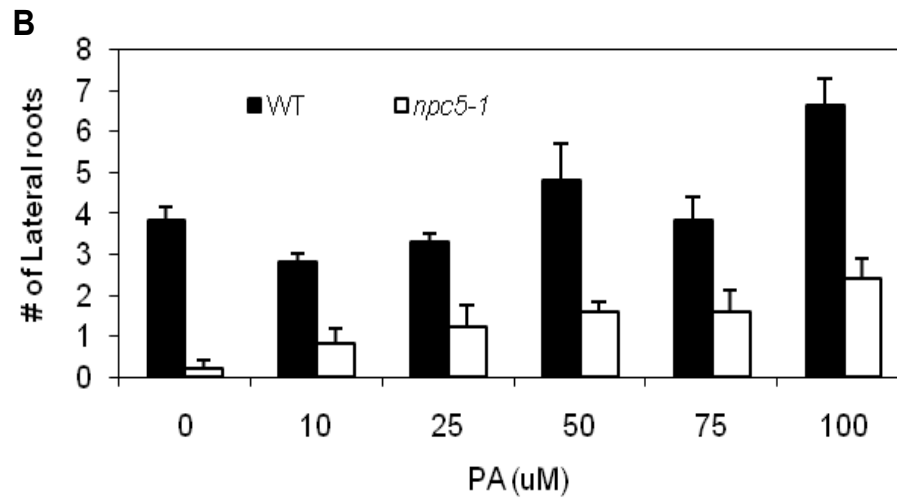
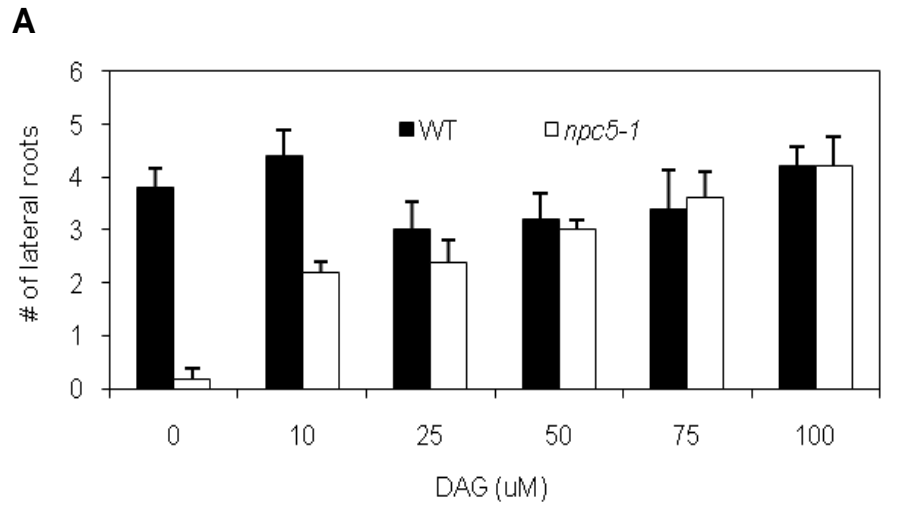


Figure 10

Chapter 6. Discussion and Conclusions

Summary, Significance and Perspectives

In this study six non specific phospholipase C (NPC) genes were cloned and *NPC3*, *NPC4*, *NPC5*, and *NPC6* were characterized. At the onset of this research no published reports existed on any members of the NPC family in Arabidopsis. *NPC4* and *NPC5* have been subsequently cloned and characterized in phosphate deprivation (Nakamura et al., 2005; Gaude et al., 2008). The NPCs are differentially expressed in Arabidopsis tissues. *NPC1*, *NPC2* and *NPC6* are highly expressed in siliques. *NPC5* is highly expressed in inflorescences and promoter GUS fusion showed that it is expressed in the vascular tissue of young and mature leaves (Figure 1B, Chapter 5). *NPC3* shows the highest expression in roots followed by *NPC6* and *NPC1*. *NPC5* expression is the lowest of the NPCs (Figure 3, Chapter 2). The NPCs are also differentially expressed under stress conditions according to Genevestigator (Figure 4, Chapter 5). *NPC4* is highly upregulated by drought, low phosphorous, low nitrate and heat stress. *NPC1* and *NPC3* were also responsive to drought stress and low nitrate. Medium term (24 h and 48 h) phosphate deprivation slightly induced expression of *NPC1*, *NPC2*, and *NPC3* whereas *NPC6* expression was not affected by phosphate deprivation and drought (Figure 4, Chapter 5).

To study the biochemical properties of the NPCs, NPC1-NPC6 were expressed in *E. coli*. NPC5 expression could not be detected by immunoblotting, thus *NPC5* was expressed in Arabidopsis under the control of the 35S promoter with a C-terminus fused STREP tag. Attempts to purify the protein from plants using STREP-Tactin superflow agarose (Novagen) failed. For this reason, the biochemical properties of NPC5 were not determined in this study. NPC1, NPC2, NPC3, NPC4, and NPC6 proteins were successfully expressed in *E. coli* and the biochemical properties of NPC3, NPC4 and NPC6 were determined in this study. Induction of the proteins at 25°C resulted in the proteins being expressed in the insoluble fraction, thus protein expression was induced at 12°C. The three NPCs tested in this study are active phospholipases that do not require calcium for their activity. In vitro assays show that NPC4 uses minor phospholipids such as PA, PS and lysoPC as substrates (Figure 3, Chapter 3). NPC3 and NPC6 hydrolyze

PC and PE, but NPC3 is more active towards PE and PC than NPC6 (Figure 8, Chapter 4). NPC4 is also more active than NPC3 and NPC6. Our results show that the subcellular localization of the NPC family members differs. NPC2 is cytosolic (Figure 1, Chapter 3), and NPC5 was observed in the nucleus, the cytosol and a small portion was seen on the chloroplasts (Figure 1C, Chapter 5). NPC5 was predicted to be cytosolic and nuclear localized according to PSORT. NPC6 was observed in the cytosol and GFP points were visible, indicating that NPC6 may also be associated with organelles (Figure 1C, Chapter 4). NPC4 associates with the plasma membrane (Figure 1C, Chapter 3). NPC3 associated with the plasma membrane and cytosol (Figure 1C, Chapter 4). The NPC-GFP fusion proteins were transformed into Arabidopsis. Analysis of the subcellular localization using the stable transformed lines will further augment the results obtained from transient expression using tobacco. In addition, membrane fractionation experiments will be useful in augmenting the GFP- fusion experiment. NPC1 subcellular localization was not determined in this study. These differences in expression pattern, biochemical properties, and subcellular localization indicate that the NPC family functions are diverse.

Phosphorous limitation in soils greatly affects plant growth and productivity. Unlike animals, plants are non-motile and have developed mechanisms to cope with environmental stresses. During phosphate starvation morphological and metabolic changes occur. The root to shoot ratio increases, number of roots hairs increases and organic acids are exuded in an attempt to sequester the available phosphate in soil. At the metabolic level, phosphate containing compounds are hydrolyzed to release organic phosphate. One such molecule is phospholipid, which is replaced with non-phosphorous containing digalactosyldiacylglycerol (DGDG). Phospholipases catalyze this reaction. In this study we show that *NPC4*, *NPC3* and *NPC6* are involved in lipid metabolism under phosphate deprived conditions (Figures 2D-2F, Chapter 3; Chapter 4). *NPC4* basal level of expression is lower than both *NPC3* and *NPC6* under phosphate sufficient conditions. Under phosphate deprived conditions, *NPC4* is highly expressed, while *NPC3* and *NPC6* expression is not greatly affected (Figure 6A, Chapter 2). Despite the level of induction of *NPC4*, the major classes of phospholipids were not affected under phosphate starvation. However, minor membrane lipids such as phosphatidylserine (PS),

phosphatidic acid (PA) and lyso-phosphatidylcholine (L-PC) were altered. *In vitro* activity assays also confirmed that PS, PA and L-PC serve as substrates for NPC4. In addition, *NPC4* does not affect DGDG accumulation under phosphate deprived conditions. NPC3 and NPC6 hydrolyze PC under phosphate sufficient conditions. During phosphate deprivation, ablation of *NPC3* and *NPC6* affected lysolipid and PC hydrolysis. DGDG accumulation was not altered in *npc3-1*, but more MGDG accumulated in *npc6-1*. In *npc3-1npc6-1* roots DGDG accumulation was lower than wild-type. Under phosphate deprivation diacylglycerol (DAG), the direct product of NPCs, is used as the backbone for DGDG synthesis. In phosphate starved wild-type roots a two fold increase in DAG is observed. This increase in DAG was not seen in *npc3-1*, *npc6-1* and *npc3-1npc6-1*. Furthermore, *npc6-1* and *npc3-1npc6-1* plants DAG were 50% of wild-type levels and *npc3* was 65% wild-type levels. From the results obtained from this study, it is evident that *NPC4* does not play a major role in supplying inorganic phosphate under phosphate starvation. However, it is possible that *NPC4* may play a role in signaling at the onset of phosphate deprivation. Further evidence to support such a hypothesis would be needed. *NPC3* and *NPC6* play different roles in phosphate starvation. Over-expression of *NPC3* increases primary root growth and tolerance to phosphate deprivation. It would be worth while to investigate if the effect is the same in crop plants.

Salt stress and hyperosmotic stress such as drought negatively impact plant growth and productivity. Here we show that *NPC4* is involved in ABA signaling and hyperosmotic stress responses. ABA is a phytohormone that is involved in stress adaptation. *NPC4* is a positive regulator of ABA signaling, since *npc4-1* showed reduced sensitivity to ABA. ABA is known to affect the expression of genes related to stress adaptation. Over-expression of *NPC4* causes increased tolerance to hyperosmotic and salt stress. *NPC4-OE* plants produced more biomass than wild-type plants under salt and drought stress. Under mild salt stress *NPC5* is involved in lateral root formation. *NPC4* and *NPC5* are highly similar (85% a.a identity), but their cellular functions are distinct.

According to Genevestigator, *NPC4* and *NPC6* are slightly induced by IAA (Figure 4, Chapter 2). Double Knockout of *NPC3* and *NPC6* display defective seedling

development, reduced sensitivity to IAA, and loss of apical dominance earlier than wild-type (Figure 12, Chapter 2). Further characterization of *npc3-1npc6-1* will elucidate its role in auxin responses. Low nitrogen induced the expression of *NPC4*, *NPC3* and *NPC2* (Figure 12, Chapter 2). In this study, the NPCs were tested on 0.5 mM nitrogen and *npc5-1* grew shorter roots than wild-type. Since nitrogen is an important macronutrient required for plant growth and development, further experiments testing various concentrations of nitrogen will be useful in determining the functions of the NPC gene family in low nitrate conditions.

Our results show that this family of enzymes has important functions in plants ranging from seedling development to stress adaptation. However, little is known about the function of diacylglycerol (DAG) in plants. Further studies are needed to determine the direct target(s) of DAG in plants.

Conclusions

The main conclusions from this research are as follows:

1. All NPCs tested, NPC3, NPC4, and NPC6 encode functional phospholipase C. NPC4 is the most active followed by NPC3.
2. The *NPCs* are differentially expressed in Arabidopsis tissues. *NPC3* and *NPC4* are highly expressed in roots. *NPC6* is highly expressed in siliques and roots.
3. The subcellular localization of the *NPCs* varies. NPC4 localizes to the plasma membrane. NPC6 is cytosolic and NPC3 is predominantly plasma membrane localized.
4. NPC4 is a positive regulator of ABA signaling and is involved in hyperosmotic stress signaling. Knockout (KO) of *NPC4* increases sensitivity to hyperosmotic stress while overexpression (OE) reduces sensitivity.
5. PA produced via the NPC/DGK pathway is involved in ABA responses.

6. *NPC3* is involved in phosphate starvation in Arabidopsis roots. *NPC3* contributes to 25% of the DAG pool under phosphate deprivation in roots.

7. *NPC6* affects lipid metabolites in Arabidopsis leaves and roots under phosphate deprivation. *NPC6* contributes to more than 50% of the DAG pool in Arabidopsis roots.

8. Double KO of *NPC3* and *NPC6* reduces DGDG accumulation by 36% in Arabidopsis roots.

9. *NPC5* is involved in lateral root formation under mild salt stress. DAG produced by *NPC5* is important for lateral root growth under mild salt stress.